A DISSERTATION FOR THE DEGREE OF DOCTOR OF PHILOSOPHY

Development of a process-based model with higher applicability using deep learning for hydroponic sweet peppers

딥러닝 방법론을 이용한 높은 적용성을 가진 수경재배 파프리카 대상 절차 기반 모델 개발

BY

TAEWON MOON

AUGUST, 2022

MAJOR IN HORTICULTURAL SCIENCE AND BIOTECHNOLOGY

DEPARTMENT OF AGRICULTURE, FORESTRY, AND BIORESOURCES

THE GRADUATE SCHOOL OF SEOUL NATIONAL UNIVERSITY

Development of a process-based model with higher applicability using deep learning for hydroponic sweet peppers

UNDER THE DIRECTION OF DR. JUNG EEK SON
SUBMITTED TO THE FACULTY OF THE GRADUATE SCHOOL
OF SEOUL NATIONAL UNIVERSITY

BY

TAEWON MOON

MAJOR IN HORTICULTURAL SCIENCE AND BIOTECHNOLOGY
DEPARTMENT OF AGRICULTURE, FORESTRY, AND BIORESOURCES

AUGUST, 2022

APPROVED AS A QUALIFIED DISSERTATION OF TAEWON MOON
FOR THE DEGREE OF DOCTOR OF PHILOSOPHY
BY THE COMMITTEE MEMBERS

CHAIRMAN _____
CHANGHOO CHUN, PH.D.

VICE-CHAIRMAN _____
JUNG EEK SON, PH.D.

MEMBER _____
HAK-JIN KIM, PH.D.

MEMBER _____
YOUNG-YEOL CHO, PH.D.

MEMBER _____
HYUN KWON SUH, PH.D.

Development of a process-based model with higher applicability using deep learning for hydroponic sweet peppers

Taewon Moon

Department of Agriculture, Forestry, and Bioresources

The Graduate School of Seoul National University

ABSTRACT

Many agricultural challenges are entangled in a complex interaction between crops and the environment. As a simplifying tool, crop modeling is a process of abstracting and interpreting agricultural phenomena. Understanding based on this interpretation can play a role in supporting academic and social decisions in agriculture. Process-based crop models have solved the challenges for decades to enhance the productivity and quality of crop production; the remaining objectives have led to demand for crop models handling multidirectional analyses with multidimensional information. As a possible milestone to satisfy this goal, deep learning algorithms have been introduced to the complicated tasks in agriculture. However, the algorithms could not replace existing crop models because of the research fragmentation and low

accessibility of the crop models. This study established a developmental protocol for a process-based crop model with deep learning methodology. Literature Review introduced deep learning and crop modeling, and it explained the reasons for the necessity of this protocol despite numerous deep learning applications for agriculture. Base studies were conducted with several greenhouse data in Chapters 1 and 2: transfer learning and U-Net structure were utilized to construct an infrastructure for the deep learning application; HyperOpt, a Bayesian optimization method, was tested to calibrate crop models to compare the existing crop models with the developed model. Finally, the process-based crop model with full deep neural networks, DeepCrop, was developed with an attention mechanism and multitask decoders for hydroponic sweet peppers (*Capsicum annuum* var. *annuum*) in Chapter 3. The methodology for data integrity showed adequate accuracy, so it was applied to the data in all chapters. HyperOpt was able to calibrate food and feed crop models for sweet peppers. Therefore, the compared models in the final chapter were optimized using HyperOpt. DeepCrop was trained to simulate several growth factors with environment data. The trained DeepCrop was evaluated with unseen data, and it showed the highest modeling efficiency (=0.76) and the lowest normalized root mean squared error (=0.18) than the compared models. With the high adaptability of DeepCrop, it can be used for studies on various scales and purposes. Since all methods adequately solved the given tasks and underlay the DeepCrop development, the established protocol can be a high throughput for

enhancing accessibility of crop models, resulting in unifying crop modeling studies.

Additional keywords: artificial intelligence, crop simulation model, machine learning, multitask learning, Transformer

Student number: 2019-35122

CONTENTS

Chapter 1. Infrastructure for applying deep learning algorithms to crop modeling

LIST OF TABLES

LIST OF FIGURES

LITERATURE REVIEW

Deep learning as an accelerator for process-based crop modeling

ABSTRACT

Agriculture has to undergo an intensification for sustainable production. In this regard, crop models are a versatile tool for obtaining a sense of future crop production. However, the relevant studies have been fragmented because of the differences in research scales and purposes. This disjunction interrupts the productive cooperation and progress of agricultural systems. Therefore, a deep-learning-based crop model would provide a breakthrough in solving the fragmentations of crop modeling research. From this perspective, the current status of the crop production and crop models, the advantages and requirements of the deep learning, deep learning applications in the other fields, deep learning applications for crop production research, and the limitations and reasons for the applications in crop production were discussed. Finally, what the crop model with deep learning should be was outlined. Deep-learning-based crop models will derive standardization and cooperation from heterogenous crop modeling groups based on the accessibility and applicability of the deep learning algorithms.

Additional keywords: agricultural system model, crop simulation model, climate change, horticulture, sustainability

Background

Plant production has been inextricable from humanity since the agricultural revolution 10,000 years ago. Diverse plants have been domesticated as crops, and their productivity and quality have significantly increased with several agricultural innovations (Evenson and Gollin 2003; Bisbis et al. 2018; Eshed and Lippman 2019). Therefore, crop production has been able to meet global demand. However, agriculture has faced some future challenges: overpopulation, climate change, and degradation of arable lands. According to a recent report, climate change is inevitable, and global environmental conventions are boosting the demand for sustainability (UN 2019; IPCC 2021). Agricultural innovations also strain Earth, similar to other industries, although they significantly improved crop productivity and quality (FAO 2018). Therefore, agriculture is required to achieve intensification for sustainability.

Horticultural crops, such as fruits and vegetables, are also the mainstays in agricultural production (Dohlman et al. 2022). The horticultural industry has improved productivity and quality by introducing diverse technologies and expanding the cultivational area, so fruit and vegetable production has also been sufficient to meet global demand. However, the consumption of fruits and vegetables was reported to increase steadily through 2050: the ratio of fruits and vegetables in diet per capita will increase because of improvements in the national limits, such as undernourishment and economic status (FAO 2018). At

the same time, irrigated area and greenhouse gas emissions should be reduced according to the recent necessity of sustainable production; therefore, high-level intensification is required to simultaneously accomplish sustainable horticulture and sufficient supply.

Greenhouse horticulture has been studied and developed as an intensification methodology for horticultural crop production. Greenhouse productivity can be significantly higher than that in open fields; greenhouse-grown crops could have higher resource footprints (Fig. 1). Greenhouses have high variances in productivity and resource use efficiency (RUE) according to cultivation conditions such as local climate, introduced technology, and cultivating crops. With an improper cultivation strategy, high energy and carbon use worsen global warming, and increased water use could cause salinization and desertification in nearby ecosystems (Thomas and Middleton 1993; Singh 2009; Shi et al. 2009). The productivity and RUE of greenhouses could be improved with adequate technologies and strategies for cultivational conditions. Therefore, a suitable cultivation strategy should be selected to improve greenhouse production that can vary with cultivation conditions.

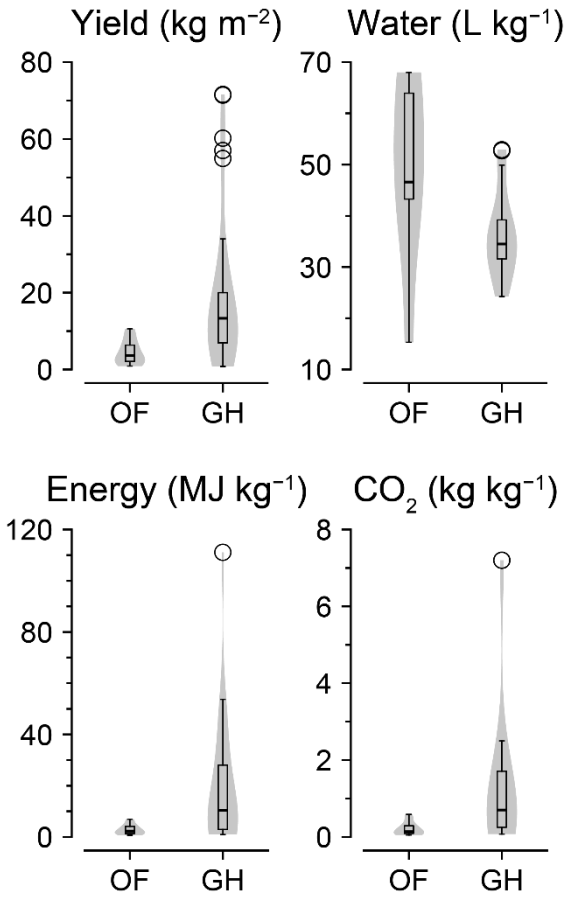

Fig. 1. Crop yield and resource footprints of open fields (OF) and greenhouses (GH). The data of eight vegetables from 18 scientific reports from 2005 to 2022 were meta-analyzed. The boxes and markers represent quantiles and outliers, respectively. Black solid line in the box represents the median. Refer to Appendix for the analyzed references.

Improving greenhouse production involves many study fields (Fig. 2). Greenhouse production is a multifactorial optimization problem that accompanies engineering, biological, chemical, and economic considerations (Gijzen et al. 1998; Vanthoor et al. 2012; Gruda et al. 2019; Ahn et al. 2021). The properties of greenhouse structure are restricted, and the exchange of energy and materials in greenhouse environments is relatively immediate; however, crops change by their environment in the long term, and the response of crops can be diverse according to genotype and management (Hajjarpoor et al. 2018; Peng et al. 2020). High planting density and semiclosed microclimate in greenhouses can drastically change the internal environment (Vanthoor et al. 2011; van Beveren et al. 2015). Therefore, optimal control of greenhouse environment for better crop productivity should be based on understanding crop growth (Katzin et al. 2022). Crop modeling would be an adequate tool for the analysis.

Fig. 2. Word clouds of study fields covering greenhouse horticulture. Topics from 1,845 journals were analyzed. The font sizes were determined by multiplying the number of related papers published after 2018 and the SJR factor on a log scale. The searching keywords for those papers were "crop greenhouse −gas −gases." The minus sign represents that the keywords have not to be included in the search results. Note that the relevant papers covering climate change could also be excluded because of the search term.

A system can be condensed into a model as necessary; the model can be used for mathematical analysis and simulation to explain the target phenomenon. In agriculture, agroecological research covers interactions of agricultural production, environmental resources, and human factors; therefore, agricultural system modeling was introduced to understand and evaluate the performance of the overall agroecosystem (Jones et al. 2017). Among the specialized agricultural system models, crop models have been developed to analyze crop growth (Muller and Martre 2019). Crop models can quantify the influence of crops, agricultural management, and the environment based on adequate information (Hoogenboom et al. 2020).

Crop models were also developed for various horticultural crops by miscellaneous research groups; however, horticultural crop models have low accessibility and fragmentation problems (Gary et al. 1998; Marcelis et al. 1998; Vos et al. 2010; Altes-Buch et al. 2019; Katzin et al. 2022). Some accessible crop models seemed not to be suitable for current greenhouse cultivation. DSSAT has major vegetable models, such as tomatoes and cabbages, but the models have outdated parameters calibrated for open field data (Jones et al. 2003; Antle et al. 2017). Detailed information about advanced horticultural crop models such as HORTISIM and KASPRO are not available to the public, and relevant reports on formulas and parameters are decades old (Gijzen et al. 1998; Altes-Buch et al. 2019; Katzin et al. 2022). Newly modeling a crop requires nontrivial efforts and resources, and the existing modeling processes are

fragmented according to the research purpose and scale (Antle et al. 2017; Janssen et al. 2017). Cultivars and managements could be diverse with locations and purposes even for the same crop (van Straten et al. 2000; van Ploeg and Heuvelink 2005; Muller and Martre 2019; Wang et al. 2019b; Peng et al. 2020). Therefore, horticultural crop models were not successful in adequately keeping up with technological advances in greenhouses.

Since high technologies have been introduced to greenhouse cultivation, the collected information and data have become diverse (Wolfert et al. 2017; Kamilaris et al. 2017; Misra et al. 2020). Recently, data-driven cultivations in high-tech greenhouses were not able to be predicted with advanced greenhouse climate model and crop model (Hemming et al. 2019, 2020). That is, cultivation management out of the reasonable simulated range achieved higher productivity and benefits than existing model-based inference and green-thumb intuition. Therefore, it can be said that existing crop models for greenhouse horticulture failed to deal with the data accumulations of high-tech greenhouses.

The fragmentation problem is not limited to horticulture; it is prevalent in general crop modeling studies. Researchers at various scales have recognized that fragmentation is the common cause of tardy updates in crop models. The fragmentation resulted in unspecified uncertainty of crop model outputs. The independent models were studied in various growths, managements, and local conditions; therefore, the cause of uncertainty is rarely distinguishable (Li et al. 2015). Crop models should be evaluated with multiscale conditions rather than

a single season and crop for a better understanding of uncertainty (Rötter et al. 2018). Cooperation through diverse scales and fields is necessary to solve the common challenges of crop models (Hammer et al. 2019; Peng et al. 2020). Numerous improvements for food and feed crop models have been suggested based on problem recognition; however, fragmentation has not yet been solved (Wang et al. 2017a; Roberts et al. 2017; Rötter et al. 2018; Müller et al. 2021; Schierhorn et al. 2021). Therefore, the accessibility to crop models should be improved first to foster global cooperation and mutual development.

Based on this background in greenhouse horticulture and crop models, this chapter reviewed current status of deep learning applications and introduced a possible approach to use deep learning for improving the accessibility of crop models. Since deep learning was introduced a sufficient number of years ago, plant and agricultural applications of deep learning have been surveyed, and advanced technologies, including deep learning as a partial section, have been reviewed in high quality (Table 1). The articles emphasized the potential of deep learning algorithms for crop production; however, the innate advantages of deep learning and the way to make the most of it for crop production were not discussed clearly. Therefore, this chapter outlined the strength of deep learning according to advancement in the other fields and how to improve the accessibility of the crop models utilizing that strength of deep learning.

Table 1. Ranges of environmental data used for the experiment.

	Summary	References
Comprehensive	Machine learning and deep learning have promising potential to handle challenges in agriculture. Most of them were conducted for research purposes. Deep learning outperformed existing techniques, but additional technology is required to address agricultural specificity.	Kamilaris and Prenafeta-Boldú 2018 Benos et al. 2021 Osinga et al. 2022
Crop yield prediction and fruit detection	Yield prediction and fruit detection can help achievement of optimum crop yield. Deep learning is suited for studies requiring future predictions from raw data, but the best model is uncharacterized. The choice of features depends on availability and quality of the dataset and research purposes. Models with more features did not always provide the best performance for the yield prediction. The research changed to modify existing deep learning models suitable for a specific application.	Koirala et al. 2019 van Klompenburg et al. 2020 Bali and Singla 2022
Phenotyping	Genome engineering exceeded the capacity to measure the effects of genetic changes on plant traits. Plant phenotyping is also essential to select stress-resistant varieties and develop better stress-management strategies. Genomics-assisted breeding has become a popular approach to food security. Machine learning is a promising solution for improving image-based phenotyping. High-throughput crop phenotyping could help standardize crop traits, and the growing capabilities of the methodology can extract new insights across varied crops.	Singh et al. 2021 Jin et al. 2021 Sarić et al. 2022
Plant diseases and pest detection	Plant diseases and pests are essential factors determining the yield and quality of plants. Detecting and monitoring them over vast areas could also enhance plant protection. Machine learning plays an important role in modeling diseases and pest detection; especially, deep learning has made breakthroughs in digital image processing. Deep learning has great development potential, although practical production and application are still unrealizable. A large number of labeled samples is the main challenge of the application. Therefore, collecting big data for plant diseases and pests should be a priority for applying deep learning methods.	Zhang et al. 2019b Liu and Wang 2021
Weed detection	Weeds are one of significant factors that could diminish crop productivity. Deep learning has enabled rapid detection, localization, and recognition of objects from vision. With technological advances, image processing techniques have become a promising tool for precise real-time weed and crop detection in the field. Most studies achieved high accuracy by fine-tuning pre-trained models and availability of labeled big data. The future is promising, although some challenges still exist. generalized large datasets and tailored machine learning models in weed-crop settings are necessary for future research.	Wang et al. 2019a Hasan et al. 2021

Remarkable applicability and accessibility of deep learning

Deep learning algorithms show state-of-the-art performance in broad engineering and scientific fields (Goodfellow et al. 2014; LeCun et al. 2015; Aloysius and Geetha 2017; Shinde and Shah 2018; Pan et al. 2019; Liu et al. 2020; Dhillon and Verma 2020; Gm et al. 2020; Otter et al. 2021; Wang et al. 2021; Tan et al. 2021; Han et al. 2022). Before the introduction of deep learning, diverse algorithms competed in computer vision, such as classification and object detection (Liu et al. 2020); however, existing algorithms have been overwhelmed since 2012, and deep learning has been applied by all teams (Huang 2016). Natural language processing, such as voice recognition and text-to-speech, requires data processing technology based on the target languages' linguistic and cultural backgrounds; however, deep learning's abstraction capability enables the use of unprocessed raw data (Otter et al. 2021; Tan et al. 2021). This resulted in higher accessibility that nonspecialized institutions can develop and improve the models (Tan et al. 2021). Generative models have rarely been created because of the innate complexity of analyzing the generation task (Gm et al. 2020), and the research field is booming with the introduction of deep learning (Goodfellow et al. 2014; Pan et al. 2019; Gm et al. 2020; Wang et al. 2021). Deep learning models have also been broadly applied in other fields (Shinde and Shah 2018; Dhillon and Verma 2020). High performances and increasing study groups ensure that deep learning is superior to existing methods in many studies.

A famous reason for the high performances is enormous data accumulation in a specific field (Fig. 3). The data related to human activity, such as images, text, and gameplays, are sufficiently accumulated and powered by global internet networks and storage, and the data have high integrity in nature: that is, big data with sufficient common features and a similar distribution space can be utilized. In addition, the advent of computation powers to deal with big data is also a core of the model performance. The concepts of deep learning are decades-long, but the computing power and data amount to realize the methodology were recently satisfied (McCulloch and Pitts 1943; Rosenblatt 1958; Fukushima 1988; Hochreiter and Schmidhuber 1997).

Another well-known strength is a high performance in generalizing big data: automated feature extraction (LeCun et al. 2015). With conventional data science, humans should extract features of the target data based on domain knowledge and empirical data analysis skills. Deep learning can autonomously extract necessary features for a given task with sufficient data (Lee et al. 2009; Siegel et al. 2016). Therefore, more complicated data relations, such as images of gameplays and required actions for high scores, can be interpreted from the raw data (Mnih et al. 2015), and the background knowledge becomes less important (Silver et al. 2018; Schrittwieser et al. 2020).

As mentioned above, big data, progress in computation power, and high-level abstraction are often noted to explain deep learning performance. However, the explanations are a perspective of computer science and engineering, and the prevalent application and utilization of deep learning regardless of the research fields could be more derivative: the high accessibility and adaptability of the developed deep learning model with less domain knowledge. Many areas where deep learning stands out have been organically connected and developed faster than before based on high accessibility to the algorithms (Fig. 4). Scientific reports, including deep learning applications for complicated tasks, are frequently published, although the technologies were studied exclusively by private institutions and companies before. Deep neural networks, a core structure of deep learning, are an assembly of many linear calculations; therefore, deep learning models have shown high adaptability regardless of the input and output types. (Yoon et al. 2018; Shu et al. 2019; Brown et al. 2020; Wang et al. 2021; Ramesh et al. 2021). Algorithms that are in completely different fields influence and develop each other based on adaptability. Based on accessibility and adaptability, deep learning has increased opportunities for scientific and engineering contributions; therefore, deep learning algorithms have led to unprecedented progress in that field.

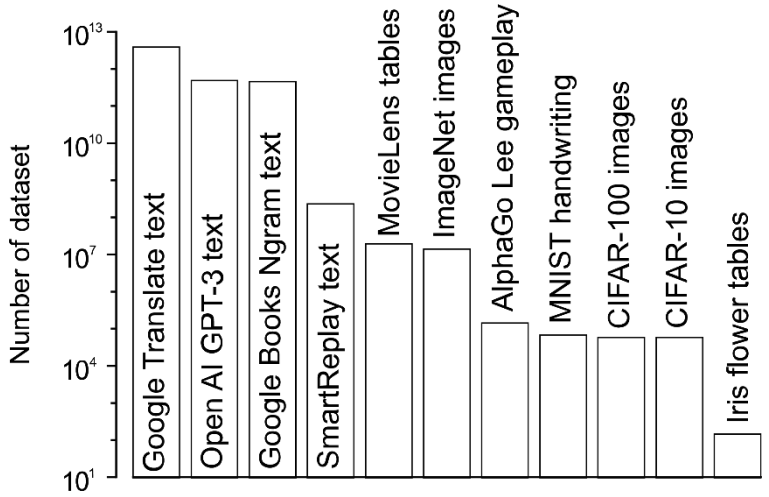

Fig. 3. Numbers of datasets used to train machine learning or deep learning models.

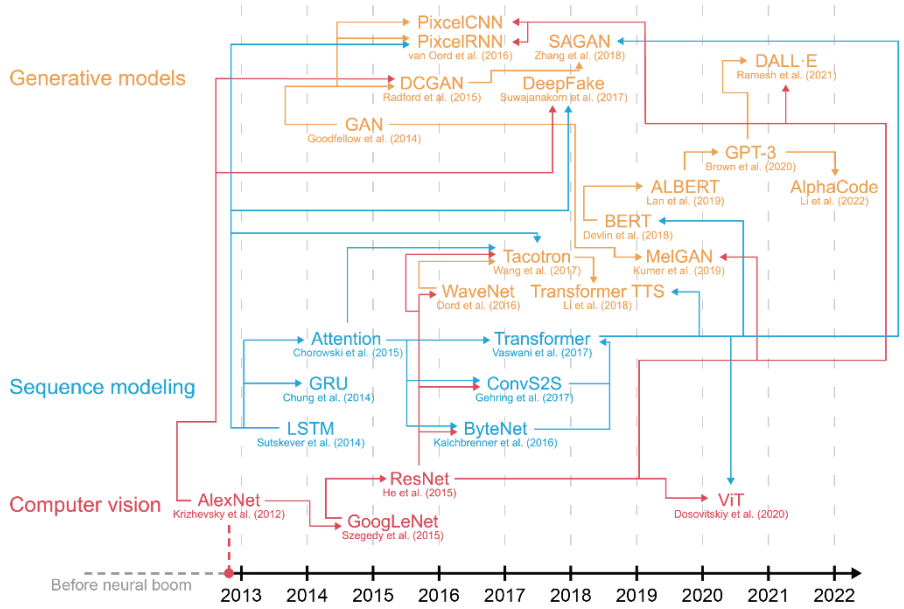

Fig. 4. A brief timeline of progress in computer vision, sequence modeling, and generative models after the deep learning introduction. Solid arrows represent the structural and motivational reuse of the previous algorithm. Note that some remarkable inventions were omitted for convenience of depiction. Refer to Appendix for the used references.

Deep learning applications for crop production

Since scientific reports covering deep learning applications for crop models are infrequent, pros and cons can be inferred from those for the broader topic: crop production. Advanced technologies, including deep learning applications in agriculture, have been actively studied and reviewed. Diverse applications have also been frequently tried over the last decade, although the topic of crop production is a relatively narrow scope (Table 1). Computer vision such as fruit, pest, and weed detection and classification was relatively favorable because the data were easily collectible and relevant pre-trained models were affordable; meanwhile, the cases of hyperspectral imaging and external phenotyping suggested securing data first because collecting adequate output data is challenging.

Studies commonly remarked that deep learning is a promising tool because of its abstraction ability; however, they also indicated that firm infrastructure, such as standardized data collection and accessible tools for popularization, should precede the application for stable model training. The necessity of hyperparameter tunning and specialized model structures for agricultural purpose was also mentioned. However, most of the studies still concentrated on improving the end-to-end model accuracies for limited dataset with existing deep learning structures. Unlike the high-tech fields that have made great strides in a decade after the introduction of deep learning, the applications for crop production are still in infancy. The results in crop production can be

regarded as preliminary experiments, and they did not show reportable advantages that can substitute for crop models except for high accuracy in specific and partial conditions. Inactivated research in crop model applications could also be explained with these thresholds.

Thresholds to apply deep learning to crop models

Deep learning applications for crop models share challenges with those for crop production: lack of infrastructure. The obvious infrastructure to make the most of the deep learning is the securement of standardized and generalized dataset. As previously discussed, deep learning algorithms established superiority in the fields where various datasets with high data integrity were affordable. That is, establishing standards for data collection and feature selection can solve the majority of the challenges; however, crop cultivation data have some distinctive characteristics.

1. Cultivation takes relatively long time than other famous tasks such as playing games or autonomous driving. Crop productivity and quality change with crop developmental stages and cumulative influences of crop environments; therefore, high quality data should be collected in long-term periods with various locations. It makes space and time constraints for constructing datasets.
2. Features of agricultural data are scattered. Standardized agricultural data should include crop genotypes, climatic impacts, crop management,

cultivation scales, etc. Standardizing anthropogenic features such as management could be impractical because they can differ by crop, farming scale, and farmer; therefore, recording every feature from microscopic to macroscopic would require unaffordable funding. Even if a standard for the data collection is established, labeling the data will be a second hurdle. Providing answer sheets for an ambiguous target is difficult unlike sentiments in texts, facial expressions, and moves in the game of Go.

3. Agricultural research groups using crop models have different research scales and objectives; therefore, necessary datasets and mainstream crop models are also varied (Jones et al. 2003; Steduto et al. 2009; Wang et al. 2017; de Wit et al. 2019). Several interdisciplinary academic meetings will have to be held, and relevant research groups should agree (Antle et al. 2017; Janssen et al. 2017; Jones et al. 2017). However, crop production involves various fields, from genetics to classical mechanics. This breadth makes it challenging to understand studies of each other group and assemble datasets together for a single purpose, such as object detection or classification. Therefore, making a common dataset could require a long time unlike other fields where the deep learning algorithms have taken a leading role.

Therefore, an immediate and practicable way is required. To make the most of deep learning as an accelerator, it must be applied to the distinctive

infrastructure of agriculture. Rather than simply applying the end-to-end model to increase the accuracy following the precedent, we need to find a way to make modeling convenient by focusing on the accessibility and applicability of the deep learning algorithms.

Necessity to prioritize deep-learning-based crop models

In this regard, the disseminating accessible tools should be solved first. Deep-learning-based crop models can be shared on any scale and for any purpose with their strengths. Deep learning models can be retrained with semantically different input unless the dimension of the input tensor change. Moreover, well-trained deep learning models can be retrained with different input and output tensors by eliminating some layers, called transfer learning (Pan and Yang 2010; Weiss et al. 2016; Zhuang et al. 2020). If the amount of crop data increases, relations of crop data can be embedded into another vector space (Mikolov et al. 2013; Rong 2016). Therefore, the features of the datasets will converge to optimized items with the common deep crop model.

Progress in the deep crop model can also improve in agricultural data science. In the case of games and driving, space and time constraints can be alleviated with a simulation. Data shortage for model training could be complemented with an imperfect simulation like autonomous driving (Chao et al. 2020; Huang and Chen 2020; Kiran et al. 2021). Similarly, neural networks are a function approximator; therefore, deep crop models can be trained with

data from existing crop models. However, simulation and reality are not completely equal, so sim-to-real methodology should be introduced to avoid overfitting to the simulation condition.

Requirements of the deep-learning-based crop models

While end-to-end models with a direct structure from input vectors to output vectors can yield higher accuracy than existing models, they are not sufficient to share and maintain the developed model in the current stage. It can easily be an isolated study in which the models are robust only for the private data, and follow-up studies are rarely conducted. The deep crop model should have a structure similar to existing crop models.

As a warming-up step, the high-level abstraction property of deep learning should be utilized. Human intervention and manual feature extraction can be replaced. For example, simplified input such as daily maximum temperature or cumulative radiation can be conducted with some neural layers (Jones et al. 2003; Steduto et al. 2009; Mikolov et al. 2013; de Wit et al. 2019). However, only using the deep learning for the feature extraction with conventional crop models cannot solve the fragmentation of the related studies. A deep crop model that is fully structured with deep neural networks is adequate for using, maintaining, and developing by anyone. In this manner, explainable parameters with the target output should be encouraged. Above all, the developed model must be competitive to the existing crop models.

Opening remarks and thesis objectives

In this chapter, crop modeling and deep learning applications were reviewed. Then, a practical way to develop a deep-learning-based crop model was suggested. The deep-learning-based crop model can accelerate crop modeling research, which can provide insights into sustainable production in agriculture. It would result in the progress in agricultural data science like other cases. However, the agricultural distinctiveness is also a hurdle for the practical way. Partial solutions could cause more fragmentations, so a complete protocol for the model development from scratch can be an example for new other deep learning applications.

This study focused to establish a developmental protocol for a process-based crop model with full deep learning architecture. Base studies were conducted with several greenhouse data in Chapters 1 and 2. In Chapter 1, transfer learning and U-Net structure were utilized to construct an infrastructure for the deep learning application. In Chapter 2, HyperOpt, a Bayesian optimization method, was tested to calibrate crop models to compare the existing crop models with the developed model. In Chapter 3, the process-based crop model with full deep neural networks, DeepCrop, was developed with an attention mechanism and multitask decoders for hydroponic sweet peppers. The established protocol expected to be a high throughput for enhancing accessibility of crop models.

LITERATURE CITED

Ahn TI, Yang J-S, Park SH, Im Y-H, Lee JY (2021) Nutrient recirculating soilless culture system as a predictable and stable way of microbial risk management. J Clean Prod 298:126747.

Aloysius N, Geetha M (2017) A review on deep convolutional neural networks. In: 2017 International Conference on Communication and Signal Processing (ICCSP). IEEE, pp 0588–0592.

Altes-Buch Q, Quoilin S, Lemort V (2019) Greenhouses: A Modelica Library for the Simulation of Greenhouse Climate and Energy Systems. pp 533–542.

Antle JM, Jones JW, Rosenzweig CE (2017) Next generation agricultural system data, models and knowledge products: Introduction. Agric Syst 155:186–190.

Bisbis MB, Gruda N, Blanke M (2018) Potential impacts of climate change on vegetable production and product quality – A review. J Clean Prod 170:1602–1620.

Brown TB, Mann B, Ryder N, Subbiah M, Kaplan J, Dhariwal P, Neelakantan A, Shyam P, Sastry G, Askell A, et al. (2020) Language Models are Few-Shot Learners. arXiv Preprint arXiv:2005.14165.

Chao Q, Bi H, Li W, Mao T, Wang Z, Lin MC, Deng Z (2020) A Survey on Visual Traffic Simulation: Models, Evaluations, and Applications in

Autonomous Driving. Comput Graph Forum 39:287–308.

de Wit A, Boogaard H, Fumagalli D, Janssen S, Knapen R, van Kraalingen D, Supit I, van der Wijngaart R, van Diepen K (2019) 25 years of the WOFOST cropping systems model. Agric Syst 168:154–167.

Dhillon A, Verma GK (2020) Convolutional neural network: a review of models, methodologies and applications to object detection. Prog Artif Intell 9:85–112.

Dohlman E, Hansen J, David B (2022) USDA Agricultural Projections to 2031. USDA, Washington, USA.

Eshed Y, Lippman ZB (2019) Revolutions in agriculture chart a course for targeted breeding of old and new crops. Science 366:eaax0025.

Evenson RE, Gollin D (2003) Assessing the Impact of the Green Revolution, 1960 to 2000. Science 300:758–762.

FAO (2018) The future of food and agriculture – Alternative pathways to 2050. FAO, Rome.

Fukushima K (1988) Neocognitron: A hierarchical neural network capable of visual pattern recognition. Neural Net 1:119–130.

Gary C, Jones JW, Tchamitchian M (1998) Crop modelling in horticulture: state of the art. Sci Hortic 74:3–20.

Gijzen H, Heuvelink E, Challa H, Marcelis LFM, Dayan E, Cohen S, Fuchs M (1998) HORTISIM: a model for greenhouse crops and greenhouse climate. Acta Hortic 441–450.

Gm H, Gourisaria MK, Pandey M, Rautaray SS (2020) A comprehensive survey and analysis of generative models in machine learning. Comput Sci Rev 38:100285.

Goodfellow I, Pouget-Abadie J, Mirza M, Xu B, Warde-Farley D, Ozair S, Courville A, Bengio Y (2014) Generative Adversarial Nets. In: Z G, M. W, C C, N L, K.Q. W (eds) Advances in Neural Information Processing Systems. Curran Associates, Inc., Montréal Canada.

Gruda N, Bisbis M, Tanny J (2019) Impacts of protected vegetable cultivation on climate change and adaptation strategies for cleaner production – A review. J Clean Prod 225:324–339.

Hajjarpoor A, Vadez V, Soltani A, Gaur P, Whitbread A, Suresh Babu D, Gumma MK, Diancoumba M, Kholová J (2018) Characterization of the main chickpea cropping systems in India using a yield gap analysis approach. Field Crops Res 223:93–104.

Hammer G, Messina C, Wu A, Cooper M (2019) Biological reality and parsimony in crop models—why we need both in crop improvement! in silico Plants 1:diz010.

Han K, Wang Y, Chen H, Chen X, Guo J, Liu Z, Tang Y, Xiao A, Xu C, Xu Y, Yang Z, Zhang Y, Tao D (2022) A Survey on Vision Transformer. IEEE Trans Pattern Anal Mach Intell 1–1.

Hasan ASMM, Sohel F, Diepeveen D, Laga H, Jones MGK (2021) A survey of deep learning techniques for weed detection from images. Comput Electron

Agric 184:106067.

Hemming S, de Zwart F, Elings A, Righini I, Petropoulou A (2019) Remote Control of Greenhouse Vegetable Production with Artificial Intelligence—Greenhouse Climate, Irrigation, and Crop Production. Sensors 19:1807.

Hemming S, Zwart F de, Elings A, Petropoulou A, Righini I (2020) Cherry Tomato Production in Intelligent Greenhouses—Sensors and AI for Control of Climate, Irrigation, Crop Yield, and Quality. Sensors 20:6430.

Hochreiter S, Schmidhuber J (1997) Long Short-Term Memory. Neural Comput 9:1735–1780.

Hoogenboom G, Justes E, Pradal C, Launay M, Asseng S, Ewert F, Martre P (2020) iCROPM 2020: Crop Modeling for the Future. J Agric Sci 158:791–793.

Huang J-H (2016) Accelerating the race to self-driving cars. CES, Las Vegas, p 10.

Huang Y, Chen Y (2020) Autonomous Driving with Deep Learning: A Survey of State-of-Art Technologies. arXiv Preprint arXiv:2006.06091.

IPCC (2021) Climate Change 2021: The Physical Science Basis. Contribution of Working Group I to the Sixth Assessment Report of the Intergovernmental Panel on Climate Change. Cambridge University Press, Cambridge, UK.

Janssen SJC, Porter CH, Moore AD, Athanasiadis IN, Foster I, Jones JW, Antle JM (2017) Towards a new generation of agricultural system data, models

and knowledge products: Information and communication technology. Agric Syst 155:200–212.

Jones JW, Antle JM, Basso B, Boote KJ, Conant RT, Foster I, Godfray HCJ, Herrero M, Howitt RE, Janssen S, et al. (2017) Brief history of agricultural systems modeling. Agric Syst 155:240–254.

Jones JW, Hoogenboom G, Porter CH, Boote KJ, Batchelor WD, Hunt LA, Wilkens PW, Singh U, Gijsman AJ, Ritchie JT (2003) The DSSAT cropping system model. Eur J Agron 18:235–265.

Kamilaris A, Kartakoullis A, Prenafeta-Boldú FX (2017) A review on the practice of big data analysis in agriculture. Comput Electron Agric 143:23–37.

Katzin D, van Henten EJ, van Mourik S (2022) Process-based greenhouse climate models: Genealogy, current status, and future directions. Agric Syst 198:103388.

Kiran BR, Sobh I, Talpaert V, Mannion P, Sallab AAA, Yogamani S, Pérez P (2021) Deep Reinforcement Learning for Autonomous Driving: A Survey. IEEE Trans Intell Transp Syst 1–18.

LeCun Y, Bengio Y, Hinton G (2015) Deep learning. Nature 521:436–444.

Lee H, Grosse R, Ranganath R, Ng AY (2009) Convolutional deep belief networks for scalable unsupervised learning of hierarchical representations. In: Proceedings of the 26th Annual International Conference on Machine Learning. Association for Computing Machinery, New York, USA, pp 609–

616

Li T, Hasegawa T, Yin X, Zhu Y, Boote K, Adam M, Bregaglio S, Buis S, Confalonieri R, Fumoto T, et al. (2015) Uncertainties in predicting rice yield by current crop models under a wide range of climatic conditions. Glob Change Biol 21:1328–1341.

Liu L, Ouyang W, Wang X, Fieguth P, Chen J, Liu X, Pietikäinen M (2020) Deep Learning for Generic Object Detection: A Survey. Int J Comput Vis 128:261–318.

Marcelis LFM, Heuvelink E, Goudriaan J (1998) Modelling biomass production and yield of horticultural crops: a review. Sci Hortic 74:83–111.

McCulloch WS, Pitts W (1943) A logical calculus of the ideas immanent in nervous activity. Mull Math Biol 5:115–133.

Mikolov T, Chen K, Corrado G, Dean J (2013) Efficient Estimation of Word Representations in Vector Space. arXiv Preprint arXiv:1301.3781

Misra NN, Dixit Y, Al-Mallahi A, Bhullar MS, Upadhyay R, Martynenko A (2020) IoT, big data and artificial intelligence in agriculture and food industry. IEEE Internet Things J 1–1.

Mnih V, Kavukcuoglu K, Silver D, Rusu AA, Veness J, Bellemare MG, Graves A, Riedmiller M, Fidjeland AK, Ostrovski G, et al. (2015) Human-level control through deep reinforcement learning. Nature 518:529–533.

Muller B, Martre P (2019) Plant and crop simulation models: powerful tools to link physiology, genetics, and phenomics. J Exp Bot 70:2339–2344.

Müller C, Franke J, Jägermeyr J, Ruane AC, Elliott J, Moyer E, Heinke J, Falloon PD, Folberth C, Francois L, et al. (2021) Exploring uncertainties in global crop yield projections in a large ensemble of crop models and CMIP5 and CMIP6 climate scenarios. Environ Res Lett 16:034040.

Otter DW, Medina JR, Kalita JK (2021) A Survey of the Usages of Deep Learning for Natural Language Processing. IEEE Trans Neural Netw Learn Syst 32:604–624.

Pan SJ, Yang Q (2010) A Survey on Transfer Learning. IEEE Trans Knowl Data Eng 22:1345–1359.

Pan Z, Yu W, Yi X, Khan A, Yuan F, Zheng Y (2019) Recent Progress on Generative Adversarial Networks (GANs): A Survey. IEEE Access 7:36322–36333.

Peng B, Guan K, Tang J, Ainsworth EA, Asseng S, Bernacchi CJ, Cooper M, Delucia EH, Elliott JW, Ewert F, et al. (2020) Towards a multiscale crop modelling framework for climate change adaptation assessment. Nat Plants 6:338–348.

Ramesh A, Pavlov M, Goh G, Gray S, Voss C, Radford A, Chen M, Sutskever I (2021) Zero-Shot Text-to-Image Generation. arXiv Preprint arXiv:2102.12092.

Roberts MJ, Braun NO, Sinclair TR, Lobell DB, Schlenker W (2017) Comparing and combining process-based crop models and statistical models with some implications for climate change. Environ Res Lett

12:095010.

Rong X (2016) word2vec Parameter Learning Explained. arXiv Preprint arXiv:1411.2738

Rosenblatt F (1958) The perceptron: A probabilistic model for information storage and organization in the brain. Psychol Rev 65:386–408.

Rötter R, Hoffmann M, Koch M, Müller C (2018) Progress in modelling agricultural impacts of and adaptations to climate change. Curr Opin Plant Biol 45:255–261.

Schierhorn F, Hofmann M, Gagalyuk T, Ostapchuk I, Müller D (2021) Machine learning reveals complex effects of climatic means and weather extremes on wheat yields during different plant developmental stages. Climatic Change 169:39.

Schrittwieser J, Antonoglou I, Hubert T, Simonyan K, Sifre L, Schmitt S, Guez A, Lockhart E, Hassabis D, Graepel T, et al. (2020) Mastering Atari, Go, chess and shogi by planning with a learned model. Nature 588:604–609.

Shi W-M, Yao J, Yan F (2009) Vegetable cultivation under greenhouse conditions leads to rapid accumulation of nutrients, acidification and salinity of soils and groundwater contamination in South-Eastern China. Nutr Cycl Agroecosyst 83:73–84.

Shinde PP, Shah S (2018) A Review of Machine Learning and Deep Learning Applications. In: 2018 Fourth International Conference on Computing Communication Control and Automation (ICCUBEA). pp 1–6.

Shu DW, Park SW, Kwon J (2019) 3D Point Cloud Generative Adversarial Network Based on Tree Structured Graph Convolutions. CVF, Seoul, Korea, pp 3859–3868.

Siegel C, Daily J, Vishnu A (2016) Adaptive neuron apoptosis for accelerating deep learning on large scale systems. In: 2016 IEEE International Conference on Big Data (Big Data). Washington D.C., USA, pp 753–762.

Silver D, Hubert T, Schrittwieser J, Antonoglou I, Lai M, Guez A, Lanctot M, Sifre L, Kumaran D, Graepel T, et al. (2018) A general reinforcement learning algorithm that masters chess, shogi, and Go through self-play. Science 362:1140–1144.

Singh G (2009) Salinity-related desertification and management strategies: Indian experience. Land Degrad Dev 20:367–385.

Steduto P, Hsiao TC, Raes D, Fereres E (2009) AquaCrop—The FAO crop model to simulate yield response to water: I. Concepts and underlying principles. Agron J 101:426–437.

Tan X, Qin T, Soong F, Liu T-Y (2021) A Survey on Neural Speech Synthesis. arXiv Preprint arXiv:2106.15561.

Thomas DSG, Middleton NJ (1993) Salinization: new perspectives on a major desertification issue. J Arid Environ 24:95–105.

UN (2019) World Population Prospects 2019: Highlights. United Nations, New York, USA.

van Beveren PJM, Bontsema J, van Straten G, van Henten EJ (2015) Optimal

control of greenhouse climate using minimal energy and grower defined bounds. Appl Energy 159:509–519.

Van Ploeg D, Heuvelink E (2005) Influence of sub-optimal temperature on tomato growth and yield: a review. J Hortic Sci Biotechnol 80:652–659.

van Straten G, Challa H, Buwalda F (2000) Towards user accepted optimal control of greenhouse climate. Computers and Electronics in Agriculture 26:221–238.

Vanthoor BHE, Stanghellini C, van Henten EJ, de Visser PHB (2011) A methodology for model-based greenhouse design: Part 1, a greenhouse climate model for a broad range of designs and climates. Biosyst Eng 110:363–377.

Vanthoor BHE, Stigter JD, van Henten EJ, Stanghellini C, de Visser PHB, Hemming S (2012) A methodology for model-based greenhouse design: Part 5, greenhouse design optimisation for southern-Spanish and Dutch conditions. Biosyst Eng 111:350–368.

Vos J, Evers JB, Buck-Sorlin GH, Andrieu B, Chelle M, de Visser PHB (2010) Functional–structural plant modelling: a new versatile tool in crop science. J Exp Bot 61:2101–2115.

Wang A, Zhang W, Wei X (2019a) A review on weed detection using ground-based machine vision and image processing techniques. Comput Electron Agric 158:226–240.

Wang E, Brown HE, Rebetzke GJ, Zhao Z, Zheng B, Chapman SC (2019b)

Improving process-based crop models to better capture genotype×environment×management interactions. J Exp Bot 70:2389–2401.

Wang E, Martre P, Zhao Z, Ewert F, Maiorano A, Rötter RP, Kimball BA, Ottman MJ, Wall GW, White JW, et al. (2017) The uncertainty of crop yield projections is reduced by improved temperature response functions. Nat Plants 3:1–13.

Wang Z, She Q, Ward TE (2021) Generative Adversarial Networks in Computer Vision: A Survey and Taxonomy. ACM Comput Surv 54:37:1-37:38.

Weiss K, Khoshgoftaar TM, Wang D (2016) A survey of transfer learning. J Big Data 3:9.

Wolfert S, Ge L, Verdouw C, Bogaardt M-J (2017) Big Data in Smart Farming – A review. Agric Syst 153:69–80.

Yoon J, Jordon J, Schaar M (2018) GAIN: Missing Data Imputation using Generative Adversarial Nets. In: Proceedings of the 35th International Conference on Machine Learning. PMLR, Stockholm, Sweden, pp 5689–5698.

Zhuang F, Qi Z, Duan K, Xi D, Zhu Y, Zhu H, Xiong H, He Q (2020) A Comprehensive Survey on Transfer Learning. arXiv Preprint arXiv:1911.02685.

CHAPTER 1

Infrastructure for applying deep learning algorithms to crop modeling

Chapter 1-1

Knowledge transfer for adapting deep neural models to different greenhouses with a low quantity of data

Chapter 1-2

Two-dimensional convolutional neural networks for imputation of missing greenhouse environment data

CHAPTER 1-1

Knowledge transfer for adapting deep neural models to a different greenhouse with a low quantity of data

ABSTRACT

Deep learning is a state-of-the-art application in many fields, and this methodology has also been applied in agriculture. Deep learning algorithms require a large quantity of data in the model training; however, sufficient data may not be provided when considering agriculture applications. Transfer learning, a learning strategy for rapid and easy adaptation of a pre-trained model, can be a solution for limited agricultural data. The objective of this study was to verify the adaptability of a pre-trained model that predicts the greenhouse environment factors. The pre-trained models were retrained with data from new cultivation conditions, using transfer learning. Five greenhouse environment factors from twenty-seven greenhouses (14 sweet peppers and 13 tomato cultivations) in various regions of South Korea were predicted. Before the transfer learning procedure, some layers from pre-trained models were replaced with new layers; then, the models were retrained with unseen test dataset. The best model showed the highest training accuracy (R^2=0.69) was BiLSTM. BiLSTM also adequately predicted the transfer dataset showing the highest

accuracy of an average R^2 of 0.78 and 0.81 for sweet pepper and tomato datasets, respectively. The accuracies of most transferred models are higher than those of the corresponding deep learning models. Therefore, transfer learning can be used to predict the microclimates of a greenhouse with scarce data adapting previously trained deep learning models. Furthermore, the models can be adapted to heterogeneous tasks based on the high applicability and adaptability of deep learning algorithms.

Additional keywords: long short-term memory, machine learning, multilayer perceptron, sweet pepper, tomato

*Chapter 1-1 was previously published by Computers and Electronics in Agriculture [Moon T, Son JE (2021) Knowledge transfer for adapting pre-trained deep neural models to predict different greenhouse environments based on a low quantity of data. Comput Electron Agric 185:106136].

INTRODUCTION

The data amount is increasing in agriculture, and methodologies for data analyses are diversifying (Muangprathub et al. 2019; Sarker et al. 2019). Wireless networks with IoT applications are the main cause of increasing data accumulation (Kochhar and Kumar, 2019). Novel data types, such as hyperspectral imaging, have also been utilized in previous research for yield prediction (Hassanzadeh et al. 2020). Collecting and monitoring multidimensional data have continuously been studied due to the improvements in sensors and computers (Wolfert et al. 2017; Khanna and Kaur 2019). Many methodologies have been adapted in agriculture with an expectation to understand phenomena from accumulated and new data.

As deep learning represents state-of-the-art performances in many areas, it has also been applied to solve problems in agriculture, such as fruit segmentation, autonomous greenhouse control, and crop environment estimation (Barth et al. 2019; Hemming et al. 2019; Moon et al. 2019a). Deep learning became prevalent because of its adaptability for diverse tasks; a same deep learning model can be retrained with different input and output without domain knowledge.

However, the data amount of agriculture could be insufficient for deep learning. Greenhouses generally have high temperature and humidity, and sensors are vulnerable to these conditions resulting in data loss (Moon et al.

2019b). The limited number of crops could also restrict the sufficient data collection (Lee et al. 2020). Moreover, differences in crop environment and growth due to target species, season, and cultivation strategy lead to the requirement of more diversified data (Jones et al. 1991; Van Henten and Van Straten 1994; Wubs et al. 2012). Collecting sufficient data for deep learning is a difficult task in agriculture. Deep learning models could not show the state-of-the-art performances like other fields, resulting in fragmented studies of the applications (Kamilaris and Prenafeta-Boldú 2018).

Therefore, the adaptability of the deep learning models for the distinctive agricultural conditions are verified. Transfer learning, one of the machine learning studies, may be a means to identify the performance, as it can be applied to limited available data. In machine learning, In the transfer learning methodology, the knowledge derived from data can be transferred from some previous tasks (Pan and Yang 2009).

As a result, pre-trained models have been actively adopted, by varying the structure of the network, and, afterward, retrained with a new dataset (Shin et al. 2016; Gómez-Valverde et al. 2019; Thenmozhi and Reddy 2019). Moreover, this methodology has improved the performance of the model (Devlin et al. 2018). Therefore, the deep learning model can perform better if the pre-trained models can be adapted to a new cultivation condition.

In this regard, greenhouse environment data can be utilized for transfer learning of deep learning models. The environment data relatively abundant

and diverse. In addition, the environment is worth to predict for greenhouses studies. Active control of the internal environment improves crop quality and yield when analyzing phenomena in greenhouses. The active control of the environment surmounts the regional limitations of plant growth (Sethi et al. 2013; Shamshiri and Ismail, 2013). As a result, optimal control of the internal environment is considered an important goal regarding greenhouse cultivation. Therefore, the target task for deep learning models was set to predict greenhouse environment. This chapter aimed to verify the adaptability of a pre-trained model of a greenhouse environment by retraining it using transfer learning with a new cultivation condition.

MATERIALS AND METHODS

Deep learning models

The transfer learning methodology was applied in this work based on five common deep learning models, as indicated in Fig. 1-1-1: Feedforward neural network (FFNN), long short-term memory (LSTM), bidirectional long short-term memory (BiLSTM), and LSTMs with autoencoder (AE-LSTM and AE-BiLSTM). FFNN is a basic neural network architecture that is the core structure of deep learning algorithms (Schmidhuber 2015). LSTM is commonly used to analyze sequence data (Hochreiter and Schmidhuber 1997). Meanwhile, BiLSTM is a countermeasure model applied when the LSTM outputs are highly influenced by a backward context (Graves et al. 2005). Autoencoder (AE) is an algorithm that can reduce the dimension of the data (Wang et al. 2014). AEs have the same input and output with a narrow hidden layer in the middle of the architecture. Meaningful information could be encoded in the middle layer, so the other models can be easily trained with the encoded vector. AEs were coupled with the LSTM (AE-LSTM) and BILSTM (AE-BiLSTM), as this combination has generated models with higher performance in comparison with the original version (Fan et al. 2018; Mirsky et al. 2018). In this case, the LSTM and BiLSTM predicted the encoded values of the five environment factors, and AEs encoded and decoded the five factors.

The architectures of the models differed in evaluating the influence of the

depth of the model on transfer learning, as shown in Table 1-1-1. The nodes in the layer represent the number of neurons in the layer. Encoders and decoders had the same structures as the first four and the last three layers of the AE, respectively. Layer normalization is a normalizing method for the stability of neural networks (Ba et al. 2016). The extracted features were supposed to be located in the middle of the hidden layer, so the first and the last layers were replaced and retrained.

In contrast, the batch size (32) and learning rate (0.001) were the same in all experiments. Furthermore, the mean square error (MSE) was set as the variable to be optimized by the models. All deep learning models were requested to predict the behavior of five environmental factors in the next 24 h based on the data collected from the previous 24 h. This task was a kind of regression procedure, so the training results were compared considering the R^2 and root mean square error (RMSE) as a performance indicator and the model accuracy, and the TensorFlow (v. 2.0) software was used to build the model (Abadi et al. 2016).

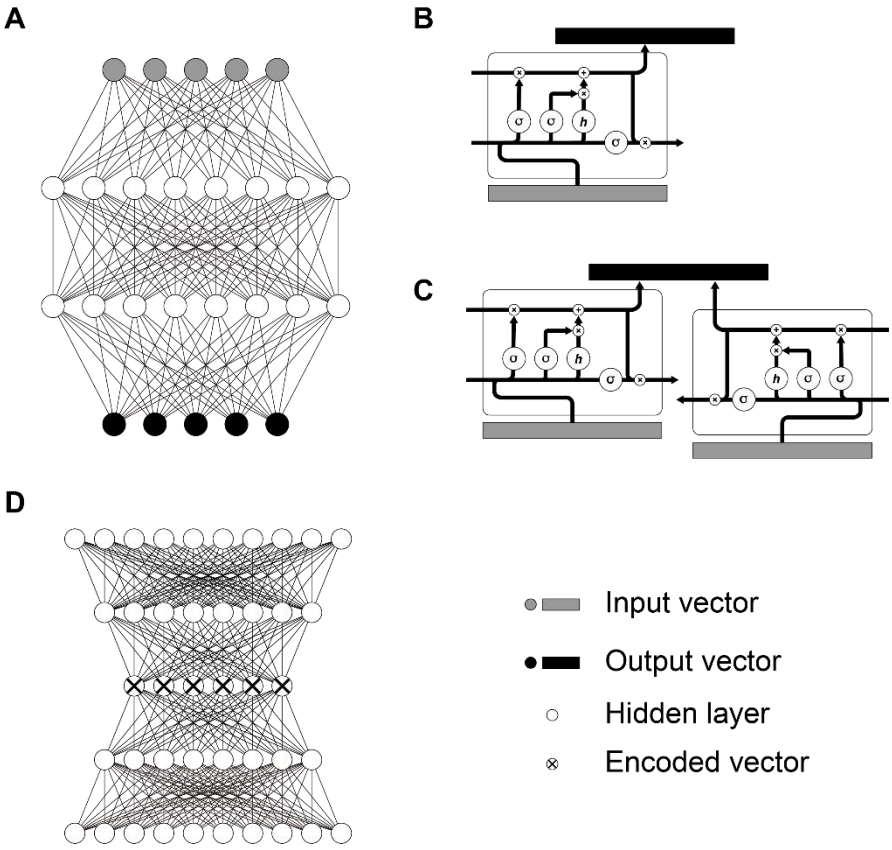

Fig. 1-1-1. Deep learning models used in this study: feedforward neural network (A), long short-term memory (B), bidirectional long short-term memory (C), and autoencoder (D). The encoded vector from the autoencoder was used as inputs and outputs of combined long short-term memory. All common forms of the models were coupled with batch or layer normalization for impartial comparisons.

Table 1-1-1. Model architectures. The layers were represented as the 'type of layer'-'number of nodes in the layer' ('number of parameters'). A dense layer represents the basic-form of a fully-connected layer, and LayerNorm indicates layer normalization. FFNN, LSTM, BiLSTM, and AE mean feedforward neural network, long short-term memory, bidirectional long short-term memory, and autoencoder, respectively.

FFNN	LSTM	BiLSTM	AE-LSTM	AE-BiLSTM	AE[z]
Dense-256[y] (1,536)	LSTM-256 (268,288)	BiLSTM-128 (35,840)	Encoder (1,912)	Encoder (1,912)	Dense-32[y] (192)
LayerNorm	LayerNorm	LayerNorm	LSTM-256 (271,360)	BiLSTM-256 (140,288)	Dense-32 (1,056)
Dense-256 (65,792)	Dense-5[y] (1,285)	BiLSTM-128 (98,816)	LayerNorm	LayerNorm	Dense-16 (528)
LayerNorm		LayerNorm	Dense-8 (2,056)	BiLSTM-256 (394,240)	Dense-8 (136)
Dense-5[y] (1,285)		Dense-5[y] (645)	Decoder (853)	LayerNorm	Dense-16 (144)
				Dense-8 (2,056)	Dense-32 (544)
				Decoder (853)	Dense-5[y] (165)

[z]Encoded values were used for the input of AE-LSTM and AE-BiLSTM.

[y]These layers were replaced and retrained for transfer learning.

Experimental greenhouse environment data

The data collected from greenhouses, where sweet peppers (*Capsicum annuum* L.) and tomatoes (*Solanum lycopersicum* L.) were cultivated, in various regions of South Korea, were used as the experimental dataset. The covering materials were arch-type plastic or glasses. The minimum and maximum sizes of the greenhouses where sweet peppers were cultivated were 7 W × 80 L × 5 H (m) and 100 W × 110 L × 5.7 H (m), respectively, while those of the greenhouses where tomatoes were cultivated were 7 W × 53 L × 3 H (m) and 66 W × 100 L × 4.5 H (m), respectively.

As the growth strategies used for the cultivation were diverse, the microclimates and the cultivation periods also varied (Figs. 1-1-2, 1-1-3). The dataset was divided into two groups that were used in the training procedure and transfer learning tests, respectively. The deep learning models could be transferred for different crops, but greenhouses with the same crop can have distinct microclimates because of the management. Therefore, transfer learning was supposed for two cases: transferring models for similar and different conditions. The condition was set by cultivated crop. Therefore, the deep learning models were trained and validated only using the data collected from 10 selected sweet pepper cultivations. The remaining data, collected from four sweet pepper greenhouses and 13 tomato greenhouses, were used in the transfer learning tests.

The data were collected from Jan 1st, 2017 to May 4th, 2019, at intervals

of 1 h using complex sensors (GreenCS, Daejeon, Korea; Shinhan A-Tec Co., Ltd., Changwon, Korea). The total days of the dataset were 9,054. The days of datasets for model training (10 sweet pepper greenhouses) were 2,461. The days of datasets for transfer learning from four sweet pepper greenhouses and 13 tomato greenhouses were 1,344 and 5,249, respectively. The monthly solar radiation and external temperature values showed a similar tendency in this period (Fig. 1-1-3).

The target environmental variables were internal temperature, internal relative humidity, internal CO_2 concentration, external temperature, and radiation (Fig. 1-1-4). The range of each variable is shown in Table 1-1-2. These data were randomly separated into training and validation datasets, which did not overlap, at ratios of 7:3 and 2:8 for the model training and transfer learning tests, respectively. This ratio was deliberately reduced in the transfer learning test when compared to the model training procedure to simulate the short quantity of data commonly collected from greenhouses. Therefore, the number of training data for transfer learning tests was approximately 269 d for sweet pepper greenhouses and 1,050 d for tomato greenhouses, which were 20% of the whole data.

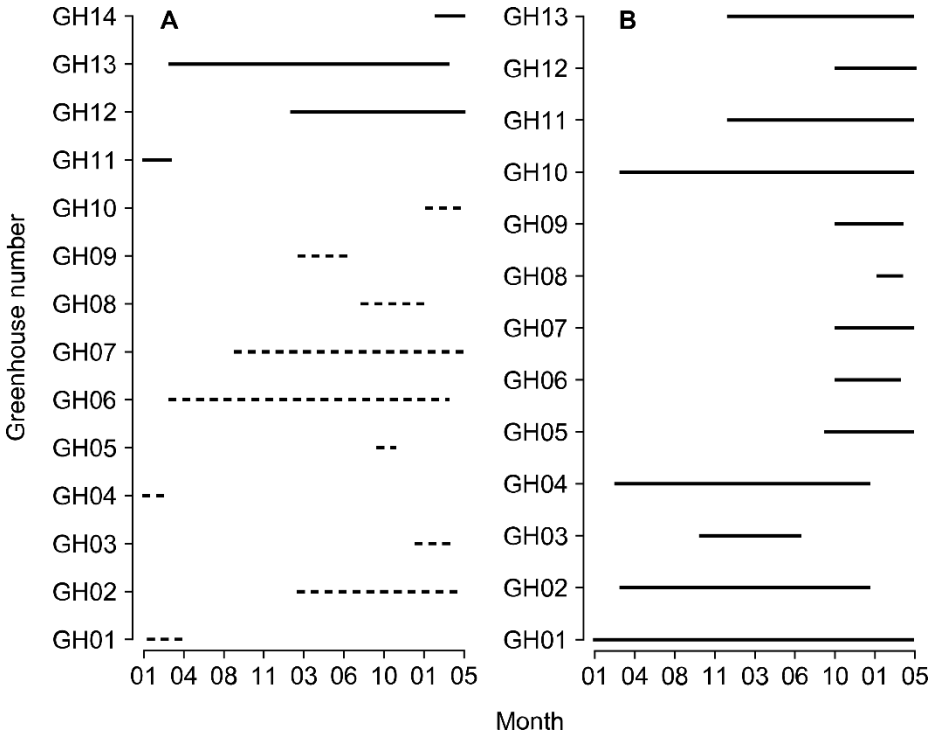

Fig. 1-1-2. Cultivation periods of sweet pepper (A) and tomato (B) based on the data collected from the corresponding greenhouses. The broken and solid lines represent the data used in the training and transfer learning tests, respectively.

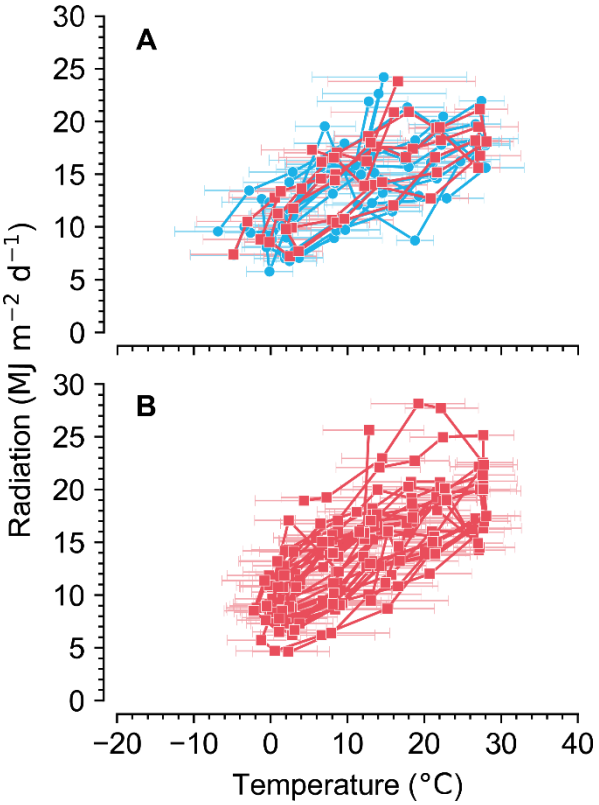

Fig. 1-1-3. Daily radiation based on average, minimum, and maximum daily temperatures (°C) per month for 14 sweet pepper (A) and 13 tomato (B) greenhouses. The blue and red solid lines represent the data used in the training and transfer learning tests, respectively.

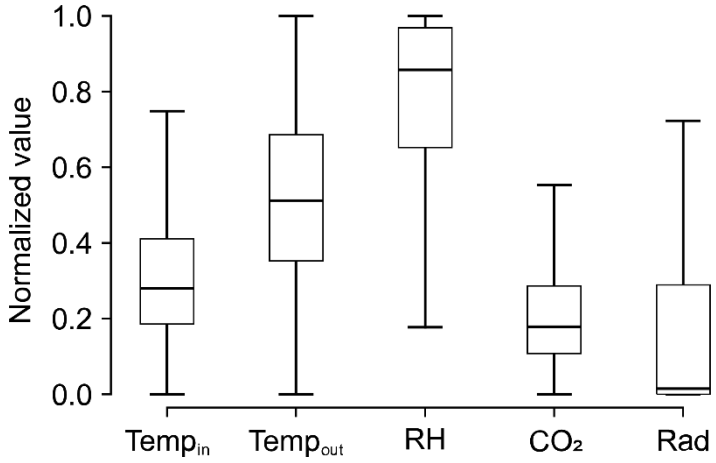

Fig. 1-1-4. Box plot of five environmental variables. The whole data were normalized in a range from 0 to 1. The outliers were not represented.

Table 1-1-2. Range of input data.

Input data (unit)	Range
Inside temperature (°C)	5.32-54.88
Inside relative humidity (%)	19.38-100.00
Inside CO_2 concentration (μmol mol^{-1})	101.67-2999.00
Outside temperature (°C)	−21.18-37.35
Radiation (W m^{-2})	0.00-1027.70

Transfer learning

In the transfer learning tests, some layers of the pre-trained models were replaced, depending on the similarity between the trained and transferred objectives, with new layers, which were retrained considering the test dataset (Tan et al. 2018). However, as the input and output of the dataset for transfer learning test were similar, one or two layers were replaced to use most parts of the trained models (Table 1-1-1). The trained layers and the new layers can be trained at the same time, but a sufficient number of datasets are required to compare to the original datasets. In this study, it was supposed that the models have to be retrained with small agricultural data. The weights of the trained layers were locked and the weights of the new layers were trained when transfer learning was conducted with the small datasets. Therefore, only the new layers were retrained for transfer learning in this study. R^2 and RMSE were also used to evaluate the accuracy of the transferred models. The transferred models were compared with pre-trained models, which were trained with previous data and were not used in the transfer learning, and raw-trained models, which were only trained with new datasets.

RESULTS

Accuracies of the deep learning models

Five models showed adequate test accuracies after the model training procedure; however, their performances varied for each target factor (Fig. 1-1-5). The model with the highest accuracy was BiLSTM, with an average R^2 of 0.69. The accuracy of each environmental variable was different based on the model. Furthermore, the highest and lowest accuracies for each model were always attributed to the external temperature and CO_2 concentration, respectively. The increased complexity of the models, particularly when evaluating the AE-BiLSTM model, which was the most complex model based on its architecture, did not contribute to the accuracy.

After the model training, for the situations in which the lowest RMSE values were obtained, some models generated highly accurate results when predicting the behavior of environmental variables in the future 24 h (Fig. 1-1-6). Furthermore, when comparing these models, relatively low accuracies were obtained from models coupled with AE in external temperature and relative humidity, even in the best cases. In contrast, the output had a similar timestamp for situations where the highest RMSE values were obtained. Each predicted variable was underestimated for these models, except the internal temperature estimated by AE-BiLSTM. However, all models grasped the tendencies of each environmental variable.

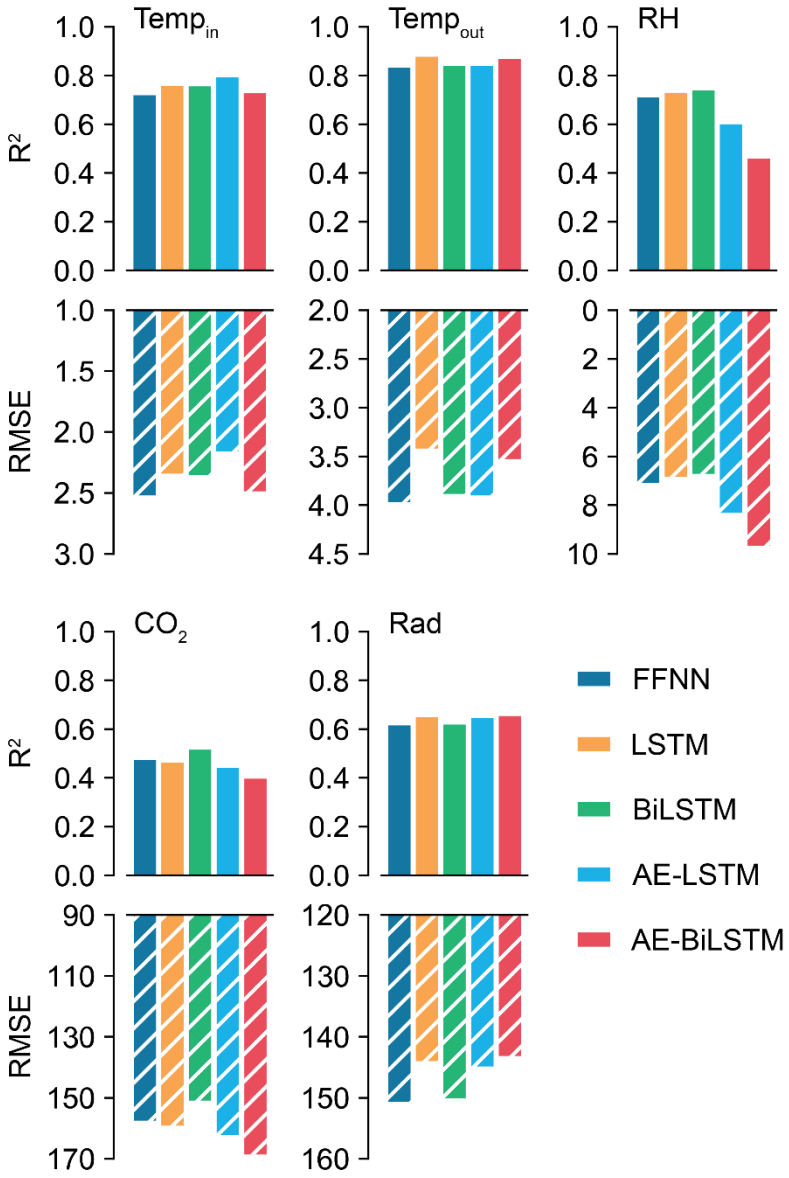

Fig. 1-1-5. R^2 and RMSE of the trained models used to predict the behavior of environmental variables of 10 sweet pepper cultivations.

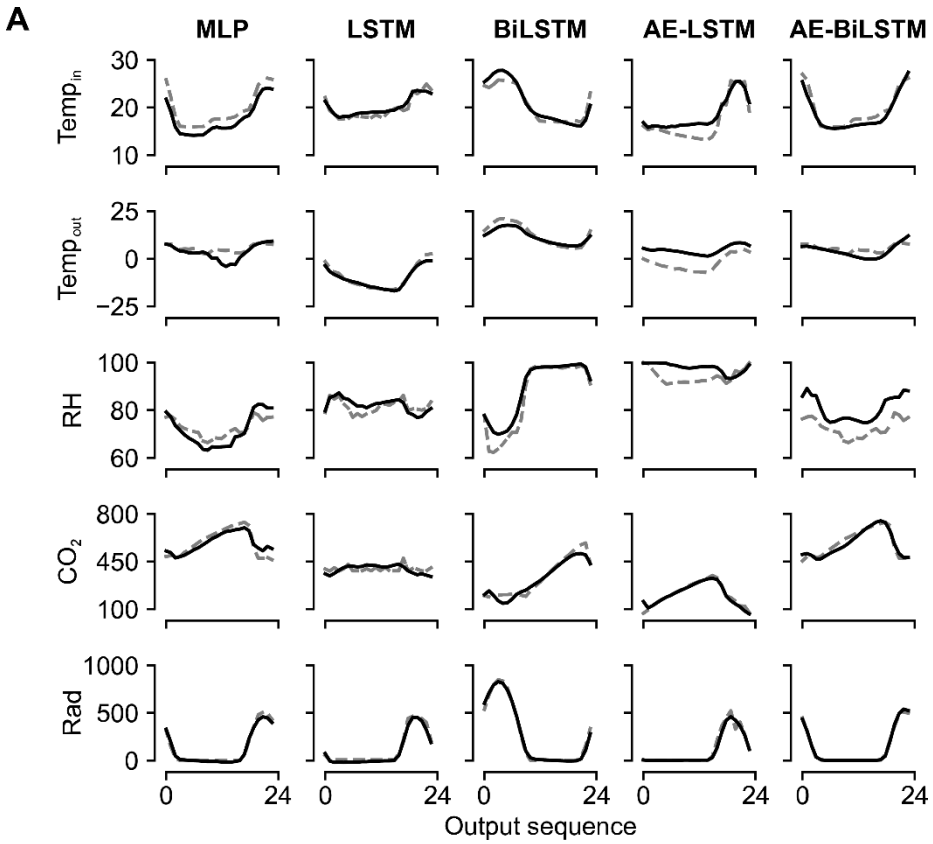

Fig. 1-1-6. Comparison models with lowest (A) and highest (B) RMSE values in the model training procedure. $Temp_{in}$, $Temp_{out}$, RH, CO_2, and Rad represent internal temperature, external temperature, relative humidity, internal CO_2 concentration, and radiation, respectively. The solid black line represents the measured values.

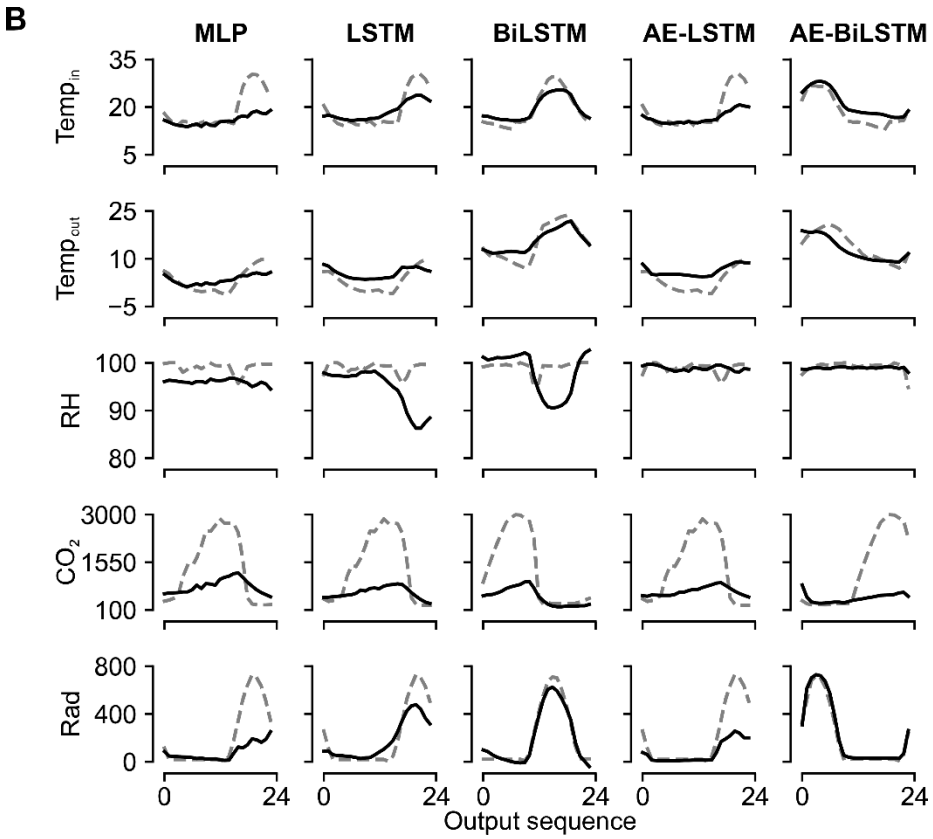

Fig. 1-1-6. (Continued from the previous page)

Performance of the transfer learning methodology

Regarding the models that used the transferred dataset, the most accurate deep-learning model was the transferred BiLSTM, with an average R^2 of 0.78 and 0.81, followed by the transferred LSTM, with an average R^2 of 0.76 and 0.79, when considering the environmental variables of sweet pepper and tomato greenhouses, respectively (Fig. 1-1-7). Among the trained FFNNs, the transferred FFNN was not the model that generated the most accurate results (raw-trained FFNN), as its average R^2 was 0.72; however, its accuracy was satisfactory. The accuracies of the transferred models were largely higher than those of the pre-trained and raw-trained models, except those of FFNN and AE-BiLSTM. In particular, the trained AE-LSTMs and AE-BiLSTMs could not predict the dataset used in the transfer test corresponding to sweet peppers. In addition, an accuracy lower than those obtained from other trained models was achieved; therefore, the increase in the model complexity due to AE did not improve the performance of the corresponding model in this case. Furthermore, higher accuracies were obtained from the models trained with the data collected from tomatoes than those trained with the data collected from sweet peppers, despite the low training/test ratio.

For each environmental variable, the prediction accuracy of the CO_2 concentration and relative humidity were the lowest, considering the sweet pepper and tomato greenhouses, respectively (Fig. 1-1-8). The AE coupled with pre-trained models did not effective the accuracy when the models predicted the transfer dataset. In contrast, the accuracy of the FFNN was similar to those

of the other models. In some cases, the raw-trained FFNN was relatively highly accurate, although the training data of the transfer dataset were scarce. However, most transferred models were highly accurate.

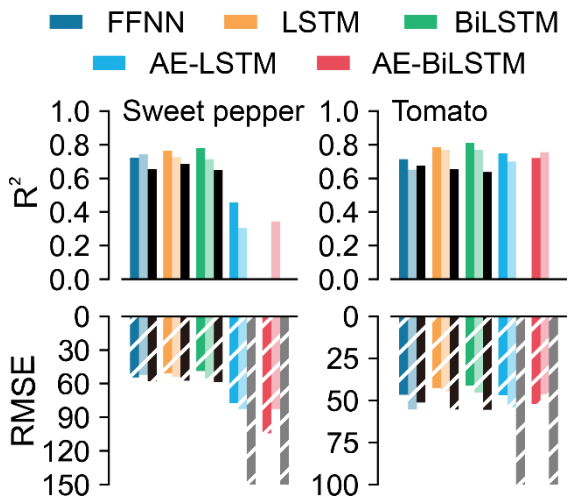

Fig. 1-1-7. Average test R^2 and RMSE of the models in which the transfer methodology was applied. Results obtained from predicting the environmental variables of four sweet pepper (A) and 13 tomato (B) greenhouses. R^2 and RMSEs were averaged by each model output. Pap and Tom represent sweet peppers and tomatoes, respectively. Black bars represent the R^2 and RMSEs of the raw-trained model, in which only a transfer test dataset was used. Light-color bars represent pre-trained models trained with the previously used dataset. Gray bars represent RMSE exceeding the axis scale. Negative R^2s were not depicted in the graph for the legibility.

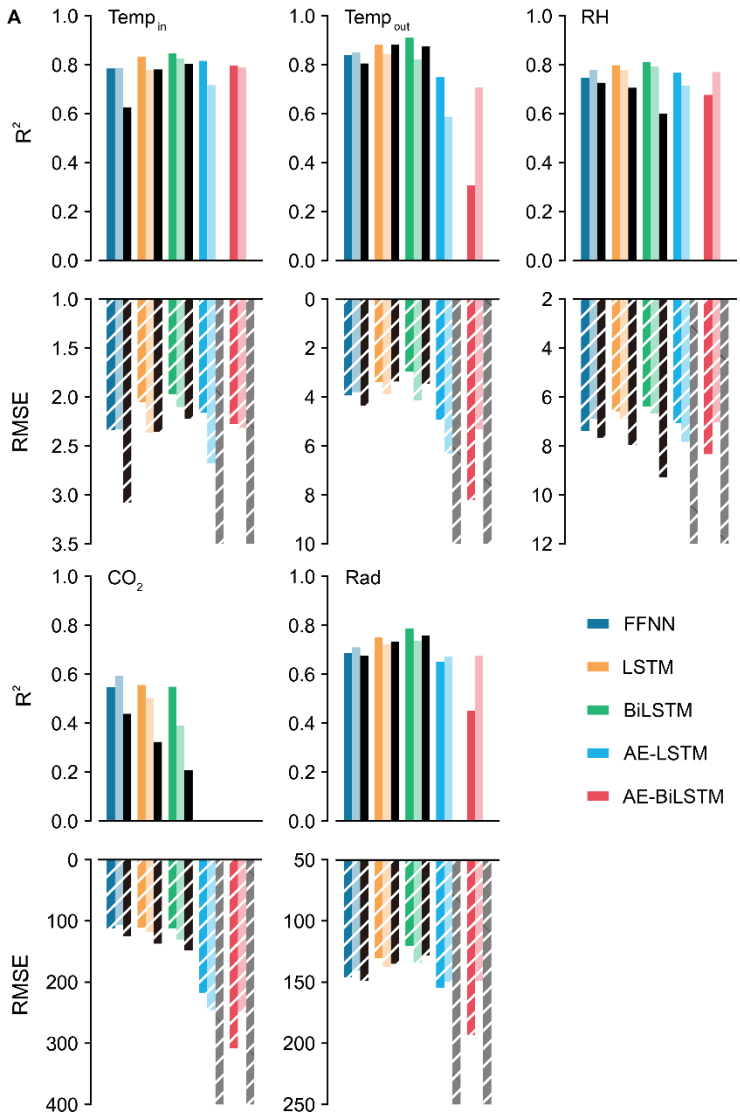

Fig. 1-1-8. Test R^2 and RMSE of the transfer models, considering the dataset of four sweet pepper (A) and 13 tomato (B) greenhouses. The black bars represent the R^2 and RMSEs of the raw-trained models, while Light-color bars represent pre-trained models. Gray bars represent RMSE exceeding the axis scale. Negative R^2s were not depicted in the graph.

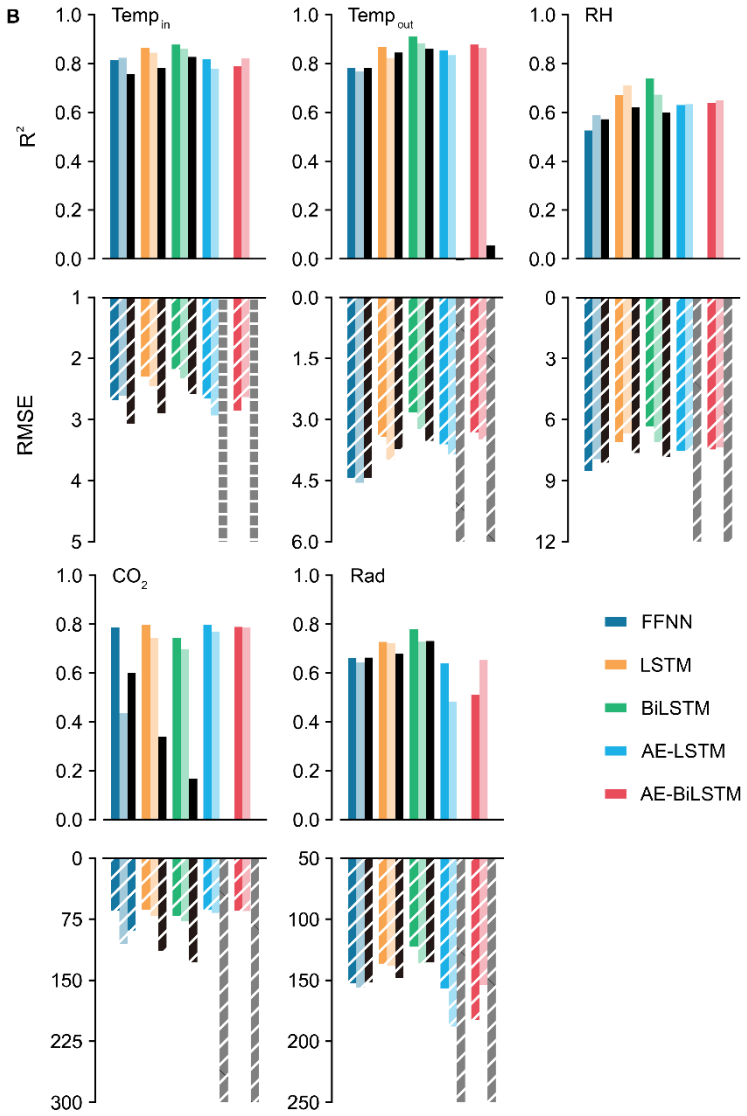

Fig. 1-1-8. (Continued from the previous page)

DISCUSSION

The accuracies obtained from the deep-learning models were relatively low, although the models generated by some methodologies resulted in highly accurate results in comparison with those obtained from canonical methods (Zhou et al. 2016; Fischer and Krauss 2018; Khan and Yairi 2018). The CO_2 concentrations influenced the accuracy of the predictions, resulting in a low average R^2 (Fig. 1-1-5). As a high CO_2 concentration can enhance crop production, most sweet pepper greenhouses adopted CO_2 fertilization (Del Amor 2007; Serret et al. 2018). As a result, the measured CO_2 concentration exceeded the concentration during daytime (approximately 400 μmol mol^{-1}), as shown in Table 1-1-2. This fertilization strategy could also vary for each greenhouse; therefore, the predictions of CO_2 concentrations were affected, as the data were collected from several greenhouses with different control strategies. Furthermore, the greenhouse microclimate may differ based on the implemented strategies to adapt to the weather, even though the same crop is cultivated (Villarreal-Guerrero et al. 2012; Choi et al. 2019). Since the data were gathered from several greenhouses having different control strategies, the CO_2 fertilization could be hard to predict. However, the models predicted the tendencies of the environmental variables, indicating that they were adequately trained, and their performance during the transfer learning process could be

evaluated.

Furthermore, the difference in the accuracies of the results generated based on the data from sweet pepper and tomato cultivations in transfer learning was due to the accuracy of CO_2 concentration (Fig. 1-1-7). For models with the lowest accuracy, the CO_2 concentrations were underestimated (Fig. 1-1-6). Although the accuracies obtained from the transferred models were the highest, the predictions of relative humidity in tomato greenhouses were relatively discrepant from the other predictions (Fig. 1-1-8). Nederhoff et al. (1992) reported the different tendencies in transpiration between tomatoes and sweet peppers, which induced the different relative humidities when comparing this cultivation (Jolliet 1994). Furthermore, the ventilation strategy adopted by the greenhouse was different for each crop (Boulard et al. 2004). As a result, universal control parameters are required to increase the accuracy of microclimate prediction, enabling an integrated multi-crop prediction.

The application of the transfer learning methodology was successful, as the accuracies of most transferred models were the highest among those obtained from different training methods (Fig. 1-1-7). Only the most common form of transfer learning was conducted in this study. As a result, the application of advanced variations of transfer learning, which have already been studied, would increase the adaptability of the model and, therefore its accuracy (Pan and Yang 2009; Zhang et al. 2019).

Coarse fitting may also influence the high deviations of the environmental

variables (Fig. 1-1-4). In this study, a parameter fitting commonly used was conducted, as the objective of this research was to compare different deep-learning models. Comprehensive search or hard fitting of these parameters could improve the accuracies due to overfitting; however, the overfitting could reduce the generalization of the models, harming the impartial comparison between them. Most trained models resulted in adequate accuracies, indicating that they could be equally compared.

Among the analyzed deep-learning models, the results obtained by BiLSTM were the most accurate, considering the training and transfer datasets. Furthermore, this model had a suitable architectural complexity. The trained LSTM also generated results with relatively high accuracies; however, more parameters were used than in BiLSTM (Table 1-1-1).

In some transfer tests, the raw-trained FFNN was the most accurate, despite the scarcity of the data used to train the models (Fig. 1-1-8). In fact, a form of attention is being developed that eliminates recurrent structures for easy parallelization (Vaswani et al. 2017; Lan et al. 2019). Predicting the environment is relatively simple, so extensive data and complex models are not required for predicting a stable environment. Therefore, in some scenarios, minimized models do not demand a high computation cost, enabling in-field applications of deep-learning models without a cloud service or a high-performance workstation. However, a complex model is required for long prediction periods or if more variables, such as control factors, must be

predicted (Jung et al. 2020).

The most complex model, AE-BiLSTM, was not the most accurate among all the experiments conducted in this research (Fig. 1-1-5), probably owing to the low complexity of data used in this study. AEs compress and restore their input as an abstractor (Baldi 2012). When an AE is coupled with a predictor, it reduces the data dimension, supporting the improvement of the predictor. The AE module could generate benefits for situations in which complex data are used, such as natural language processing (Li et al. 2015). However, in this research, the input and output dimensions were five, which may not be sufficient to improve the predictor. In addition, the raw-trained models with AEs could not predict the environments in transfer tests. It could represent that the AEs were overfitted to the original data, and the overfitting could not be resolved by replacing some layers. However, AEs could be helpful for complicated tasks, so AE complex models should be tested when the data with more input and output features are learned.

The instability in the accuracy of transferred models could be caused by the optimized parameters of the training dataset composed of data from the cultivation of sweet pepper. This complex and large model is not necessary for a simple task, such as aerial environmental prediction, but will be helpful if both the control and growth factors are considered.

CONCLUSION

To improve the adaptability of deep-learning models using the transfer learning technique, deep-learning models were trained and transferred using sweet pepper and tomato datasets obtained from 14 sweet pepper and 13 tomato greenhouses. The objective of this study was to analyze and predict the aerial environment of greenhouses. As a result, BiLSTM was the most accurate model, resulting in an R^2 of 0.69 for the training dataset, 0.78 considering the data collected from sweet peppers in transfer learning and 0.81 considering the data collected from tomatoes in transfer learning. As a basic fitting strategy was conducted, the accuracy obtained from the models was relatively low; however, the trained models could be compared to the transfer learning methodology because the overfitting was deliberately avoided. The accuracies of most transferred models were higher than those of the corresponding methods with different training strategies. As a result, transfer learning can be used to adapt trained deep learning models to predict the greenhouse microclimate with scarce data; it was verified that the deep learning models have high adaptability and applicability to the agricultural data.

LITERATURE CITED

Abadi M, Agarwal A, Barham P, Brevdo E, Chen Z, Citro C, Corrado GS, Davis A, Dean J, Devin M, et al. (2016) Tensorflow: Large-scale machine learning on heterogeneous distributed systems. arXiv preprint arXiv:1603.04467.

van Beveren PJM, Bontsema J, Van Straten G, Van Henten EJ (2015) Optimal control of greenhouse climate using minimal energy and grower defined bounds. Appl Energy 159:509-519.

Ba JL, Kiros JR, Hinton GE (2016) Layer normalization. arXiv Preprint arXiv:1607.06450.

Baldi P (2012) Autoencoders, unsupervised learning, and deep architectures. In: Proceedings of International Conference on Machine Learning (ICML), Scotland: Edinburgh, pp. 37-49.

Barth R, IJsselmuiden J, Hemming J, Van Henten EJ (2019) Synthetic bootstrapping of convolutional neural networks for semantic plant part segmentation. Comput Eelctron Agric 161:291-304.

Boulard T, Fatnassi H, Roy JC, Lagier J, Fargues J, Smits N, Rougier M, Jeannequin B (2004) Effect of greenhouse ventilation on humidity of inside air and in leaf boundary-layer. Agric Forest Meteorol 125:225-239.

Choi H, Moon T, Jung DH, Son JE (2019) Prediction of air temperature and relative humidity in greenhouse via a multilayer perceptron using environmental factors. Prot Hortic Plant Fact 28:95-103.

Del Amor FM (2007) Yield and fruit quality response of sweet pepper to organic and mineral fertilization. Renew Agric Food Syst 22:233-238.

Devlin J, Chang MW, Lee K, Toutanova K (2018) BERT: Pre-training of deep bidirectional Transformers for language understanding. arXiv Preprint arXiv:1810.04805.

Fan C, Xiao F, Zhao Y, Wang J (2018) Analytical investigation of autoencoder-based methods for unsupervised anomaly detection in building energy data. Applied Energy 211:1123-1135.

Fischer T, Krauss C (2018) Deep learning with long short-term memory networks for financial market predictions. Eur J Oper Res 270:654-669.

Gómez-Valverde JJ, Antón A, Fatti G, Liefers B, Herranz A, Santos A, Sánchez CI, Ledesma-Carbayo MJ (2019) Automatic glaucoma classification using color fundus images based on convolutional neural networks and transfer learning. Biomed Opt Express 10:892-913.

Graves A, Fernández S, Schmidhuber J (2005) Bidirectional LSTM networks for improved phoneme classification and recognition. In: International Conference on Artificial Neural Networks (ICANN), Poland: Warsaw. pp. 799-804.

Hassanzadeh A, Van Aardt J, Murphy SP, Pethybridge SJ (2020) Yield modeling of snap bean based on hyperspectral sensing: a greenhouse study. J. Appl. Remote. Sens. 14, 024519.

Hemming S, De Zwart F, Elings A, Righini I, Petropoulou A (2019) Remote

control of greenhouse vegetable production with artificial intelligence—greenhouse climate, irrigation, and crop production. Sensors 19:1807.

van Henten EJ, Van Straten G (1994) Sensitivity analysis of a dynamic growth model of lettuce. J Agr Eng Res 59:19-31.

Hochreiter S, Schmidhuber J (1997) Long short-term memory. Neural Computation 9:1735-1780.

Jolliet O (1994) HORTITRANS, a model for predicting and optimizing humidity and transpiration in greenhouses. J Agric Eng Res 57:23-37.

Jones JW, Dayan E, Allen LH, Van Keulen H, Challa H (19910 A dynamic tomato growth and yield model (TOMGRO). Trans ASAE 34:663-0672.

Jung DH, Kim HS, Jhin C, Kim HJ, Park SH (2020) Time-serial analysis of deep neural network models for prediction of climatic conditions inside a greenhouse. Comput Electron Agric 173:105402.

Kamilaris A, Prenafeta-Boldú FX (2018) Deep learning in agriculture: A survey. Comput Electron Agric 147:70-90.

Khan S, Yairi T (2018) A review on the application of deep learning in system health management. Mech Syst Signal Process 107:241-265.

Khanna A, Kaur S (2019) Evolution of Internet of Things (IoT) and its significant impact in the field of Precision Agriculture. Comput Electron Agric 157:218-231.

Kochhar A, Kumar N (2019) Wireless sensor networks for greenhouses: An end-to-end review. Comput Electron Agric 163:104877.

Lan Z, Chen M, Goodman S, Gimpel K, Sharma P, Soricut R (2019) ALBERT: A lite BERT for self-supervised learning of language representations. arXiv preprint arXiv:1909.11942

Lee JW, Kang WH, Moon T, Hwang I, Kim D, Son JE (2020) Estimating the leaf area index of bell peppers according to growth stage using ray-tracing simulation and a long short-term memory algorithm. Hortic Environ Biotechnol 61:255-265.

Li J, Luong MT, Jurafsky D (2015) A hierarchical neural autoencoder for paragraphs and documents. arXiv preprint arXiv:1506.01057.

Pan SJ, Yang Q (2009) A survey on transfer learning. IEEE Trans Knowl Data Eng 22:1345-1359.

Mirsky Y, Doitshman T, Elovici Y, Shabtai A (2018) Kitsune: an ensemble of autoencoders for online network intrusion detection. arXiv preprint arXiv:1802.09089.

Moon T, Ahn TI, Son JE (2019a) Long short-term memory for a model-free estimation of macronutrient ion concentrations of root-zone in closed-loop soilless cultures. Plant Methods 15:59.

Moon T, Hong S, Choi HY, Jung DH, Chang SH, Son JE (2019b) Interpolation of greenhouse environment data using multilayer perceptron. Comput Electron Agric 166:105023.

Muangprathub J, Boonnam N, Kajornkasirat S, Lekbangpong N, Wanichsombat A, Nillaor P (2019) IoT and agriculture data analysis for

smart farm. Comput Eelctron Agric 71:467-474.

Nederhoff EM, Rijsdijk AA, De Graaf R (1992) Leaf conductance and rate of crop transpiration of greenhouse grown sweet pepper (*Capsicum annuum* L.) as affected by carbon dioxide. Sci Hortic 52:283-301.

Sarker MNI, Wu M, Chanthamith B, Yusufzada S, Li D, Zhang J (2019) Big data driven smart agriculture: Pathway for sustainable development. In: International Conference on Artificial Intelligence and Big Data (ICAIBD), China: Chengdu. pp. 60-65.

Schmidhuber J (2015) Deep learning in neural networks: An overview. Neural Networks 61:85-117.

Sethi VP, Sumathy K, Lee C, Pal DS (2013) Thermal modeling aspects of solar greenhouse microclimate control: A review on heating technologies. Solar Energy 96:56-82.

Shamshiri R, Ismail WIW (2013) A review of greenhouse climate control and automation systems in tropical regions. J Agric Sci Appl 2:176-183.

Shin HC, Roth HR, Gao M, Lu L, Xu Z, Nogues I, Yao J, Mollura D, Summers RM (2016) Deep convolutional neural networks for computer-aided detection: CNN architectures, dataset characteristics and transfer learning. IEEE Trans Med Imaging 35:1285-1298.

Tan C, Sun F, Kong T, Zhang W, Yang C, Liu C (2018) A survey on deep transfer learning. In: International Conference on Artificial Neural Networks (ICANN). Greece: Rhodes, pp. 270-279.

Thenmozhi K, Reddy US (2019) Crop pest classification based on deep convolutional neural network and transfer learning. Comput Electron Agric 164:104906.

Vaswani A, Shazeer N, Parmar N, Uszkoreit J, Jones L, Gomez AN, Kaiser Ł, Polosukhin I (2017) Attention is all you need. In: Proceedings of Advances in Neural Information Processing Systems (NIPS), California: Long beach, pp. 5998-6008.

Villarreal-Guerrero F, Kacira M, Fitz-Rodríguez E, Linker R, Kubota C, Giacomelli GA, Arbel A (2012) Simulated performance of a greenhouse cooling control strategy with natural ventilation and fog cooling. Biosyst Eng 111:217-228.

Wang W, Huang Y, Wang Y, Wang L (2014) Generalized autoencoder: A neural network framework for dimensionality reduction. In: Proceedings of the IEEE Conference on Computer Vision and Pattern Recognition (CVPR), Ohio: Colombus. pp. 490-497.

Wolfert S, Ge L, Verdouw C, Bogaardt MJ (2017) Big data in smart farming–a review. Agric Sys 153:69-80.

Wubs AM, Ma YT, Heuvelink E, Hemerik L, Marcelis LF (2012) Model selection for nondestructive quantification of fruit growth in pepper. J Am Soc Hortic Sci 137:71-79.

Zhou P, Shi W, Tian J, Qi Z, Li B, Hao H, Xu B (2016) Attention-based bidirectional long short-term memory networks for relation classification.

In: Proceedings of the Association for Computational Linguistics (ACL), Germany: Berlin, pp. 207-212.

Zhuang F, Qi Z, Duan K, Xi D, Zhu Y, Zhu H, Xiong H, He Q (2019) A comprehensive survey on transfer learning. arXiv Preprint arXiv:1911.02685.

CHAPTER 1-2

Imputation of missing greenhouse environment data utilizing two-dimensional convolutional neural networks

ABSTRACT

Greenhouses require accurate and reliable data to interpret the microclimate and maximize resource use efficiency. However, greenhouse conditions are harsh for electrical sensors collecting environmental data. Convolutional neural networks (ConvNets) enable complex interpretation by multiplying the input data. The objective of this study was to impute missing tabular data collected from several greenhouses using a ConvNet architecture called U-Net. Various data-loss conditions with errors in individual sensors and all sensors were assumed. The U-Net with a screen size of 50 exhibited the highest coefficient of determination values and the lowest root-mean-square errors for all environmental factors used in this study. U-Net_{50} correctly learned the changing patterns of the greenhouse environment from the training dataset. Therefore, the U-Net architecture can be utilized for the imputation of tabular data in greenhouses if the model is correctly trained. Growers can secure data integrity with imputed data, increasing crop productivity and quality in greenhouses.

Additional keywords: artificial intelligence, deep learning, interpolation, machine learning, plant environment

*Chapter 1-2 was previously published by Sensors [Moon T, Lee JW, Son JE (2021) Accurate Imputation of Greenhouse Environment Data for Data Integrity Utilizing Two-Dimensional Convolutional Neural Networks. Sensors 21:2187].

INTRODUCTION

Agricultural systems and their models vary across spatial and temporal scales (Jones et al. 2017). Greenhouses, which represent a small agricultural system, increase the yield and quality of crops (van Straten et al. 2010). The greenhouse microclimate is manipulated to reduce energy input and increase crop yield and quality (Aaslyng et al. 2003; van Beveren et al. 2015; Graamans et al. 2018). Growers' strategies make distinctive microclimates to maximize resource use efficiency. Therefore, the microclimate is partly or totally anthropogenic in any form of greenhouses.

Since the greenhouse environment should be monitored for precise control, multidimensional information is accumulated and interpreted differently (Wang et al. 2006; Köksal et al. 2019; Xie and Yang 2020). The collected data can explain the interactions between the environment and the crops (Zhao et al. 2011; Wolfert et al. 2017). Recent developments in sensors and algorithms have also allowed machine learning and deep learning to be applied to agricultural data (Kamilaris and Prenafeta-Boldú 2018).

However, the internal environment of a greenhouse can be harsh for electrical sensors. The greenhouse may be close to water, and high solar radiation could heat the sensors (Mobtaker et al. 2019). Root-zone sensors could also be blocked by irrigational problems (Cho et al. 2018). In this case, sensors cannot obtain complete data without errors, resulting in low data

integrity. In addition, sensors in greenhouses are likely to lose their connection because of various external causes, such as blackouts or floods. Under such conditions, relatively long-term datasets could be lost, distorting the accumulated environmental data (Moon et al. 2019). Because past environments cannot be inferred from distorted data, a method to restore lost data is required.

Because environmental factors in greenhouses influence each other interactively and temporally, complex interpretation should be considered in interpolating environmental data. Convolutional neural networks (ConvNets) enable complex interpretation by multiplying the input data (Rawat and Wang 2017). ConvNets are mainly used for image processing, but they also exhibit high performance in extracting interactive features within inputs (Silver et al. 2017; Senior et al. 2020). Therefore, data imputation using a two-dimensional ConvNet can be performed for the obtained greenhouse environmental data. The objective of this study is to impute missing tabular data collected from several greenhouses using a ConvNet.

MATERIALS AND METHODS

U-Net model architecture and prediction workflow

A fully convolutional network architecture called U-Net was used for data imputation (Fig. 1-2-1). From the original input size, N, the size was compressed to one-quarter, and the abstracted features were restored in stages. U-Net is often used for image segmentation tasks in medical image datasets where the output has similar features and the same size as the input (Ronneberger et al. 2015). The architecture was the same as that of vanilla U-Net, which has a skip connection.

Every layer in a neural network algorithm is expected to abstract the relationship between the input and output hierarchically (LeCun et al. 2015). However, the layers could become short-sighted and learn only the relation between the previous and subsequent layers. This can reduce the model performance, especially when the model should restore the original input size. The skip connection architecture directly delivers the previous abstraction to the deeper layers (Orhan and Pitkow 2017). In this study of data imputation, not only did the output have to be the same size as the input, but also, the output was largely related to the original input. Therefore, the U-Net architecture was expected to be effective for the data imputation. Zero padding was added to sustain even-numbered inputs for the convolutional layer. The cost function was the mean square error.

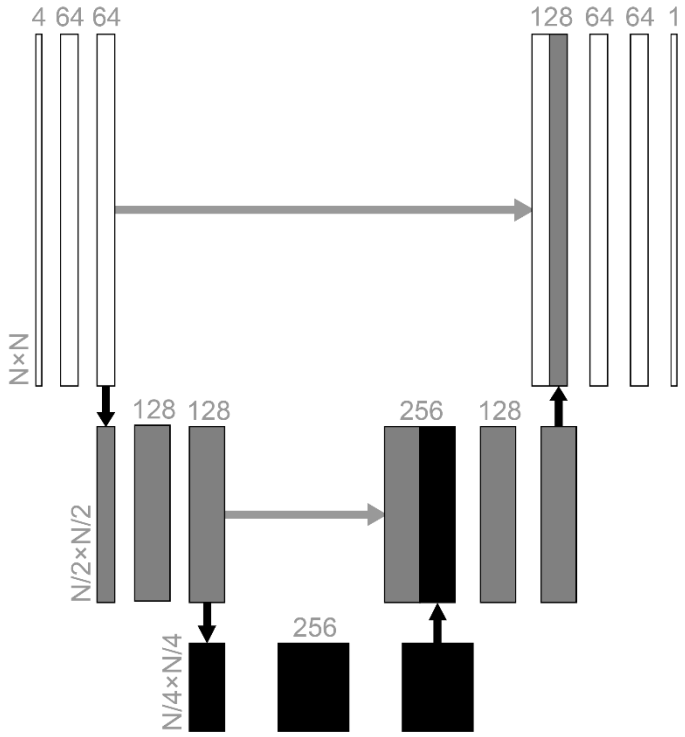

Fig. 1-2-1. U-Net structure used in this study. N was 5, 10, 20, or 100, the same as screen and input sizes. The numbers with horizontal writing represent the dimensions of the relevant vectors. Black and gray arrows represent max pooling and skip connection.

Experimental greenhouse environmental data

Greenhouses cultivating sweet peppers (*Capsicum annuum* L.) and tomatoes (*Solanum lycopersicum* L.) in various regions of South Korea were used to obtain the experimental datasets. The covering materials varied from arch-type plastic to Venlo-type glasses. The minimum and maximum sizes of the sweet pepper greenhouses (width × length × height) were 7 m × 80 m × 5 m and 100 m × 110 m × 5.7 m, respectively; those of the tomato greenhouses were 7 m × 53 m × 3 m and 66 m × 100 m × 4.5 m, respectively. The data collection periods varied according to the greenhouses (Fig. 1-2-2A).

The data interval was one hour, and the collected environmental factors were internal temperature (T_{in}), external temperature (T_{out}), internal relative humidity (RH), CO_2 concentration (CO_2), and radiation (Rad). The collected data included erroneous values (Table 1-2-1).

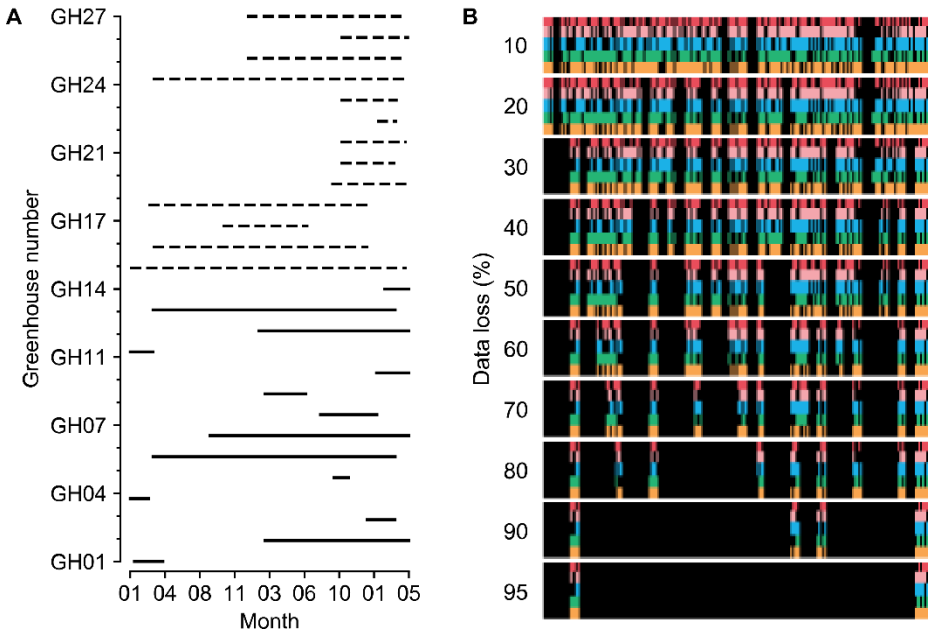

Fig. 1-2-2. Cultivation periods of the greenhouses (A) and an example of manipulated data loss (B). Solid and dashed lines represent tomato and sweet pepper greenhouses, respectively. Each color from the top represents five target factors of internal temperature, external temperature, internal relative humidity, internal CO_2 concentration, and radiation. Black blanks represent the data loss. Refer to Table 1-2-1 for the units of environmental factors.

Table 1-2-1. Ranges of environmental data used for the experiment.

Environmental factor	Abbreviation	Range
Internal temperature (°C)	T_{in}	5.3-60.3
External temperature (°C)	T_{out}	−21.2-38.0
Internal relative humidity (%)	RH	19.4-101.3
Internal CO_2 concentration (μmol mol^{-1})	CO_2	1.7-2999.0
Radiation (W m^{-2})	Rad	0.0-1669.9

Manipulation of the data-loss conditions and data preprocessing

In this study, incomplete data with errors and short-term losses were used. Outliers of the measured data were deleted, and short-term missing data were linearly interpolated. After processing, the data were considered intact. The data loss was manipulated with the collected environment factors for the experiments (Fig. 1-2-2B). The random seed for generating random numbers was fixed for the comparisons. Various data-loss conditions with errors in individual sensors and in all sensors were assumed. Losses in all sensors can result from electrical malfunctions such as a blackout, making it impossible to refer to other sensor values at the current loss time. The error rates of the individual sensors and all sensors were 30%. Because all-sensor losses usually accompany long-term loss, all-sensor loss times were set to two days (48 data indices). All losses were randomized using a random number generator.

The input matrices had specific screen sizes of 5, 10, 20, and 100 to ensure they were rectangular (Fig. 1-2-3). The screen sizes are represented as subscripts. Five input features were used; therefore, the input features were duplicated to increase the input size to match the screen size when needed. Consequently, the output also followed the screen sizes, and the duplicated outputs were averaged, except for two outliers in both extremes, expecting a similar effect to the model ensemble. To make the U-Net consider adjacent data, the tabular data in the previous and next date time from the target were used as the input. A mask matrix representing missing values was also added to the

input. Intact and missing data were 1 and 0 in the matrix, respectively. Similarly, the prediction ranges were also the same as the screen sizes. The data were normalized in the range of 0-1. Missing values were replaced with −1, which is outside the normalized range. ConvNets usually receive images in gray or RGB scale, but the networks can interpret other data types such as go board, shogi board, or chessboard (Silver et al. 2017). The ConvNets mathematically calculate the input, whatever the input is, it acts just a series of numbers. Therefore, rather than images, the input of the U-Net used in this study consisted of target tabular data with the specific screen size, previous and next data of the target, and a masking matrix for missing data of the target. The number of data input channels was four. Considering it as images, this input becomes an image with N × N pixels and one more dimension than RGB. It was expected that each feature and dimension was considered complex by convolution.

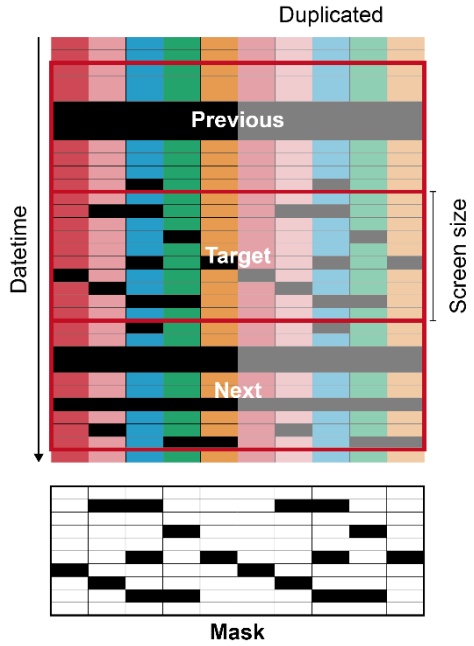

Fig. 1-2-3. Diagram of data preprocessing for U-Net. Each color represents each environmental factor. Each color from left to right represents the five target factors of internal temperature, external temperature, internal relative humidity, internal CO_2 concentration, and radiation. Black cells are missing data. The values in a mask were 0 and 1 for black and white, respectively.

Model evaluation

To compare the U-Net architecture with existing methodologies, linear interpolation (LI), a feedforward neural network (FFNN), and long short-term memory (LSTM) were selected. LI is a simple approach to imputing missing data; it simply linearly connects intact data. The FFNN is a basic architecture of a neural network algorithm (Schmidhuber 2015). LSTM is often used for sequence data and exhibits state-of-the-art performance (Greff et al. 2016). Since FFNN and LSTM showed reliable accuracies for predicting environmental changes and microclimates in greenhouses, they were selected as comparable models. Owing to structural limitations, the FFNN and LSTM could not have the same input matrices as U-Net (Table 1-2-2). The environmental factors corresponding to Target, Previous, and Next screen and the loss mask were linearly arranged for the FFNN input.

The most accurate U-Net and existing models were tested with different all-sensor losses from 10% to 95% to determine the limits of the model robustness by loss percentage (Fig. 1-2-2B). All losses were randomized using a random number generator with the same random seed. The U-Net and existing models were trained with 30% data loss. Ablation tests with input matrices were also conducted to verify the efficiency of each input component. In all evaluations, the coefficient of determination (R^2) and root-mean-square error (RMSE) were used as indicators of accuracy.

Table 1-2-2. Architectures of the compared models. Layer parameters are denoted as a type of layer and the number of nodes in the layer (number of trainable parameters). FFNN and LSTM represent a feedforward neural network and long short-term memory, respectively.

Model	FFNN	LSTM
Input size	1 × 20	100 × 20
Layers	Dense 64 (384)	BiLSTM 64 (43,520)
	Dense 64 (4160)	BiLSTM 64 (98,816)
	Dense 5 (325)	Dense 5 (645)
Output size	1 × 5	100 × 5

RESULTS

Imputation accuracies of U-Nets and other methods

U-Net_{50} exhibited the highest R^2 values (Table 1-2-3) and the lowest RMSEs (Table 1-2-4) for all environmental factors. Among them, the R^2 value for Tout was the highest, while that for CO_2 was the lowest. In particular, the prediction ability for the missing CO_2 data was relatively poor, given that the R^2 values for predicting other environmental factors were near 0.8.

The accuracies of the trained U-Nets increased with screen size, but U-Net_{100} exhibited lower accuracy than U-Net_{50}. The values imputed by U-Net_{100} tended to be biased, which could indicate overfitting (Fig. 1-2-4). Aside from the U-Nets, LI had the highest accuracy for imputation of the missing data. Similar to the U-Nets, the highest prediction accuracy was obtained with Tout, while the lowest was obtained with Rad. This result contrasts with the high imputation accuracy for radiation obtained by the trained U-Net_{50}. The FFNN and LSTM did not exhibit competitive accuracies, although they are deep learning methodologies. According to the R^2 values, they could not relate the remaining intact data with the missing data.

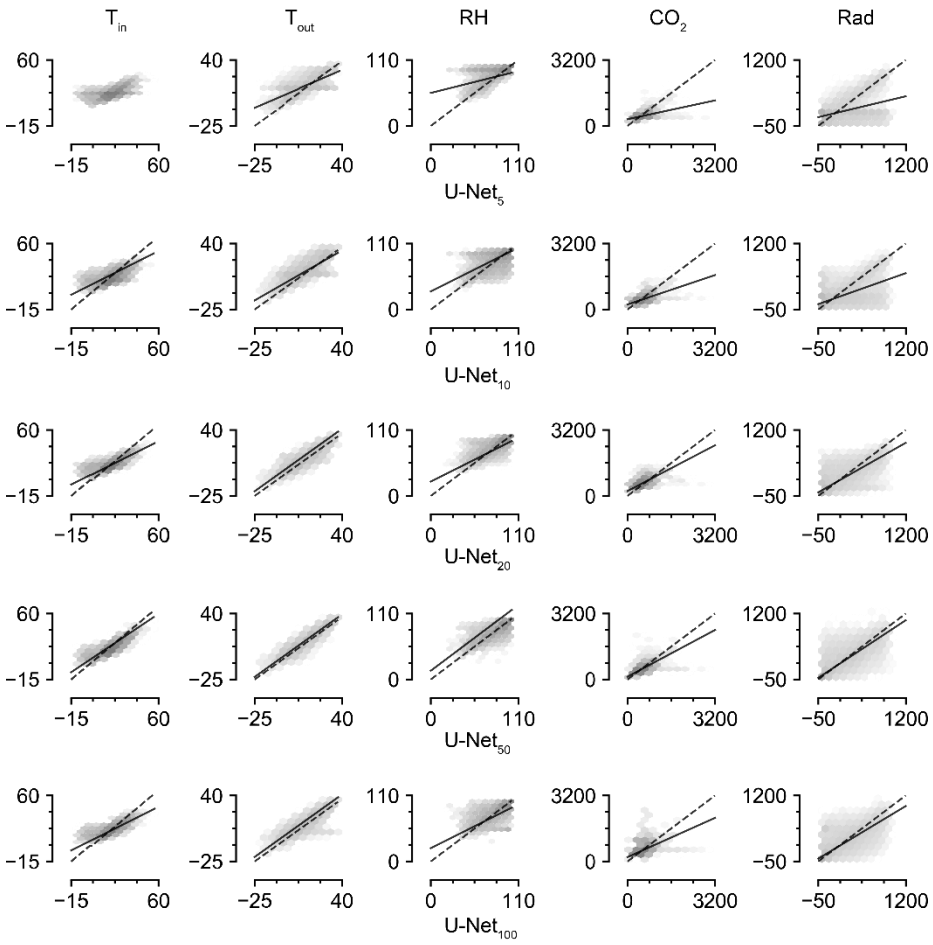

Fig. 1-2-4. Linear comparison of measured and imputed values. FFNN, LSTM, and LI represent the feedforward neural network, long short-term memory, and linear interpolation, respectively. The subscript represents the screen size. Refer to Tables 1-2-1 and 1-2-4 for the abbreviations of environmental factors and the coefficients and intercepts of regression lines, respectively.

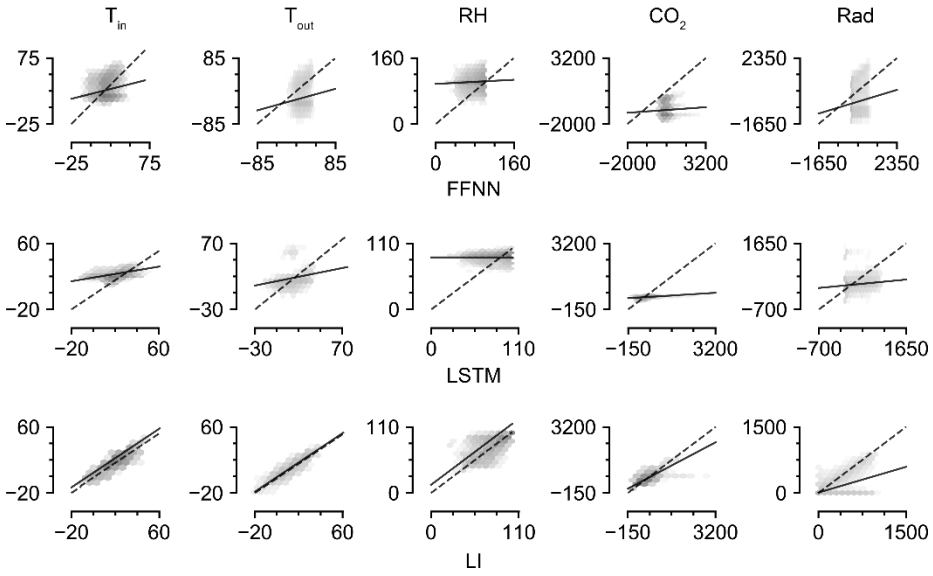

Fig. 1-2-4. (Continued from the previous page.)

Table 1-2-3. R^2 values of the models. The boldface values are the highest R^2 values for each factor. FFNN, LSTM, and LI represent the feedforward neural network, long short-term memory, and linear interpolation, respectively. The subscript represents the screen size. See Table 1-2-1 for the abbreviations of environmental factors.

	$U\text{-}Net_5$	$U\text{-}Net_{10}$	U-Net20	$U\text{-}Net_{50}$	$U\text{-}Net_{100}$	FNNN	LSTM	LI
T_{in}	0.32	0.45	0.67	**0.80**	0.66	−3.34	0.13	0.71
T_{out}	0.49	0.69	0.87	**0.92**	0.85	−14.81	0.07	0.88
RH	0.33	0.49	0.75	**0.81**	0.57	−1.74	−0.04	0.76
CO_2	0.23	0.23	0.21	**0.66**	0.23	−85.32	0.03	0.62
Rad	0.22	0.41	0.69	**0.79**	0.68	−14.25	0.01	0.17

Table 1-2-4. Root-mean-square error (RMSE) values of the models. The boldface values are the lowest RMSE values for each factor. FFNN, LSTM, and LI represent the feedforward neural network, long short-term memory, and linear interpolation, respectively. The subscript represents the screen size. Refer to Table 1-2-1 for the abbreviations of environmental factors.

	$U\text{-}Net_5$	$U\text{-}Net_{10}$	U-Net20	$U\text{-}Net_{50}$	$U\text{-}Net_{100}$	FNNN	LSTM	LI
T_{in}	5.44	4.90	3.79	**2.95**	3.88	13.82	6.18	3.57
T_{out}	7.16	5.57	3.61	**2.81**	3.83	39.98	9.69	3.54
RH	11.02	9.63	6.75	**5.91**	8.77	22.25	13.70	6.58
CO_2	141.33	141.61	143.00	**93.19**	141.17	1,494.73	158.64	99.42
Rad	210.03	182.91	132.40	**109.40**	134.71	927.42	238.57	216.69

Model robustness as ascertained by the loss percentages

Because U-Net$_{50}$ exhibited the highest accuracy among the U-Nets, it was used to compare the models by their losses. The accuracy of the trained U-Net decreased sharply in the case of CO_2 (Fig. 1-2-5). For factors other than CO_2, U-Net sustained its accuracy at loss rates of <50%. LI sustained its accuracy even with losses of >50%. The RMSE values of the FFNN and LSTM were also changed, although they could not correctly impute the missing data.

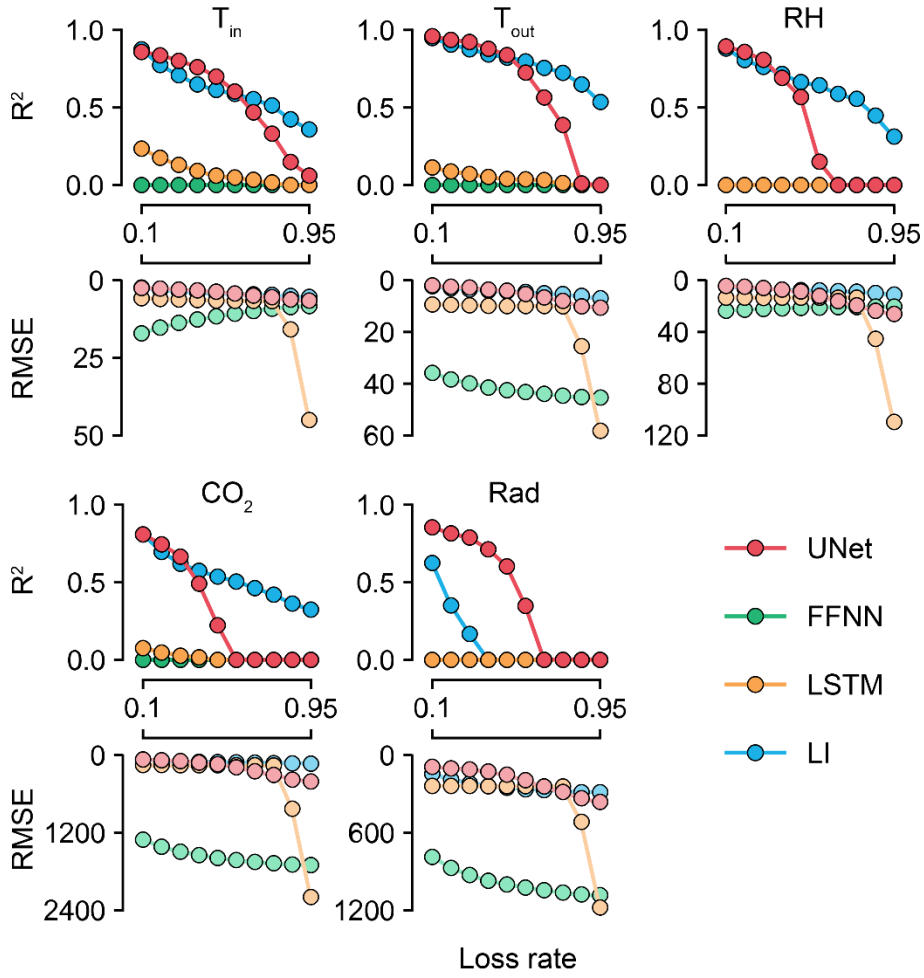

Fig. 1-2-5. R^2 and RMSE values ascertained by the loss rates. Colors with low alpha values represent RMSE values. R^2 values less than zero are depicted as 0.0. FFNN, LSTM, and LI represent the feedforward neural network, long short-term memory, and linear interpolation, respectively. Refer to Table 1-2-1 for the abbreviations of environmental factors and the units of RMSE values.

Ablations for critical components of the input

Because the R^2 values decreased by almost 0.6 without the previous and next matrices, these matrices were the most influential input components (Fig. 1-2-6). The absence of the mask matrix barely reduced the accuracy. Unexpectedly, the current matrix was the next least influential, after the mask matrix. Although the current matrix was the target, the decrease in accuracy was relatively lower compared to other input components. In contrast, the trained U-Net could not correctly impute the missing data with only current and mask matrices, although the screen size of 50 included a long-term dataset (>2 days). The magnitude of the decrease could be small, but the exclusion of each component resulted in a reduction in accuracy.

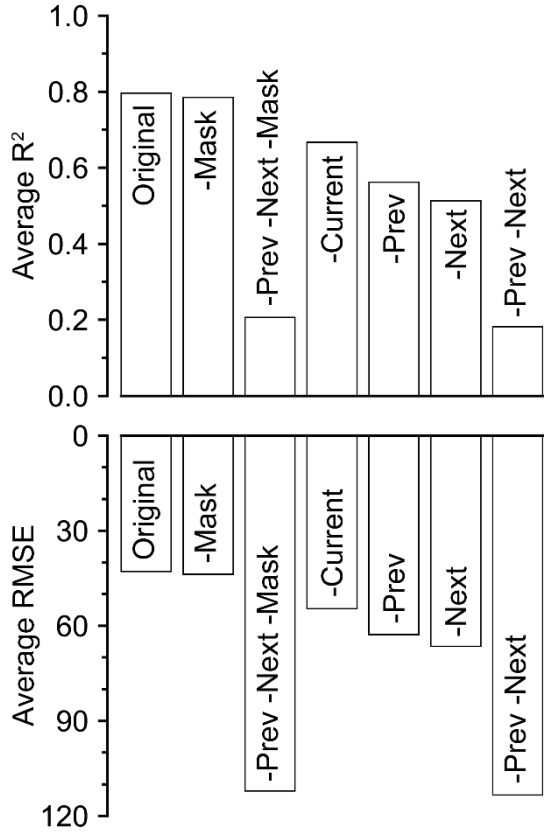

Fig. 1-2-6. Average R^2 and RMSE values of the trained U-Net_{50} by ablation of each input component. "Original" represents as intact input component. "Mask" represents the mask matrix. "Prev," "Current," and "Next" represent the Previous, the Current, and the Next matrix in input matrices. The minus symbol represents ablation.

DISCUSSION

U-Nets

Various screen sizes were compared to evaluate the U-Net architecture for data imputation, and U-Net$_{50}$ exhibited the best performance (Fig. 1-2-4). That is, U-Net was optimized with a screen size of 50. U-Nets usually handle an image size of >500×500 because the input should be compressed and abstracted in multiple layers (Ronneberger et al. 2015; Du et al. 2020). However, the optimal size was 50 for tabular data, which was 10% of the usual input size of U-Nets. The columns in the images are independent of their size. The small optimal screen size could be due to the strong relationship between duplicated columns. Likewise, the low accuracy of the trained U-Net$_{100}$ could result from overfitting because the five features of tabular data were too few for this architecture. This could also be due to receptive fields. ConvNet has specific receptive fields according to its architecture, and this could change the way of recognizing input (Lue et al. 2016). In this study, all U-Nets had the same receptive fields for model comparison. The same receptive fields could be too small for U-Net$_{100}$, resulting in a narrow view of the inputs. Changing the hyperparameters could improve the performance of the U-Nets. However, U-Net$_{100}$ with the same architecture could be used in other conditions. Environmental factors that can be used for microclimate monitoring have more

than five features (Kochhar and Kumar 2019; Zellweger et al. 2019). The optimal screen size could be >50 when more features are in the tabular dataset.

In the ablations, the absence of each input component caused different decreases in accuracy (Fig. 1-2-6). A mask with 0 and 1 can train non-image inputs using a ConvNet (Silver et al. 2017a; Silver al. 2017b). However, the mask was ineffective for U-Net$_{50}$, as shown by the barely changed accuracy. In this study, missing values were marked as −1 in the tabular data, which is outside the normalization range. Therefore, U-Net$_{50}$ could recognize the missing values without the mask matrix. Unlike in the positioning of hostile and friendly markers as in a board game, empty data could be marked as −1. In the case where target positioning is necessary with fully existing real data (e.g., proofreading of tabular data), the mask matrix could be helpful.

For the other input components, the trained U-Net$_{50}$ imputed the missing data with comparable accuracy, even without the current matrix. In the case of the current matrix only, U-Net$_{50}$ exhibited the lowest accuracy. The imputation performance was determined by patterns in the previous and next data, not adjacent data. Greenhouse environments exhibit 24-hour patterns, although they may vary by season (Baille and Baille 1994; Ma et al. 2019). Therefore, a screen size of 20 can yield high accuracy. However, all-sensor losses were designed to be 48 h. It seems that the screen size of 50 exceeded the length of all-sensor losses; therefore, it could be the optimal length. In generalizing the U-Net, high accuracy will be obtained only when it matches the appropriate

pattern range of tabular data.

However, because the accuracy slightly decreased without the current matrix, the current matrix was not inoperative. The U-Net somewhat weighted existing values adjacent to missing values, like LI. Although it could be a slight decrease, all components were likely used correctly because ablation of all components resulted in a decreased accuracy.

For U-Net$_{50}$, even when almost half of the data were missing, the accuracy was maintained to some extent (Fig. 1-2-5). Compared to the intact data, the imputation was also reasonable (Figs. 1-2-7, 1-2-8). The sustained accuracy of the U-Net could be due to the nature of machine learning (Liakos et al. 2018). The trained U-Net learned patterns from the given data, and it can fill the missing data correctly. Therefore, more data could improve the model robustness unlike the conventional interpolation methods.

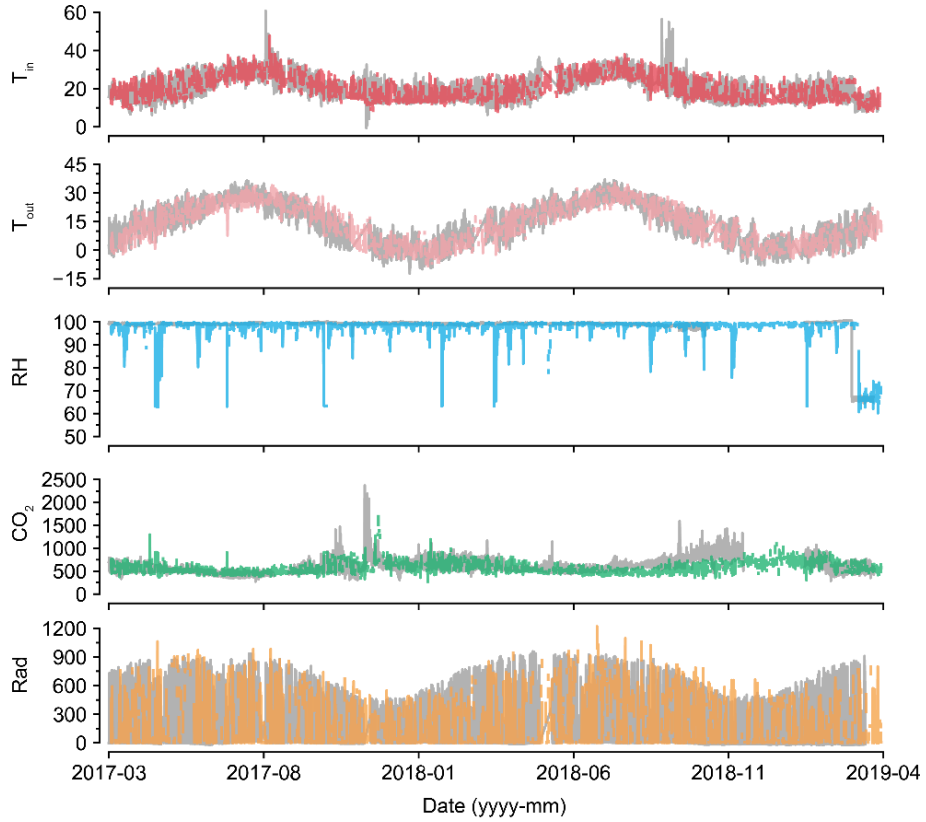

Fig. 1-2-7. Long-term examples of a recovered environmental dataset (GH24 in Fig. 1-2-2A; 50% data loss). Gray and colored lines represent intact raw data and imputed data, respectively. Refer to Table 1-2-1 for the units of environmental factors.

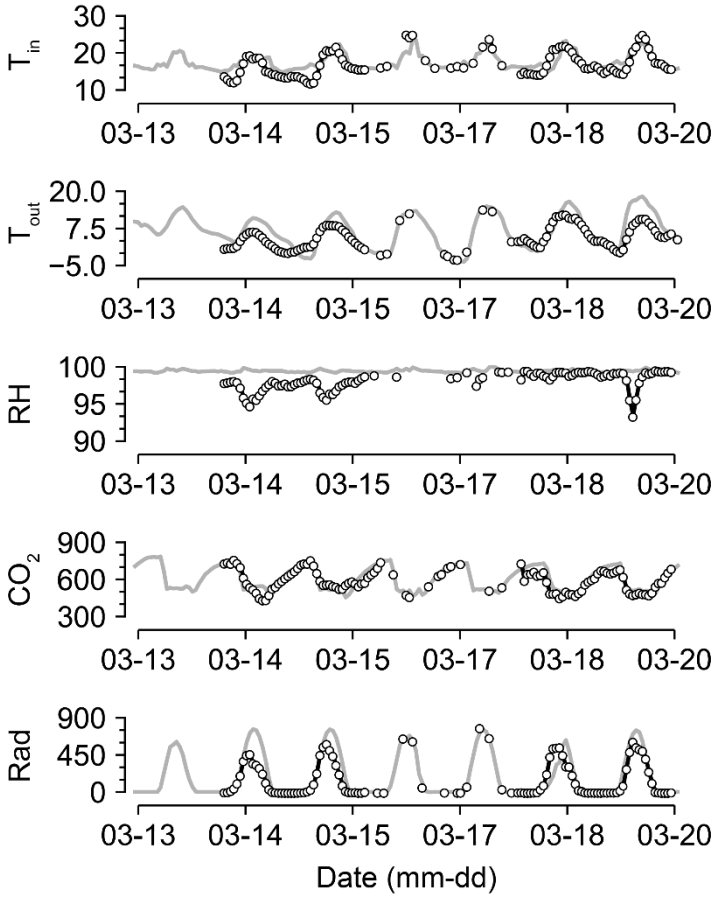

Fig. 1-2-8. Short-term examples of a recovered environmental dataset (GH24; 50% data loss). Gray and solid lines represent intact raw data and imputed data, respectively. Refer to Table 1-2-1 for the units of environmental factors.

Other models

LI is a method used to splice the nearest intact data. Although it was evident that LI did not properly interpret the two-day-long loss condition, it yielded comparable accuracy (Table 1-2-3). Therefore, a new metric is needed to compare models in missing data imputation.

The low accuracies of the FFNN and LSTM could result from clumsiness in the input (Kim et al. 2016). They exhibited comparable accuracies for agricultural estimations or predictions (Panda et al. 2010; Taki et al. 2016; Moon et al., 2019a). The inputs of the FFNN and LSTM included the previous, next, and mask matrices for comparison with the U-Nets. The matrices were expected to provide more information about the missing values and the data pattern, but FFNN and LSTM could not interpret the relations between the input features. Since the data imputation task was not a simple prediction, it seemed to require a more complicated interpretation of the input and the output. U-Nets extracted the importance of each 'pixel,' but FFNN and LSTM seemed biased by missing values.

Because the FFNN and LSTM are machine learning methodologies, changes in their accuracies yielded by different loss rates imply that the models learned something from the training (Fig. 1-2-5). However, the FFNN could not interpret a long period of the previous and next data. LSTM cannot convolute tabular target data because it reads the data sequence by sequence. Therefore, a wide range of the datasheet should be considered, and all tabular data should

be calculated beyond the sequences.

Variation in input environmental factors

U-Net$_{50}$ and LI exhibited the highest accuracy for T_{out} among the five input factors. Tout was also less affected by the loss percentages. That is, Tout could be a simple factor to impute. The chosen greenhouses were in the same climate conditions; thus, the individual datasets could share a tendency with respect to Tout. Most importantly, T_{out} was not a factor controlled by the grower. Therefore, the pattern could be easily extracted by the models.

Meanwhile, the imputation of missing T_{in} did not exhibit as high an accuracy as in the case of T_{out}. The models could not impute T_{in}, although this factor also has somewhat constant patterns because the internal environments of greenhouses are controlled to be within specific ranges (van Beveren et al. 2015). Neural network algorithms yielded high performance in previous studies (Ferreira et al. 2002; Manonmani et al. 2018). Unlike T_{out}, Tin could be affected by different grower strategies (Shamshiri et al. 2018). Therefore, the datasets did not seem to share the changing patterns; thus, the models could not impute the missing T_{in} with as high an accuracy as for T_{out}.

U-Net$_{50}$ exhibited a higher variance when imputing the RH than other environmental factors, even though the measured RH was sustained at almost 100% (Fig. 1-2-7). In greenhouses, the RH can be sustained at 100%, but it tends to drop and be restored immediately after sunrise because of thermal

screens and ventilation (Stanghellini 1992; Boulard et al. 2004). RH sensors have been reported to have high error and failure rates (Liu and Tang 2014). Therefore, the measured values could be incorrect. Consequently, it seems that U-Net$_{50}$ can be used for proofreading error data, as well as for the imputation of missing data. Based on the flexibility of the deep learning algorithm, the U-Nets could be remodeled with only a few input and output changes.

Regarding CO_2, the control strategy barely showed a pattern (Fig. 1-2-7). In particular, the imputation accuracy of CO_2 declined with an increase in the loss rate (Fig. 1-2-5). The relationship between CO_2 and other environmental factors could be weak. This could be due to the control strategies of CO_2. CO_2 fertilization is usually conducted empirically (Ting et al. 2015; Yang et al., 2020). In this study, greenhouses used manual CO_2 fertilization, except for some advanced farms. Therefore, the models could not find definite patterns of CO_2 changes. In this case, control data could improve robustness (Choi et al. 2019). However, U-Net$_{50}$ exhibited adequate accuracy for CO_2 imputation, although it was relatively lower than the accuracy for other environmental factors.

LI failed to impute Rad, but U-Net did so adequately (Table 1-2-3). This seems to be due to nighttime data, as LI simply splices the intact values; thus, the zero Rad at nighttime could cause high errors in imputing Rad. U-Nets could distinguish day and night regardless of the position of the input screen, although Rad was somewhat overestimated or underestimated. It can be said

that U-Net could learn specific patterns in tabular data that LI could not, as LI does not have model training

CONCLUSION

In this study, U-Net architectures were evaluated from the perspective of data imputation based on missing tabular data from 27 greenhouses. The trained U-Net exhibited an acceptable accuracy (average $R^2 = 0.80$), and the highest accuracy was obtained with a screen size of 50. Among the other models tested, LI exhibited comparable performance. The FFNN and LSTM could not be properly trained. Based on the accuracies for imputing five environmental factors, U-Net seemed to sufficiently learn the change patterns in the tabular data, although U-Nets are usually used for images. The trained U-Nets sustained their robustness with increasing loss rate, demonstrating their usefulness for tabular data imputation with short-term and long-term losses simultaneously.

LITERATURE CITED

Aaslyng JM, Lund JB, Ehler N, Rosenqvist E (2003) IntelliGrow: A greenhouse component-based climate control system. Environ Model Softw 18:657–666.

Baille M, Baille A, Delmon D (1994) Microclimate and transpiration of greenhouse rose crops. Agric For Meteorol 71:83–97.

van Beveren PJM, Bontsema J, van Straten G, van Henten EJ (2015) Optimal control of greenhouse climate using minimal energy and grower defined bounds. Appl Energy 159:509–519.

Boulard T, Fatnassi H, Roy JC, Lagier J, Fargues J, Smits N, Rougier M, Jeannequin B (2004) Effect of greenhouse ventilation on humidity of inside air and in leaf boundary-layer. Agric For Meteorol 125:225–239.

Cho WJ, Kim HJ, Jung DH, Kim DW, Ahn TI, Son JE (2018) On-site ion monitoring system for precision hydroponic nutrient management. Comput Electron Agric 146:51–58.

Choi H, Moon T, Jung DH, Son JE (2019) Prediction of air temperature and relative humidity in greenhouse via a multilayer perceptron using environmental factors. Prot Hortic Plant Fact 28:95–103.

Du G, Cao X, Liang J, Chen X, Zhan Y (2020) Medical image segmentation based on U-Net: A review. J Imaging Sci Technol 64:1–12.

Ferreira PM, Faria EA, Ruano AE (2002) Neural network models in greenhouse

air temperature prediction. Neurocomputing 43:51–75.

Greff K, Srivastava RK, Koutník J, Steunebrink BR, Schmidhuber J (2016) LSTM: A search space odyssey. IEEE Trans. Neural Netw Learn Syst 28:2222–2232.

Graamans L, Baeza E, van den Dobbelsteen A, Tsafaras I, Stanghellini C (2018) Plant factories versus greenhouses: Comparison of resource use efficiency. Agric Sys 160:31–43.

Jones JW, Antle JM, Basso Bm Boote KJ, Conant RT, Foster I, Godfray HCJ, Herrero M, Howitt RE, Janssen S, et al. (2017) Brief history of agricultural systems modeling. Agric Sys 155:240–254.

Kamilaris A, Prenafeta-Boldú FX (2018) Deep learning in agriculture: A survey. Comput Electron Agric 147:70–90.

Kim Y, Huang J, Emery S (2016) Garbage in, garbage out: Data collection, quality assessment and reporting standards for social media data use in health research, infodemiology and digital disease detection. J Med Internet Res 18:e41.

Kochhar A, Kumar N (2019) Wireless sensor networks for greenhouses: An end-to-end review. Comput Electron Agric 163:104877.

Köksal Ö, Tekinerdogan B (2019) Architecture design approach for IoT-based farm management information systems. Precis Agric 20:926–958.

LeCun Y, Bengio Y, Hinton, G (2015) Deep learning. Nature 521:436–444.

Liakos KG, Busato P, Moshou D, Pearson S, Bochtis D (2018) Machine

learning in agriculture: A review. Sensors 18:2674.

Liu Ym Tang N (2014) Humidity sensor failure: A problem that should not be neglected. Atmos Meas Tech 7:3909–3916.

Luo W, Li Y, Urtasun R, Zemel R (2016) Understanding the effective receptive field in deep convolutional neural networks. In: Proceedings of the Advances in Neural Information Processing Systems, Spain: Barcelona, pp. 4898-4906.

Ma D, Carpenter N, Maki H, Rehman TU, Tuinstra MR, Jin J (2019) Greenhouse environment modeling and simulation for microclimate control. Comput Electron Agric 162:134–142.

Manonmani A, Thyagarajan T, Elango M, Sutha S (2018) Modelling and control of greenhouse system using neural networks. Trans Inst Meas Control 40:918–929.

Mobtaker HG, Ajabshirchi Y, Ranjbar SF, Matloobi M (2019) Simulation of thermal performance of solar greenhouse in north-west of Iran: An experimental validation. Renew Energy 135:88–97.

Moon T, Ahn TI, Son JE (2019a) Long short-term memory for a model-free estimation of macronutrient ion concentrations of root-zone in closed-loop soilless cultures. Plant Methods 15:59.

Moon T, Hong S, Choi HY, Jung DH, Chang SH, Son JE (2019b) Interpolation of greenhouse environment data using multilayer perceptron. Comput Electron Agric 166:105023.

Orhan AE, Pitkow X (2017) Skip connections eliminate singularities. arXiv Preprint arXiv:1701.09175.

Panda SS, Ames DP, Panigrahi S (2010) Application of vegetation indices for agricultural crop yield prediction using neural network techniques. Remote Sensing 2:673–696.

Rawat W, Wang Z (2017) Deep convolutional neural networks for image classification: A comprehensive review. Neural Comput 29:2352–2449.

Ronneberger O, Fischer P, Brox T (2015) U-Net: Convolutional networks for biomedical image segmentation. In: Proceedings of the International Conference on Medical Image Computing and Computer-Assisted Intervention, Germany:Munich, pp. 234–241.

Schmidhuber J (2015) Deep learning in neural networks: An overview. Neural Network 61:85–117.

Senior AW, Evans R, Jumper J, Kirkpatrick J, Sifre L, Green T, Qin C, Žídek A, Nelson AWR, Bridgland A, et al. (2020) Improved protein structure prediction using potentials from deep learning. Nature, 577:706–710.

Shamshiri RR, Jones JW, Thorp KR, Ahmad D, Man HC, Taheri S (2018) Review of optimum temperature, humidity, and vapour pressure deficit for microclimate evaluation and control in greenhouse cultivation of tomato: A review. Int Agrophys 32:287–302.

Silver D, Hubert T, Schrittwieser J, Antonoglou I, Lai M, Guez A, Lanctot M, Sifre L, Kumaran D, Graepel T, et al. (2017a) Mastering chess and shogi by

self-play with a general reinforcement learning algorithm. arXiv Preprint arXiv:1712.01815.

Silver D, Schrittwieser J, Simonyan K, Antonoglou I, Huang A, Guez A, Hubert T, Baker L, Lai M, Bolton A, et al. (2017b) Mastering the game of go without human knowledge. Nature 550:354–359.

Stanghellini C (1992) Environmental control of greenhouse crop transpiration. J Agric Eng Res 51:297–311.

van Straten G, van Willigenburg G, van henten E, van Ooteghem R (2010) Optimal control of greenhouse cultivation. 1st ed.; CRC press: Boca Raton, FL, USA, 2010.

Taki M, Ajabshirchi Y, Ranjbar SF, Rohani A, Matloobi M (2016) Heat transfer and MLP neural network models to predict inside environment variables and energy lost in a semi-solar greenhouse. Energy Building 110:314–329.

Ting L, Man Z, Yuhan J, Sha S, Yiqiong J, Minzan L (2015) Management of CO_2 in a tomato greenhouse using WSN and BPNN techniques. Int J Agric Biol Eng 8:43–51.

Wang N, Zhang N, Wang M (2006) Wireless sensors in agriculture and food industry—Recent development and future perspective. Comput Electcron Agric 50:1–14.

Wolfert S, Ge L, Verdouw C, Bogaardt MJ (2017) Big data in smart farming–a review. Agric Sys 153:69–80.

Xie C, Yang CA (2020) review on plant high-throughput phenotyping traits

using UAV-based sensors. Comput Electron Agric 178:105731.

Yang X, Zhang P, Wei Z, Liu J, Hu X, Liu F (2020) Effects of CO_2 fertilization on tomato fruit quality under reduced irrigation. Agric Water Manag 230:105985.

Zhao CJ, Li M, Yang XT, Sun CH, Qian JP, Ji ZT (2011) A data-driven model simulating primary infection probabilities of cucumber downy mildew for use in early warning systems in solar greenhouses. Comput Electron Agric 76:306–315.

Zellweger F, de Frenne P, Lenoir J, Rocchini D, Coomes D (2019) Advances in microclimate ecology arising from remote sensing. Trends Ecol Evol 34:327–341.

CHAPTER 2

Bayesian optimization method to calibrate food and feed crop models for sweet peppers

ABSTRACT

Crop models are tools to analyze the interaction of crops and the environment. Since crop models can be applied to diverse research scales and purposes, models and their modifications vary. Therefore, the parameters of a crop model could be biased for unseen data; thus, crop models should be calibrated for the adequate simulation of the given data. This chapter aimed to calibrate food and feed crop models for sweet peppers (*Capsicum annuum* var. *annuum*) using Bayesian optimization. The algorithm does not require domain knowledge because it only considers input and output distributions based on Bayesian probability. For implementation of Bayesian optimization, HyperOpt, an algorithm for optimizing high-dimensional hyperparameters, was used. The target growth factors were fruit yield and leaf area index (LAI), and the loss function was mean squared error (MSE). As a result, the calibrated crop model showed the highest evaluation modeling efficiency (EF) of 0.53. The methodology showed adequate performance with reasonable ranges of convergence. The optimization method can be used for unknown distribution

spaces of parameters because it does not require an initial status. Among the selected food crops, the groundnut model was suitable for sweet pepper. Since the optimized crop models yielded reasonable simulations, Bayesian optimization could be introduced for horticultural purposes.

Additional keywords: crop simulation models, HyperOpt, sweet pepper, calibration

NOMENCLATURE

AMAXTB	Maximum leaf CO_2 assimilation rate as a function of development stage
CVL	Conversion efficiency of assimilates into leaves
CVO	Conversion efficiency of assimilates into storage organs
DTSMTB	Daily increase in temperature sum as a function of average temperature
DVS	Developmental stage
DVSI	Initial development stage at the start of the simulation
EFFTB	Initial light-use efficiency of CO_2 assimilation of single leaves as a function of mean daily temperature
FLTB	Fraction of above-ground dry mass increase partitioned to leaves as a function of the developmental stage
FOTB	Fraction of above-ground dry mass increase partitioned to storage organs as a function of the developmental stage
FRTB	Fraction of total dry mass increase partitioned to roots as a function of the developmental stage
FSTB	Fraction of above ground dry mass increase partitioned to stems as a function of the developmental stage
KDIFTB	Extinction coefficient for diffuse visible light as a function of the developmental stage
RFSETB	Reduction factor for senescence as a function of the developmental stage
RGRLAI	Maximum relative increase in LAI
SLATB	Specific leaf area as a function of the developmental stage
SPAN	Lifespan of leaves growing at 35 Celsius
SSATB	Specific stem area as a function of the developmental stage
TBASE	Lower threshold temperature for the aging of leaves

TBASEM	Base temperature for the emergence
TEFFMX	Maximum effective temperature for the emergence
TSUM1	Temperature sum from the emergence to the anthesis
TSUM2	Temperature sum from the anthesis to the maturity
TSUMEM	Temperature sum from the sowing to the emergence

INTRODUCTION

Crop and environment interact from farm to global scale (Jones et al. 2017). Since crops both immediately and cumulatively respond to the environmental changes, the cause and result of the interaction are entangled (Marcelis et al. 1998). Given the complexity, crops are also a target of interpretation and quantification; and crop models are used to analyze the complicated interactions (Muller and Martre 2019).

Crop models are a versatile tool to describe crop growth and development in a certain condition; and they can simulate crop growth and potential yield by calculating agricultural variables based on the climatic data (Van Diepen et al. 1989; Brisson et al. 2003; Jones et al. 2003; Steduto et al. 2009; Holzworth et al. 2014). Crop models have been modified and applied in various studies, so they have to cover broad scales with the same parameter set. Therefore, the parameters of a crop model are usually calibrated for the new data to adequately simulate the given condition (Ceglar et al. 2019; Chaki et al. 2022).

Crop models have also been developed for horticultural purposes (Gijzen et al. 1998; Marcelis et al. 2006). Horticultural crops do not necessarily prioritize food security, unlike food and feed crops, so the target crop growth and resource calculation may vary (De Corato et al. 2018; Kumar et al. 2020; Swallah et al. 2020). In addition, horticultural crops frequently accompany rigid management and controlled environment such as greenhouses. Since the given

condition differs from the open field, the crop models should be adequately modified or calibrated.

For adequate calibration, background knowledge about the target crop, such as the role of the parameters, should be required. However, the advanced models for horticultural targets are exclusive, and the related information has rarely been released. In the case of transferring food and feed crop models to the horticultural crops, they are based on different physiology of horticultural crops; therefore, background knowledge is also required. Moreover, since crop models have been updated in decades, the parameter space is too big to search randomly. An efficient way to calibrate significant parameters can help apply crop models to horticultural purposes.

Bayesian optimization is a class of machine-learning-based optimization methods focused on solving the problem to find the extrema of objective functions based on given input and a model (Frazier 2018). The optimization process changes the input to minimize or maximize the objective function based on the probability distribution of the input and the objective function output. Therefore, the method does not require domain knowledge of the target function.

One of the Bayesian optimization methods, HyperOpt, is a tool for tunning hyperparameters of deep neural networks (Bergstra et al. 2015). The high dimensional parameter sets of crop models would not exceed the neural networks, so the method could be applied to optimize crop model parameters.

The objective of this study was to calibrate existing crop models for sweet peppers with a Bayesian optimization approach for the high dimensional target, HyperOpt.

MATERIALS AND METHODS

Data collection

Crop environment and growth data collected by Rural Development Administration (RDA, South Korea) were used to fit crop models. The environment data were collected with various sensors in that location. Growth data were collected by selected inspectors, and the values were measured manually every week.

The target crops were sweet peppers (*Capsicum annuum* var. *annuum*) grown in greenhouses. Eleven greenhouses in various regions of Gangwon-do, South Korea were chosen for this study. Cultivation areas varied from 3,300 to 21,450 m^2. Cocopeats were used for the substrate. Sweet pepper cultivars were seven species, which made growth variations. Most of the crops were cultivated for a year (Fig. 2-1). Their average environments were similar, while their target growth factors differed (Fig. 2-2). The environment and growth data were collected at 1-h and 1-week intervals, respectively.

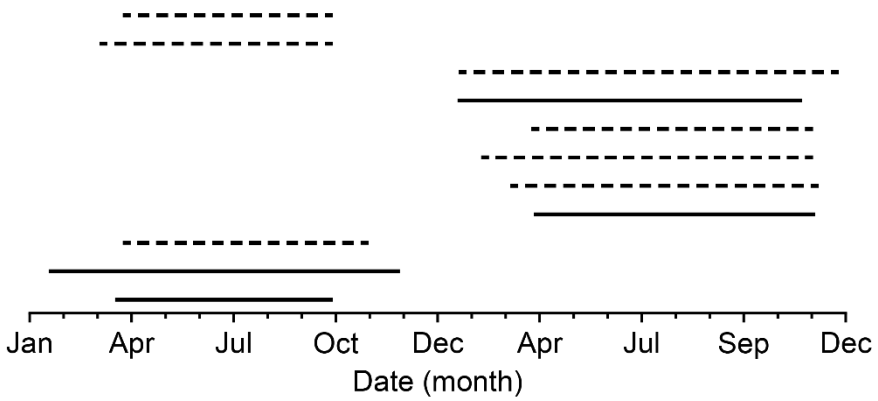

Fig. 2-1. Cultivation periods of sweet peppers in the 11 target greenhouses. Solid and dashed lines represent the dataset used for the crop model calibration and test, respectively.

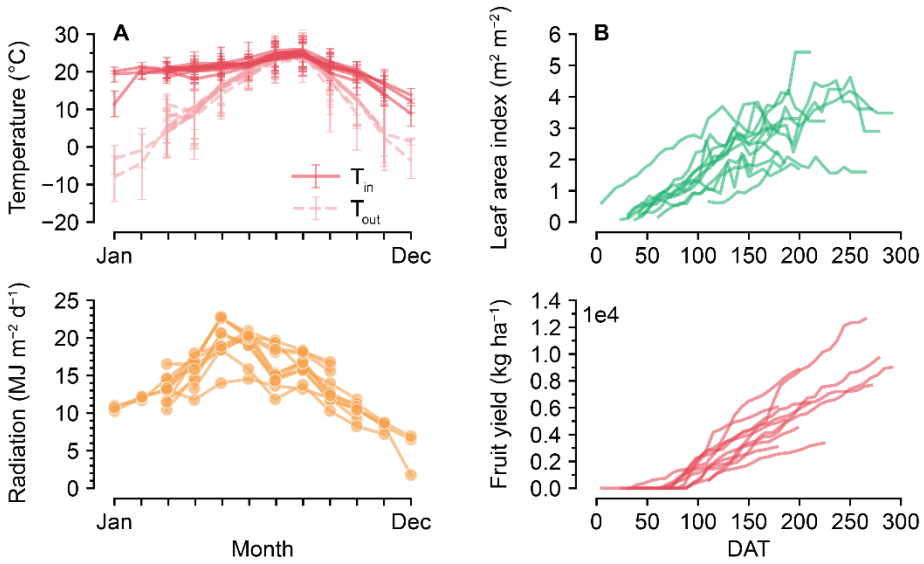

Fig. 2-2. Cultivation conditions of the 11 greenhouses: greenhouse environment (A) and crop growth (B). Daily averages of inside and outside temperatures, inside radiation, LAI, and cumulative fruit yield were depicted. The caps of each point represent the daily maximum and minimum temperatures.

Crop model implementation

To simulate and calibrate crop models, Python Crop Simulation Environment (PCSE, Wageningen UR, Wageningen, Netherlands, v. 5.5.0) was used. PCSE provides WOFOST crop models in the Python environment (de Wit et al. 2019). WOFOST 7.2 of potential production was selected for a base model of PCSE simulation. All 21 accessible food crops were used for this experiment.

For the WOFOST simulation, the input and output need to be converted to relevant forms. The 10-min interval environment data were converted to daily irradiation, minimum and maximum temperatures, and vapor pressure deficit. Considering the controlled environmental conditions of greenhouses, some factors were set to zero: wind velocity, precipitation, and snow depth. The CO_2 concentration was fixed for WOFOST, so the value was set to 360 μmol mol^{-1}. The target growth factors for the calibration were crop yield and leaf area index (LAI).

WOFOST does not distinguish between immature fruits and harvest yield; therefore, the total dry weight of storage organs (TWSO) was regarded as crop yield. The dry weight of the yield was calculated using an empirical ratio of dry weight to fresh weight of 0.075. Since LAIs were not directly measured in RDA data, leaf area per plant was estimated using leaf length, leaf width, and the number of leaves first; then, LAI was calculated by multiplying planting density. A regressor from a previous study (Lee et al. 2018) was used for the leaf area.

Among the 90 crop parameters, the parameters that can change leaf

dynamics and crop yield were selected, and broad ranges were set for each parameter (Table 2-1). Some definite parameters were fixed. Since the simulation was conducted with a potential production model, water- and nutrient-related parameters were excluded.

Table 2-1. Ranges of search spaces for parameter calibration.

Type	Parameters	Search space
Fixed	TEFFMX	100
	TBASEM	0
	TSUMEM	0
	SPAN	400
Single-point	DVSI	0.0-1.0
	TBASE	5-30
	RGRLAI	0.0-5.0[z]
	TSUM1	500-1200
	TSUM2	1200-2000
	CVO	0.0-2.0[z]
	CVL	0.0-1.0[z]
Table-form	SLATB	0.001-0.005
	SSATB	0.0-0.1[z]
	KDIFTB	0.0-0.9[z]
	AMAXTB	10-50
	RFSETB	0.0-1.0[z]
	FRTB	0.0-0.5
	EFFTB	0.1-2.1
	DTSMTB	0-100

[z]Set not to be zero.

Parameter calibration method

The crop models were calibrated to minimize errors between the observed and simulated crop yield and LAI using Bayesian optimization. The mean squared error (MSE) was normalized and set to the error. HyperOpt was used to conduct the Bayesian optimization (Bergstra et al. 2015). HyperOpt is a hyperparameter optimization tool for machine learning model selection. It provides an optimization interface that distinguishes a configuration space as a probability distribution and includes an evaluation function that assigns real-valued loss values to points within the configuration space. The tree-structured Parzen estimator approach was used to avoid local minima (Bergstra et al. 2011).

WOFOST has single-point parameters and table-form parameters. The probability distributions for single-point parameters can be set normally; however, each table-form parameter requires several points for the relevant developmental stage or environment factors, similar to a matrix. For the tables, relevant values were divided into three or four; each search space was added. For example, a table-form parameter AMAXTB had to be optimized at three points for the relevant DVS of 0.0, 1.0, and 2.0. The parameters related to partitioning required additional manipulation because the summation of the partitioning ratio must be one, and HyperOpt cannot consider external conditions, such as the fixed ratio. In the WOFOST calculation, the root-to-shoot ratio for total assimilation is determined first, and the rest is allocated to stems, leaves, and storage organs. In this study, HyperOpt optimized the

parameter for root partitioning in the same manner as the table-form; then, leaf allocation was determined. For the FSTB and FOTB, the stem-to-storage organ ratio was optimized in the range of 0-1.

Evaluation method

The optimization method HyperOpt was compared with a nonlinear optimization methodology used in the PCSE manual (Rowan 1990; de Wit et al. 2019). The Random walk, a randomized grid search, was used as a baseline. The data were divided into optimization, validation, and evaluation sets (Fig. 2-3). Each crop model was optimized based on the loss of the optimization set. The parameter set that showed the lowest loss for the average of the optimization and validation sets was selected as the best parameter set. The methods were compared with the evaluation set. Original parameter sets were compared using the same fixed parameters.

As metrics for the comparison, modeling efficiency (EF) and normalized root mean squared error (NRMSE) were used (Nash and Sutcliffe 1970).

$$RMSE = \sqrt{\sum_{i=1}^{n} \frac{\left(y_{obs,i} - y_{pred,i}\right)^2}{n}} \quad (1)$$

$$NRMSE = \frac{RMSE}{y_{obs,max} - y_{obs,min}} \quad (2)$$

$$EF = 1 - \frac{\sum_{i=1}^{n} \left(y_{obs,i} - y_{pred,i}\right)^2}{\sum_{i=1}^{n} \left(y_{obs,i} - y_{obs,mean}\right)^2} \quad (3)$$

where y_{obs} and y_{pred} represent observed and simulated target values, respectively. EF = 0 represents that the evaluated model yields the same performance as simply averaging the observed data would. Since LAI and fruit yield, the target growth factors, could be similar in all greenhouses, EF can emphasize differences in calibrated models.

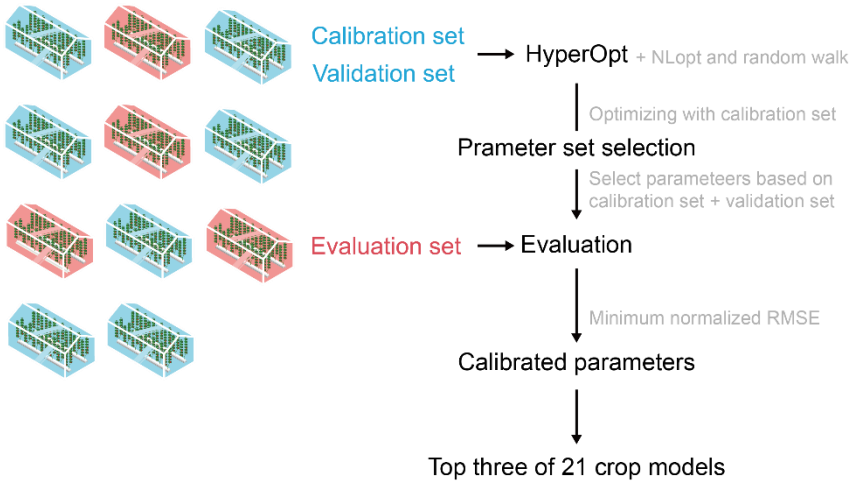

Fig. 2-3. Workflow of the calibration process and parameter set selection. Blue-colored greenhouses represent the data for calibration and validation, and red-colored greenhouses represent those for evaluation. The datasets were randomly divided. With the same datasets, HyperOpt optimized the parameter sets for all crop models in WOFOST; then, the crop models with the top three performances were selected based on the modeling efficiency.

RESULTS

Output of optimized models

Original parameter sets were unsuitable for sweet peppers (Fig. 2-4). HyperOpt showed the highest average EF of 0.74 for the calibration and validation dataset compared to −1.91 and 0.62 from NLopt and Random walk, respectively (Fig. 2-5). The top three crop models of HyperOpt that showed the highest accuracy were groundnut, barley, and potato; their evaluation EFs were 0.44, 0.53, and 0.36. The calibrated parameters by HyperOpt converged regardless of the crop species. Every optimized parameter set could follow the growth tendency for the HyperOpt result, but the simulations with low accuracy were unstable on unobserved days, such as those at the beginning of the cultivation periods (Fig. 2-6, 2-7).

NLopt could calibrate the parameters only for the LAI, although all the crops converged to a specific result. The crop yield was significantly underestimated by parameter sets from NLopt. Unobserved values were also unstably simulated by NLopt parameter sets, showing less fluctuation than HyperOpt results. The parameters could be optimized to some degree with Random walk in the fixed linear spaces; however, the results did not show a converging tendency.

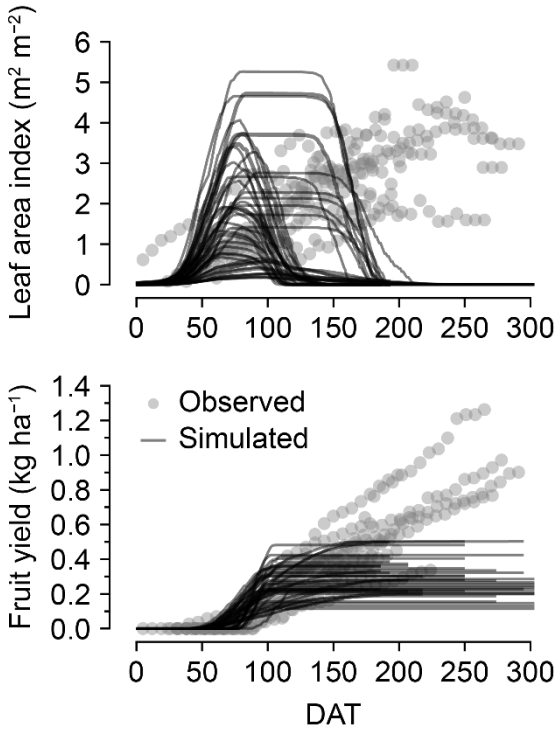

Fig. 2-4. Simulated LAIs and cumulative fruit yields using original parameter sets. All crop models in the Python Crop Simulation Environment (PCSE) were depicted. Solid lines and circle symbols represent the simulated and observed growth factors. All the simulated and observed values from the 11 greenhouses are depicted.

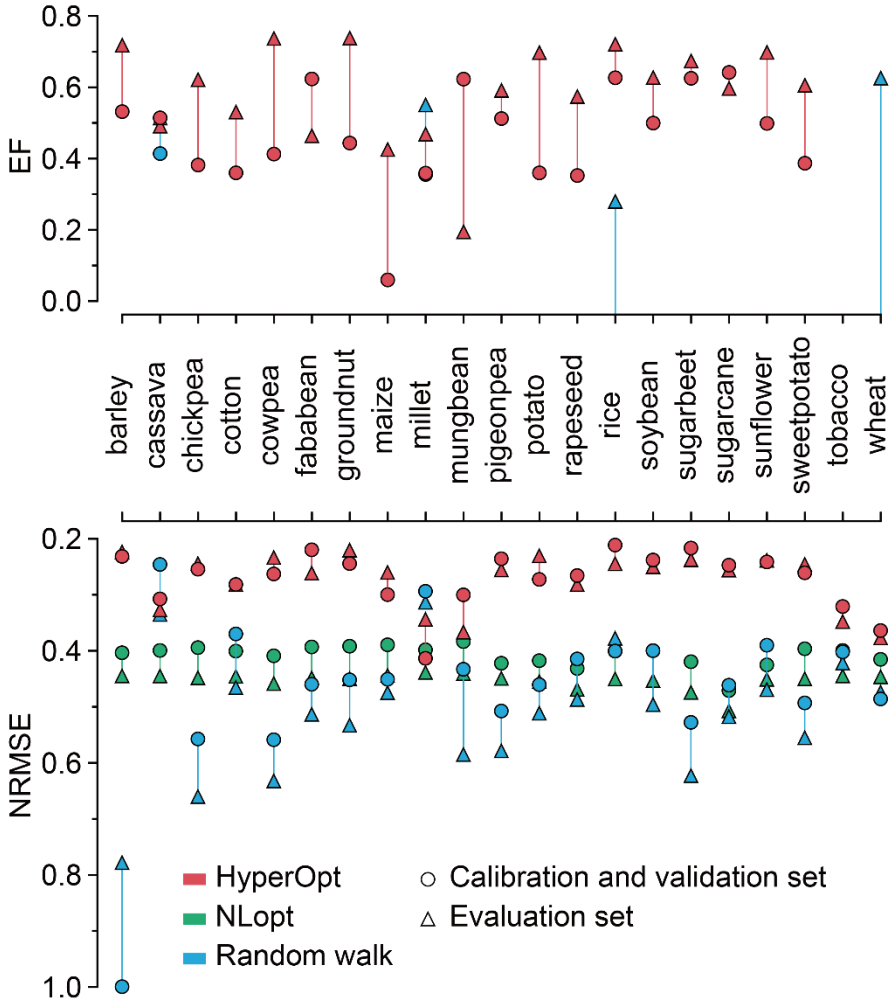

Fig. 2-5. Modeling efficiency (EF) and normalized root mean squared error (NRMSE) from the optimization methods: HyperOpt, NLopt, and Random walk. For the readability, solid lines were added between the symbols. The best crops were selected based on the EF of calibration and validation set. The top three crops were groundnut, barley, and potato.

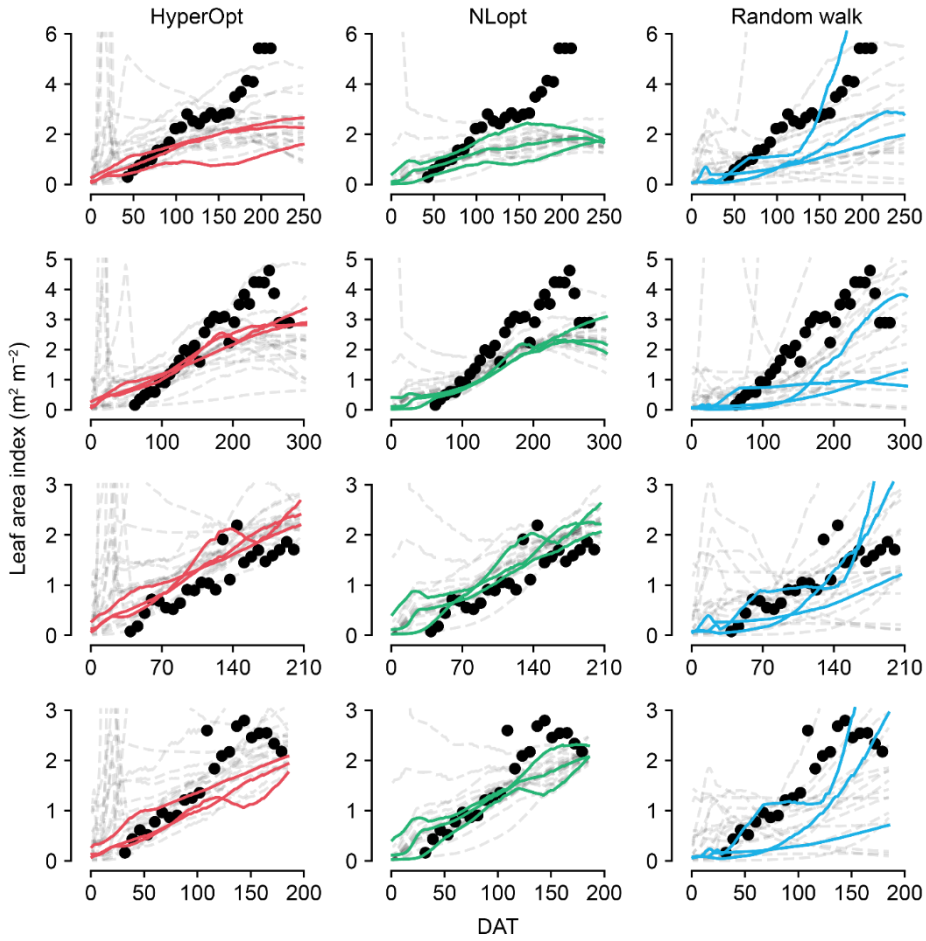

Fig. 2-6. Comparisons of observed and simulated LAIs. Each row represents the same target greenhouse. All simulation results from 21 calibrated crop models were depicted. Colored solid lines and gray dashed lines represent simulated results using the top three calibrated crop models from each method (HyperOpt, NLopt, and Random walk) and the others, respectively. The top three calibrated parameters of each model were selected based on modeling efficiency. Black markers represent observed LAIs.

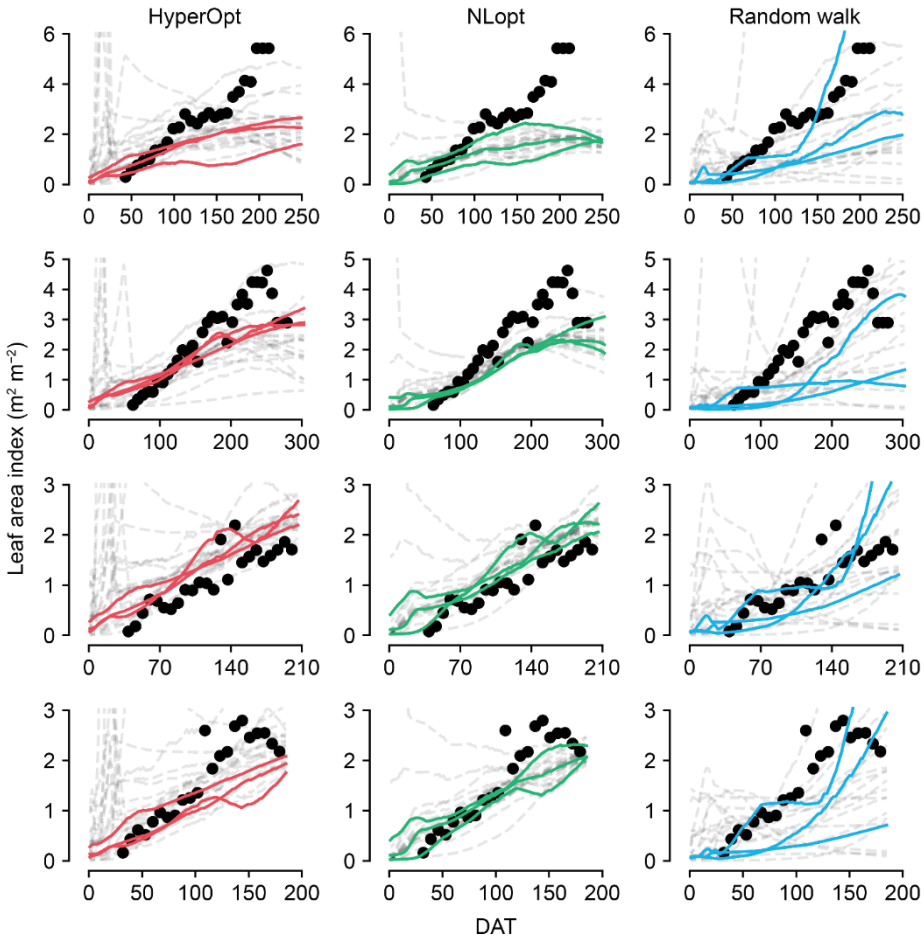

Fig. 2-7. Comparisons of observed and simulated fruit yields. Each row represents the same target greenhouse. All simulation results from 21 calibrated crop models were depicted. Colored solid lines and gray dashed lines represent simulated results using the top three calibrated crop models from the calibration methods (HyperOpt, NLopt, and Random walk) and the others, respectively. The top three calibrated parameters of each model were selected based on modeling efficiency. Black markers represent observed fruit yields.

Calibrated parameters

The calibrated parameters resulted in different variances according to the parameter and applied method. The single-point parameters converged to specific values by NLopt, and the table-form parameters showed few variations (Figs. 2-8, 2-9). For HyperOpt, both single-point and table-form parameters showed somewhat randomized distributions similar to the Random walk. However, the calibrated parameter sets with low losses showed convergence, although the values were not substantially close.

Every top-ranked single-point parameter from HyperOpt converged except TBASE and TSUM2. NLOpt had some convergence variations, and the values were located at both the boundaries and average of the search spaces. Some parameters, such as the RGRLAI from Random walk, significantly showed a converging tendency. The table-form parameters did not yield the same optimization results in all ranges but converged in a specific DVS or temperature. The HyperOpt results showed some patterns such as a decrease at the latter part, a V-shape, and an average all-time.

For the partitioning parameter sets from HyperOpt, the stem parameter was suspended in a low ratio (Fig. 2-10). The leaf and fruit parameters showed opposite patterns similar to the original parameter sets. Overall, calibrated parameters by HyperOpt showed a tendency to converge to specific values

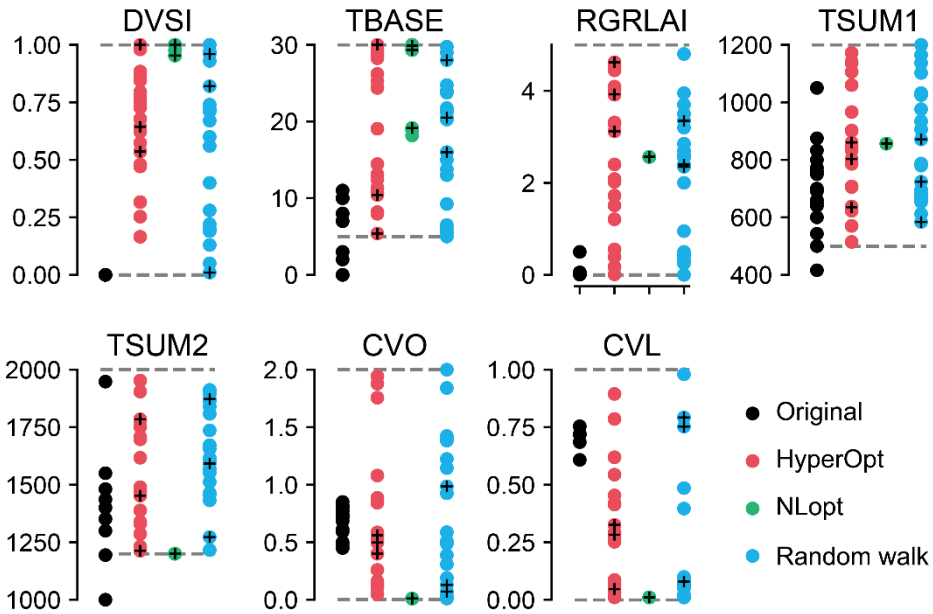

Fig. 2-8. Optimized single-point parameters. All parameters from 21 calibrated crop models were depicted. Black cross on colored markers represents the calibrated parameters of the top three crop models from the calibration methods (HyperOpt, NLopt, and random walk). Gray dashed lines represent the range of the search spaces. For the original parameter sets, the values too far from the search spaces were not depicted.

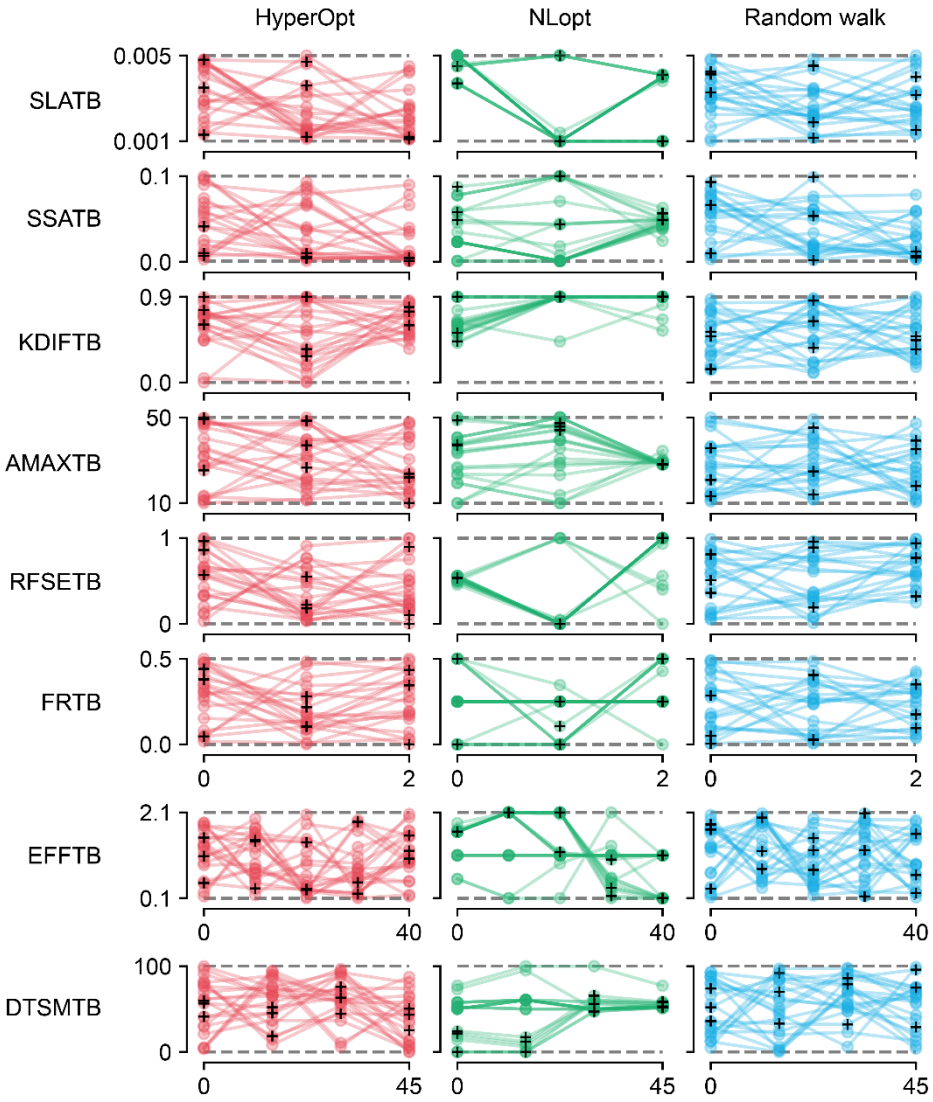

Fig. 2-9. Optimized table-form parameters. All parameters from 21 calibrated crop models were depicted. Black cross on colored markers represents the calibrated parameters of the top three crop models from the calibration methods (HyperOpt, NLopt, and Random walk). Gray dashed lines represent the range of the search spaces.

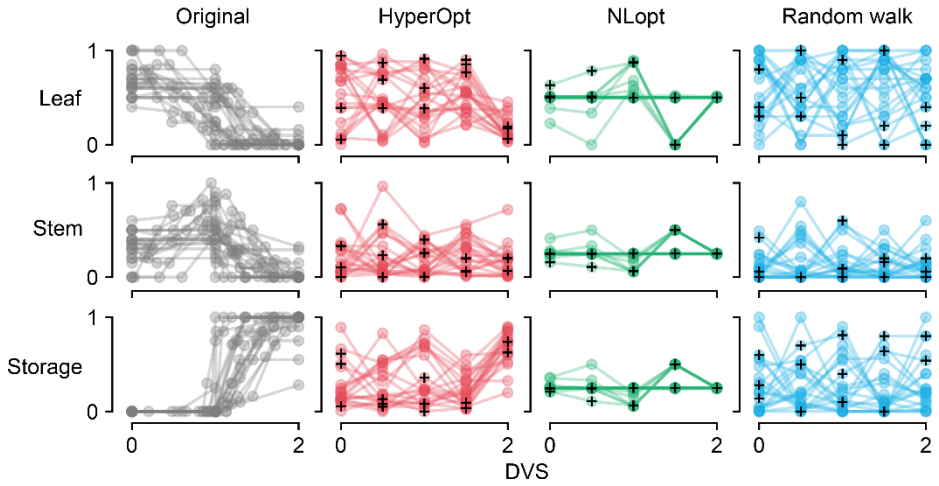

Fig. 2-10. Optimized parameters determined the dry mass allocation of leaves, stems, and storage organs. All parameters from 21 calibrated crop models were depicted. Black cross on colored markers represents the calibrated parameters of the top three crop models from the calibration methods (HyperOpt, NLopt, and Random walk).

DISCUSSION

Evaluation of optimization methods

HyperOpt showed adequate performance in calibrating existing crop parameter sets in WOFOST. However, HyperOpt results from non-top-accuracy crops were unstable on the days after transplanting (DATs) without observed data. Since the other methods were also unstable at the relevant DATs, this could be due to problems in the data. HyperOpt was able to calibrate the parameters with problematic conditions. Therefore, HyperOpt is adequate for the crop model calibration, but it should be carefully applied to avoid overfitting a given dataset. In addition, the data from the early stage should be collected to optimize the parameters of the crop model.

NLopt failed to find adequate parameters that satisfied both growth factors. The results of NLopt converged to the boundary or mean values because the method could not find the optimum parameters; and the low fluctuation with low accuracy seems to result from a weak parameter fitting. It can be inferred that NLopt could not handle the local minima. Local minima are usually not problematic for a few parameters (Gori and Tesi 1992). The optimizer had to calibrate approximately 40 parameters, including table-form parameters, simultaneously. NLopt appeared inadequate to calibrate this many parameters. The NLopt algorithm used gradient descent, but it seemed unable to support a means of escaping local minima. Therefore, NLopt could not find the global

optimum, although all the crops converge to a specific point. However, 40 parameters are not large compared to the original target of HyperOpt: neural network hyperparameters. HyperOpt uses Tree-structured Parzen Estimator to avoid local minima in high dimensions (Bergstra et al. 2011). Therefore, HyperOpt could optimize approximately 40 parameters.

Original crop models could not simulate sweet peppers correctly because of infinite growth. Sweet peppers are a fruit vegetable that can grow for almost a full year with undergoing several harvests throughout the growth period by crop management (Del Amor 2006; González-Real et al. 2008; López-Marín et al. 2013). Crop models in WOFOST target food and feed crops, and the crop harvest generally terminates cultivation. With this discordance, sweet pepper models are often developed based on crops with similar physiologies (Jones et al. 2003). However, the top three optimized crop models in this study were groundnut, barley, and potato, which have a single harvest in their cultivation period, although WOFOST includes crops with periodical harvest, such as maize. Therefore, developing a variant of a crop model may not accurately reflect the target crop. In this experiment, only WOFOST was used for the convenience, but HyperOpt can be applied to find the most suitable crop for variants of existing models.

Semantic analysis of the parameter values

After the calibration ended, major and minor parameters could be

distinguished through the distribution of optimized parameters. In single-point parameters, optimized parameters distributed in a narrow range can be considered indicators with a strong influence.

The RGRLAI converged for all of the applied methods, including Random walk. Since the value converged even though the value was randomly selected, this parameter could be the most influential factor. In WOFOST, RGRLAI regulates the maximum growth of the leaves in the early stage. Since the leaves of sweet pepper vertically distribute compared to those of food and feed crops, a high-value convergence is reasonable (Asrar et al. 1984; Delfine et al. 2001; Xie et al. 2017; Lee et al. 2020). CVO and CVL are the conversion efficiency of the assimilate; therefore, these parameters would be related to the target growth factors, LAI and fruit yield. The dry weight ratio of fruit to the other organs in fruit vegetables is higher than that in food crops (Marcelis et al. 2004; Marcelis et al. 2006); therefore, the CVL was lowered. TSUM1 and TSUM2, the parameters determining the development stage, were similar to the empirical cumulative temperatures (Sánchez-Molina et al. 2015).

For the table-form parameters that showed a converging tendency, the SSATB can affect the small crop in the early stage, so the decreasing tendency is reasonable. AMAXTB decreased by the DVS. The portion of old leaves can gradually increase because of the semi-infinite growth, and the overall performance of photosynthesis could diminish. KDIFTB showed a somewhat unusual move that decreased in the early stage and improved in the later stage.

This could be due to management such as pruning. However, the value is somewhat high, so the parameter could be overestimated because of the interruption of CVL and RGRLAI. To calibrate the interacting parameters, realistic parameters can be obtained by determining the empirical parameters in advance. In addition, each table-form parameter was correlated, but HyperOpt regarded them as independent parameters. Exponential or sigmoidal changes could be more suitable for calibration. However, the table-form parameters were calibrated in reasonable ranges, so the proposed protocol can also be adequate for calibrating table-form parameters.

In the best cases from HyperOpt, complicated partitioning parameters could be interpreted. The optimized partitioning parameters showed a similar tendency to the original parameters (Fig. 2-9); However, some details differed. For example, FOTB increased in the latter part of the DVS change, which seemed to be due to the target value because the target was fruit yield, not the dry mass, of the storage organs. Since fruits appear several weeks before harvest, using unmatured fruit could make parameters more realistic.

The calibrated parameters converged in reasonable ranges, WOFOST, which targets food and feed crops, can be calibrated for horticultural crops with adequate data collection and HyperOpt. However, the target growth factors only used total fruit yield and LAI. The other growth factors could fail to reflect the real values. A wider data collection can help to calibrate crop parameters more suitably.

CONCLUSION

In this chapter, the food and feed crop models were calibrated for sweet pepper using Bayesian optimization. The HyperOpt algorithm does not require domain knowledge because it only considers input and output distribution based on Bayesian probability. The target growth factors were fruit yield and LAI. As a result, HyperOpt showed the highest performance, followed by Radom walk and NLopt with reasonable convergence ranges. Since many optimization methods require the initial value of parameters, a randomized search can be more valuable than the inappropriate use of optimization methods. In this regard, HyperOpt can be adequate for use when there are unknown distribution spaces of parameters. Using other target growth factors such as organ dry weights can improve the calibration results to be more reasonable.

LITERATURE CITED

Antle J, Basso B, Conant RT, Godfray HCJ, Jones JW, Herrero M, Howitt RE, Keating BA, Munoz-Carpena R, Rosenzweig C, Tittonell P, Wheeler TR (2017a) Towards a new generation of agricultural system data, models and knowledge products: Design and improvement. Agric Syst 155:255–268.

Antle J, Jones JW, Rosenzweig CE (2017b) Next generation agricultural system data, models and knowledge products: Introduction. Agric Syst 155:186–190.

Asrar G, Fuchs M, Kanemasu ET, Hatfield JL (1984) Estimating Absorbed Photosynthetic Radiation and Leaf Area Index from Spectral Reflectance in Wheat1. Agron J 76:300–306.

Bergstra J, Bardenet R, Bengio Y, Kégl B (2011) Algorithms for Hyper-Parameter Optimization. In: Shawe-Taylor J, Zemel R, Bartlett P, Pereira F, Weinberger KQ (eds) Advances in Neural Information Processing Systems. Curran Associates, Inc.

Bergstra J, Komer B, Eliasmith C, Yamins D, Cox DD (2015) Hyperopt: a Python library for model selection and hyperparameter optimization. Comput Sci Discov 8:014008.

Brisson N, Gary C, Justes E, Roche R, Mary B, Ripoche D, Zimmer D, Sierra J, Bertuzzi P, Burger P (2003) An overview of the crop model STICS. Eur J Agron 18:309–332.

Campbell GS, Norman JM (1989) The description and measurement of plant canopy structure. In: Marshall B, Russell G, Jarvis PG (eds) Plant Canopies: Their Growth, Form and Function. Cambridge University Press, Cambridge, pp 1–20.

Ceglar A, van der Wijngaart R, de Wit A, Lecerf R, Boogaard H, Seguini L, van den Berg M, Toreti A, Zampieri M, Fumagalli D, Baruth B (2019) Improving WOFOST model to simulate winter wheat phenology in Europe: Evaluation and effects on yield. Agric Syst 168:168–180.

Chaki AK, Gaydon DS, Dalal RC, Bellotti WD, Gathala MK, Hossain A, Menzies NW (2022) How we used APSIM to simulate conservation agriculture practices in the rice-wheat system of the Eastern Gangetic Plains. Field Crops Research 275:108344.

de Wit A, Boogaard H, Fumagalli D, Janssen S, Knapen R, van Kraalingen D, Supit I, van der Wijngaart R, van Diepen K (2019) 25 years of the WOFOST cropping systems model. Agric Syst 168:154–167.

Del Amor F m. (2006) Growth, photosynthesis and chlorophyll fluorescence of sweet pepper plants as affected by the cultivation method. Ann Appl Biol 148:133–139.

Delfine S, Loreto F, Alvino A (2001) Drought-stress Effects on Physiology, Growth and Biomass Production of Rainfed and Irrigated Bell Pepper Plants in the Mediterranean Region. J Am Soc Hortic Sci 126:297–304.

Frazier PI (2018) A tutorial on Bayesian optimization. arXiv preprint

arXiv:1807.02811.

Gijzen H, Goudriaan J (1989) A flexible and explanatory model of light distribution and photosynthesis in row crops. Agric For Meteorol 48:1–20.

González-Real MM, Baille A, Liu HQ (2008) Influence of fruit load on dry matter and N-distribution in sweet pepper plants. Scientia Horticulturae 117:307–315.

Gori M, Tesi A (1992) On the Problem of Local Minima in Backpropagation. IEEE Trans Pattern Anal Mach Intell 14:76–86.

Hackett C, Rawson HM (1974) An Exploration of the Carbon Economy of the Tobacco Plant. II. Patterns of Leaf Growth and Dry Matter Partitioning. Funct Plant Biol 1:271–281.

Holzworth DP, Huth NI, deVoil PG, Zurcher EJ, Herrmann NI, McLean G, Chenu K, van Oosterom EJ, Snow V, Murphy C (2014) APSIM–evolution towards a new generation of agricultural systems simulation. Environ Model Softw 62:327–350.

Jones JW, Antle JM, Basso B, Boote KJ, Conant RT, Foster I, Godfray HCJ, Herrero M, Howitt RE, Janssen S, Keating BA, Munoz-Carpena R, Porter CH, Rosenzweig C, Wheeler TR (2017) Brief history of agricultural systems modeling. Agric Syst 155:240–254.

Jones JW, Hoogenboom G, Porter CH, Boote KJ, Batchelor WD, Hunt LA, Wilkens PW, Singh U, Gijsman AJ, Ritchie JT (2003) The DSSAT cropping system model. Eur J Agron 18:235–265.

Lee J, Moon T, Nam DS, Park KS, Son JE (2018) Estimation of Leaf Area in Paprika Based on Leaf Length, Leaf Width, and Node Number Using Regression Models and an Artificial Neural Network. Horticultural Science and Technology 183–192.

Lee JW, Kang WH, Moon T, Hwang I, Kim D, Son JE (2020) Estimating the leaf area index of bell peppers according to growth stage using ray-tracing simulation and a long short-term memory algorithm. Hortic Environ Biotechnol 61:255–265.

Liang H, Xu J, Chen L, Li B, Hu K (2022) Bayesian calibration and uncertainty analysis of an agroecosystem model under different N management practices. Eur J Agron 133:126429.

López-Marín J, González A, Pérez-Alfocea F, Egea-Gilabert C, Fernández JA (2013) Grafting is an efficient alternative to shading screens to alleviate thermal stress in greenhouse-grown sweet pepper. Sci Hortic 149:39–46.

Marcelis LFM, Elings A, Bakker MJ, Brajeul E, Dieleman JA, de Visser PHB, Heuvelink E (2006) Modelling dry matter production and partitioning in sweet pepper. Acta Hortic 121–128.

Marcelis LFM, Heuvelink E, Baan Hofman-Eijer LR, Den Bakker J, Xue LB (2004) Flower and fruit abortion in sweet pepper in relation to source and sink strength. J Exp Bot 55:2261–2268.

Marcelis LFM, Heuvelink E, Goudriaan J (1998) Modelling biomass production and yield of horticultural crops: a review. Sci Hortic 74:83–111.

Nash JE, Sutcliffe JV (1970) River flow forecasting through conceptual models part I — A discussion of principles. J Hydrol 10:282–290.

Oliver YM, Robertson MJ, Wong MTF (2010) Integrating farmer knowledge, precision agriculture tools, and crop simulation modelling to evaluate management options for poor-performing patches in cropping fields. Eur J Agron 32:40–50.

Rowan TH (1990) Functional stability analysis of numerical algorithms. Ph.D., The University of Texas at Austin.

Sánchez-Molina JA, Pérez N, Rodríguez F, Guzmán JL, López JC (2015) Support system for decision making in the management of the greenhouse environmental based on growth model for sweet pepper. Agric Syst 139:144–152.

Steduto P, Hsiao TC, Raes D, Fereres E (2009) AquaCrop—The FAO crop model to simulate yield response to water: I. Concepts and underlying principles. Agron J 101:426–437.

Van Diepen C van, Wolf J, Van Keulen H, Rappoldt C (1989) WOFOST: a simulation model of crop production. Soil Use Manag 5:16–24.

Wallach D, Palosuo T, Thorburn P, Hochman Z, Gourdain E, Andrianasolo F, Asseng S, Basso B, Buis S, Crout N, et al. (2021) The chaos in calibrating crop models: Lessons learned from a multi-model calibration exercise. Environ Model Softw 145:105206.

Wermelinger B, Baumgärtner J, Gutierrez AP (1991) A demographic model of

assimilation and allocation of carbon and nitrogen in grapevines. Ecol Modell 53:1–26.

Xie Y, Wang P, Bai X, Khan J, Zhang S, Li L, Wang L (2017) Assimilation of the leaf area index and vegetation temperature condition index for winter wheat yield estimation using Landsat imagery and the CERES-Wheat model. Agric For Meteorol 246:194–206.

CHAPTER 3

Process-based deep learning model of hydroponic sweet pepper with attention mechanism and multitask decoders

ABSTRACT

The crop model is an important tool to support grower decisions. However, studies on crop models have been fragmented due to the differences in research purpose and scale. Focusing on the relatively low versatility of crop models compared to the ranges of related research fields, the way to enhance accessibility and adaptability for unifying crop models was tried. Since deep neural networks have no conventional modeling parameters, they can have diverse input and output combinations with the same structure depending on the model training. Despite these advantages, no process-based crop model has been tested in full deep neural network complexes. This chapter aimed to develop a process-based deep learning model for hydroponic sweet peppers. The attention mechanism and multitask learning were selected to process distinct growth factors from the environment sequence. The developed crop model, DeepCrop, recorded the highest modeling efficiency (= 0.76) and the

lowest normalized mean squared error (= 0.18) compared to accessible crop models in the evaluation with unseen data. With the high adaptability of DeepCrop, the developed model can replace the existing crop models as a versatile tool that would reveal entangled agricultural systems with analysis of complicated information.

Additional keywords: artificial intelligence, crop simulation model, DSSAT horticultural model, HyperOpt, WOFOST

INTRODUCTION

Process-based crop models have been developed and improved to support agricultural decisions on many scales and purposes (Gijzen et al. 1998; Jones et al. 2017; Peng et al. 2020; Katzin et al. 2022); with the process-based approach, the genotypic, environmental, and management influences on crops can be quantified (Muller and Martre 2019). Food and feed crop models in open fields are representative process-based crop models (Jones et al. 2017), and horticultural crop models in greenhouses are also frequently reported (Gijzen et al. 1998; Katzin et al. 2022). These crop models have been modified and improved for decades by various research groups in various regions for diverse purposes (Newbery et al. 2016; Chenu et al. 2017; Wang et al. 2017; Holzworth et al. 2018; de Wit et al. 2019).

Because of the variation in the crop models, they have become uncoordinated: a modification or an improvement in a crop model is not ensured for the applicability to another model. Regardless of the target crops and scales, studies on the models have redundancy problems in common (Wang et al. 2017; Peng et al. 2020; Chapagain et al. 2022; Katzin et al. 2022). In the decades-long course of the crop modeling progression, the methodology has been torn into pieces due to the differences in objectives and research scales, and the disjunction has resulted in more fragments and redundancy. In addition, some advanced models have been exclusively developed, so some

improvements have low accessibility (Antle et al. 2017; Altes-Buch et al. 2019; Katzin et al. 2022).

As a potential solution, deep learning algorithms were selected to mitigate fragmentation and redundancy. Deep learning has high applicability to broad target tasks as well as remarkable abstraction ability for enormous sets of data (LeCun et al. 2015; Koirala et al. 2019; Yang and Xu 2021). With its applicability, a complicated task conducted at the enterprise became accessible with a personal computer (Tan et al. 2021). A developed model can be adopted for heterogeneous tasks with entirely different inputs and outputs (Chorowski et al. 2015; Vaswani et al. 2017; Zhang et al. 2019), and a core algorithm in a model can be shared regardless of the research fields (He et al. 2016; Silver et al. 2017). Therefore, the crop model based on deep learning could be versatile and prevalent.

The objective of this chapter was to develop a deep-learning-based crop model with a full deep neural network structure, DeepCrop. DeepCrop could be applied for various purposes and scales based on the applicability of deep neural networks. The development protocol included model development and evaluation processes, so a similar methodology can conveniently be developed, resulting in higher accessibility.

From the perspective of relating the natural environment and crop growth, deep learning can be considered and used in many directions because of its high applicability (Kamilaris and Prenafeta-Boldú 2018; Benos et al. 2021; Osinga

et al. 2022). However, the high applicability of DeepCrop necessitates some requirements in practice: (1) the model should be constructed only with neural networks; (2) DeepCrop has to calculate growth changes internally, but the input for crop simulation after the model training should only be the crop environment; (3) The developed DeepCrop can interpret sequence data with process-based calculations; and (4) DeepCrop should be competitive compared to the existing crop models.

MATERIALS AND METHODS

Overall workflow

To satisfy the requirement, the attention mechanism was used for the core algorithm of DeepCrop (Vaswani et al. 2017). Attention mechanisms have showed high performance for the sequence data; and it can also be applied to various data types (Niu et al., 2021; Han et al., 2022). Therefore, the mechanism could be suitable for application to crop growth that is highly affected by time. The model was trained with data from sweet pepper (*Capsicum annuum* var. *annuum*) data. Crop environment and growth data were fed to the model for training, and the trained DeepCrop obtained daily environment and initial growth factors for a simulation (Fig. 3-1). To interpret each organ, the model had multiple decoders (Fig. 3-2). The model included some rules for a stable simulation (Fig. 3-3).

The model was designed to predict the growth and harvest per plant from the crop environment (Table 3-1). For the simulation, target crop growth and morphology were abstracted as big organs. Since sweet peppers have several organs for a long time, average growth factors could be diluted with the fully-grown organs; therefore, the simulation was based on the total values, not on the average ones. The average growth factors can be calculated with total values and the number of organs. Some growth factors, such as plant height, that cannot be inferred from the total values were from the original plant (Fig. 3-4).

Four cultivation periods in 2020–2021 were used for the model training, validation, and test. DeepCrop was trained and validated using the 2020 data, and the sufficiently trained model was test with the 2021 data. The 2020 data were randomly divided into the training and validation set. Detailed cultivational conditions were explained in Cultivation and crop management section.

The attention mechanism can interpret complex sequence data with faster computation (Niu et al. 2021). DeepCrop was mostly based on Transformer, and the core algorithms such as positional encoding, look-ahead mask, and multi-head attention were the same (Vaswani et al. 2017); however, since the main task for Transformer was classification, some structures had to be modified (Fig. 3-5). The modified structures were inspired by the difference that the object is not linguistic sentences but sets of concrete numerical values. The data in this study can be calculated with each other if necessary; therefore, embedding is designed not to reduce the dimension of the input, but to expand it to contain diverse features. In this regard, input and output embedded by concatenating convolutional layers with different receptive fields to mimic the window in Word2Vec (Mikolov et al. 2013). The embedding layers were required to match the dimension of internal data processing. Therefore, input and output embedding layers had the same number of nodes. A gate for residual calculation was added because raw input before the encoding is also important for the target output.

Multitask decoders were added to predict each target group. The decoders had the same structure for applicability. Transformer can deal with the sequences regardless of the input and output length; however, the number of cultivations was limited, so the model should partially receive and predict the environment and growth. Therefore, the input and output length were fixed with a parameter named as memory length. The output dimensions of the multitask decoders were set to be same with the memory length. The unit of the memory length supposed to be days, so the input length was determined as 24 times of the memory length. The dimension of the datasets was matched to be same based on the batch size and the memory length. Therefore, DeepCrop always processed the same dimension of data, so the padding mask of the attention mechanism were not used in this study. Meanwhile, the positional encoding was required to mark the position of each input and output vector, although the data dimension was fixed.

The reasoning of DeepCrop was tested after the model training using two-dimensional t-distributed stochastic neighbor embedding (t-SNE) and attention weights. Both methods are generally used to explore black-box condition of the deep learning models (Mnih et al., 2015; Medina and Kalita, 2018). Some physiological tendencies, such as developmental stages, were verified.

The loss function was set to the mean squared error (MSE). The MSE of each decoder was independently calculated. To maintain the relationships among the decoders, the total fresh weights (FWs) and dry weights (DWs) of

vegetative organs were also compared. All MSEs were averaged and traced in the model training session.

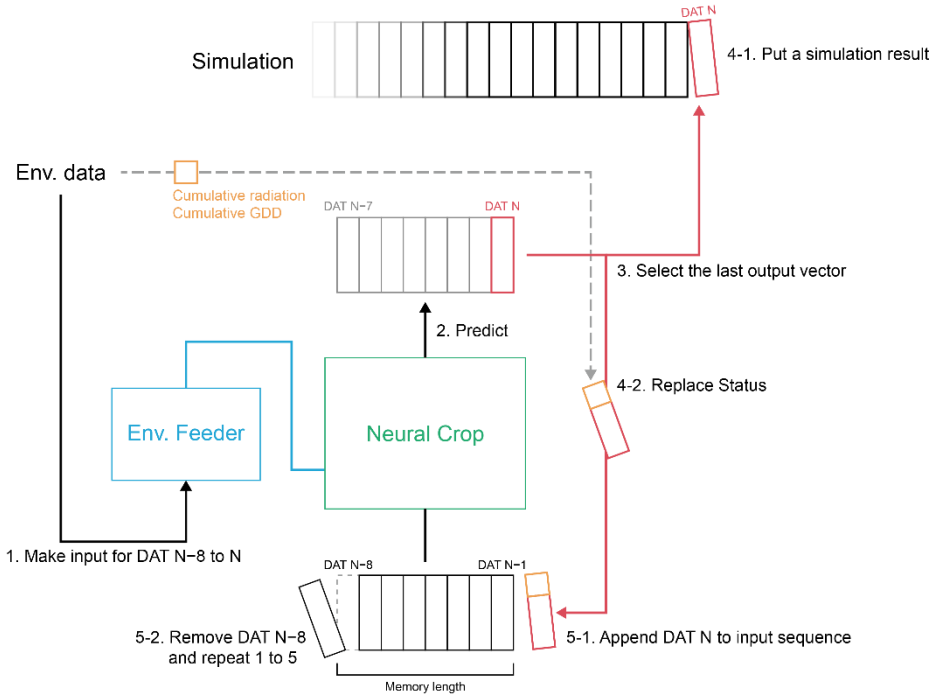

Fig. 3-1. Simulation procedure of the trained DeepCrop.

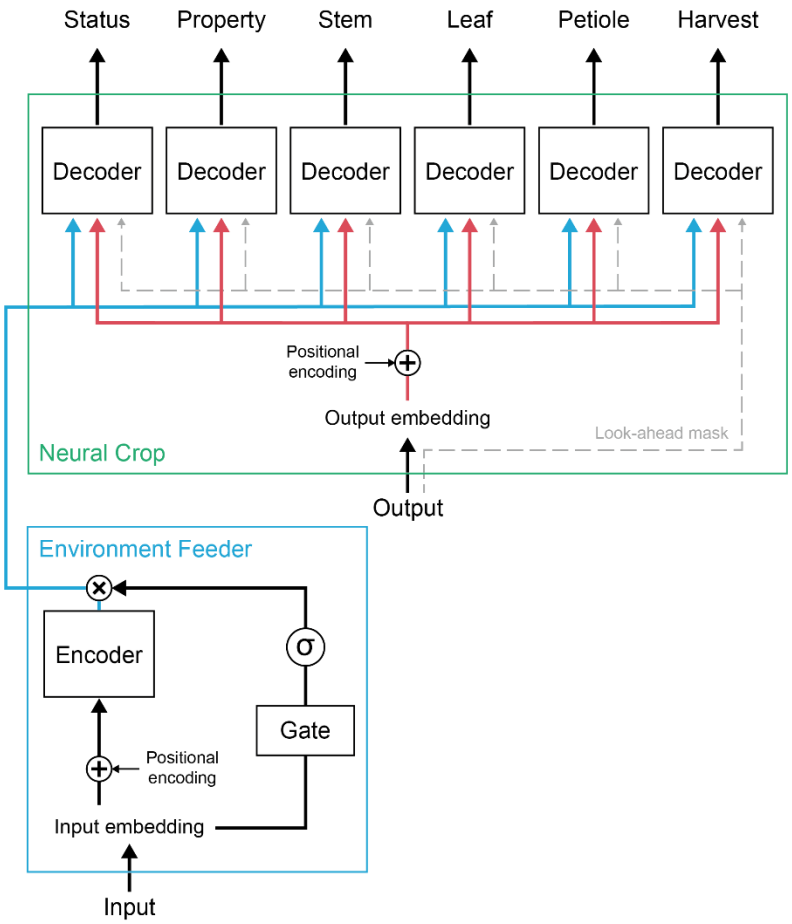

Fig. 3-2. Simulation model structure. In this study, multitask decoders and an input gate were added to the original encoder and decoder of the original Transformer algorithm. Refers to Fig. A3-1 for the detailed structure of the embedding layer.

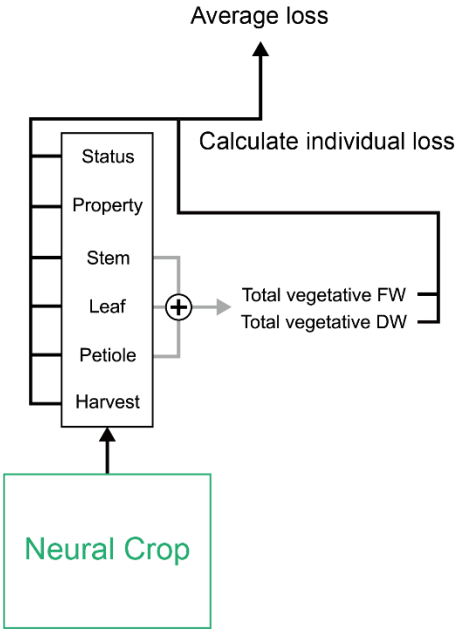

Fig. 3-3. Target loss objective of the model training. In this study, the loss function was mean squared error.

Table 3-1. Ranges of environmental data used for the experiment.

Group	Factor
Input	Internal temperature (°C)
	Internal relative humidity (%)
	Radiation (W m^{-2})
	Daily difference between the day and night temperature (°C)
	Daily cumulative radiation (kJ m^{-2} d^{-1})
	Cumulative growing degree days
	Calculated daily vapor-pressure deficit (kPa)
Status output	Total Cumulative radiation (MJ m^{-2})
	Cumulative growing degree days
Property output	Plant height (m)
	Maximum number of nodes per stem
Organ output	Leaf area (m^2)
	Total summation of node lengths (cm)
	Total summation of node diameters (mm)
	Total summation of harvested fruit heights (cm)
	Total summation of harvested fruit widths (cm)
	Number of organs
	Organ fresh weights (g)
	Organ dry weights (g)

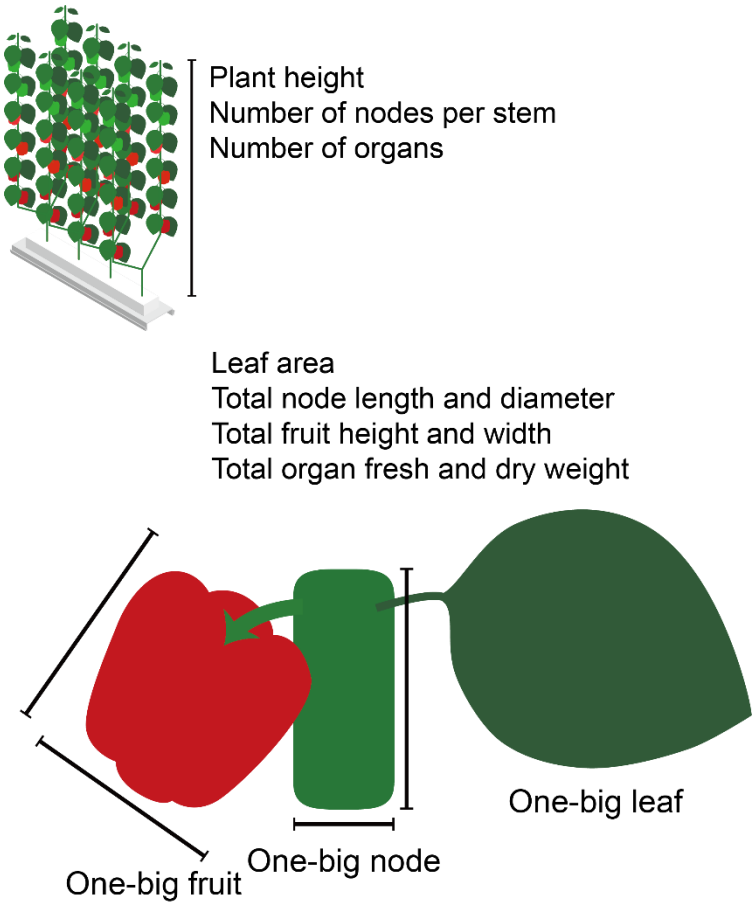

Fig. 3-4. Modeling concept. Target crop growth and morphology were abstracted as big organs. Averages can be calculated with total values and the number of organs.

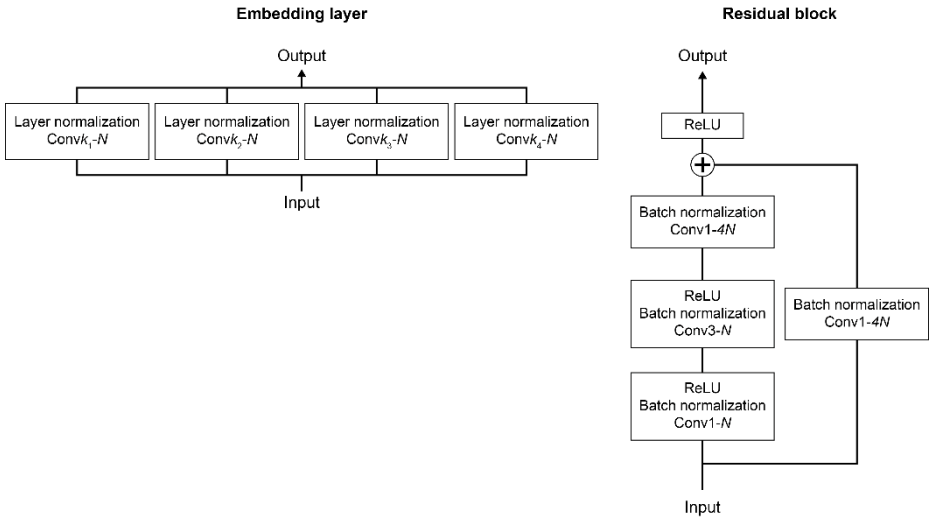

Fig. 3-5. Embedding layer for DeepCrop and residual block used for the 1D ConvNet model. Parameters for Conv are denoted as "{type of layer}{kernel size}-{number of filters}." N was set before the training as a hyperparameter. k1 to k4 for input were 1, 12, 24, and 48; those for output were 1, 2, 3, and 4.

Data preprocessing for the model training

Since the training process of DeepCrop was based on supervised learning, daily growth data in the cultivation periods had to be secured as labels; therefore, scarce growth data should be augmented. Using the output of regression or an existing formula is a way to augment the data, but it could affect the model results and lower the model accessibility. In this study, the scarce growth data and their standard deviations were interpolated linearly, and the daily output was randomly augmented (Fig. 3-6). The start date of the cultivation was set to 50% of the first growth data.

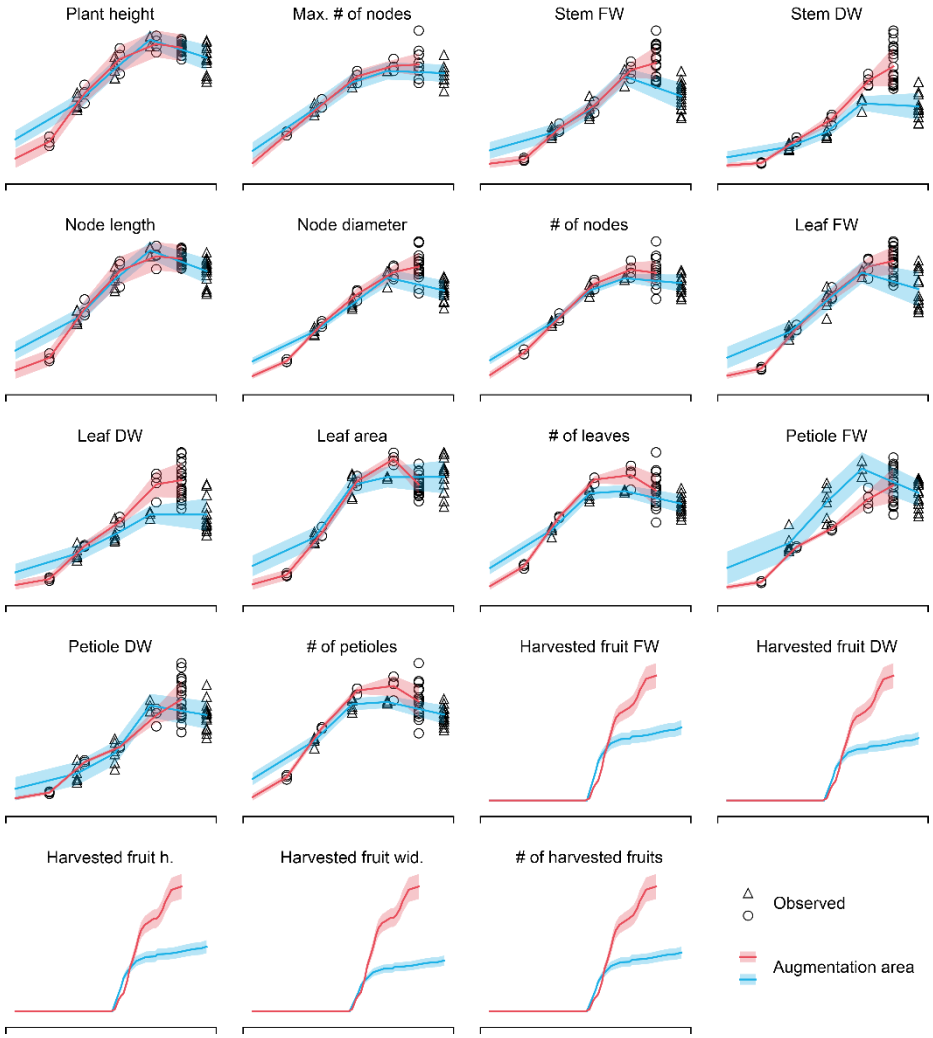

Fig. 3-6. Distribution of noised growth factors for the model training. Red and blue colors represent the first half and the second half of 2020, respectively.

Training, validation, and evaluation process.

The core algorithm of DeepCrop was the attention mechanism, so the model training and evaluation process were separated. At the training session, DeepCrop was fed sets of environment data, previous growth factors, and the target output. Since the previous growth factors do not simultaneously exist in a practical simulation, DeepCrop output recursively replaced previous growth factors. The last output vector of the output sequence was selected as the daily predicted output. The data from 2020 were used for the training and validation datasets, and those from 2021 were used for the test datasets. Cumulative temperature and radiation can be calculated with the environment data. The cumulative input factors were replaced by the measured data in practice to guide the trained DeepCrop; however, the values were not replaced to prevent training failure in the model training.

Existing crop models and deep learning models for comparison

Some accessible crop models were compared as an existing method: a simple generic crop model (SIMPLE, Zhao et al. 2019), a sweet pepper growth model for a decision support system (SW-DSS, Sánchez-Molina et al. 2015), food and feed crop models from World Food Studies (WOFOST, de Wit et al. 2019), and a sweet pepper model of Decision Support Systems for Agrotechnology Transfer (DSSAT, Hoogenboom et al. 2019). Some models were modified for comparison. The SIMPLE model yields total dry mass,

including reproductive organs; in this study, the value was changed to vegetative dry mass with a harvest index of >1. SW-DSS had an ambiguous LAI equation, so the equation changed to Eq. (3-1) based on the definition of the Gompertz growth function (Scaife and Jones 1976).

$$LAI_t = LAI_{max}\exp(\log\left(\frac{LAI_{init}}{LAI_{max}}\right)\exp\left(-C_{pLAI} \times TS\right)) \quad (3\text{-}1)$$

where LAI_{max} is the maximum LAI, LAI_{init} is the initial LAI, C_{pLAI} is a tuning parameter of the Gompertz function, and TS is the thermal time of the plant (°C d^{-1}). SW-DSS originally had a temperature-dependent gamma star for the photosynthesis calculation, but it was also calibrated as a coefficient in this study.

EF and NRMSE were selected to compare DeepCrop and the other crop models (Nash and Sutcliffe 1970; Wang et al. 2017). Since no model could cover every output of DeepCrop, the performance was calculated with the partial output, and the units of model output were converted as per plant similar to DeepCrop. Petiole FW and DW were aggregated to those of stems when the crop models could not calculate petioles independently. The leaf area index was converted to the leaf area using planting density for the models that calculated only the leaf area index. Planting density was adjusted for the crop models that were completely biased because of the conversion (Table 3-2). All models assumed sufficient irrigation without water stress.

The crop models were calibrated using the data from 2020 that were the same as the training and validation data of DeepCrop (Tables A3-1, A3-2, A3-

3, A3-4). The sweet pepper model of DSSAT was calibrated using Generalized Likelihood Uncertainty Estimation (GLUE), a built-in coefficient calibrator (He et al. 2010), and a recently calibrated model was also compared (Lee et al. 2021); the other models were calibrated using a hyperparameter optimizer algorithm, HyperOpt (Bergstra et al. 2015).

As a shallow deep learning model, a feedforward neural network (FFNN), long short-term memory (LSTM), and convolutional neural network (ConvNet) were compared. The models are representative structures of deep learning algorithms. Since the shallow models cannot efficiently interpret the same DeepCrop input and output, the optimal data structure for each model was applied (Table A3-5). The deep learning models were set as a predictor, not a process-based model; therefore, the growth factors were not recursively reprocessed by the models. Hyperparameters for the model construction and training were empirically selected (Table A3-6). The average of the growth factors in 2020 was used as a baseline.

Table 3-2. Adjusted planting density of 2020-2 for the compared crop models.

Crop model	Value
Original	5.95
DSSAT	2.00
WOFOST	5.95
Sánchez-Molina et al. (2015)	2.56
SIMPLE	3.70

Cultivation and crop management

Sweet peppers (*Capsicum annuum* var. *annuum*) were cultivated in a Venlo-type greenhouse at the experimental farm of Seoul National University, Suwon, Korea (37.3°N, 127.0°E). The cultivations were conducted twice a year, and the total number was four, under various conditions (Table 3-3).

Open-loop hydroponic systems were used for all cultivations. Two or four cultivation lines from the total eight lines in the system were used for the experiment. A stone wool slab and cubes (Grodan GT Master, Grodan, Roermond, the Netherlands) were used as substrates for all cultivations. Two main stems of the crops were maintained with trellis strings. PBG nutrient solution from the Netherlands was used for irrigation. Electrical conductivity (EC) of the nutrient solutions was maintained between 2.6-3.1 dS m^{-1}. The fruits were harvested two to three times a week when the surfaces of the fruits were mostly colored.

Table 3-3. Cultivation and management conditions.

Condition	2020–1	2020–2	2021–1	2021–2
Planting date	Feb 26	Oct 26	Mar 8	Oct 23
End date	Jul 7	Jan 25	Jul 5	Jan 19
Planting density (plants/m^2)	4.08	3.06	5.95	3.06
Number of plants	96	84	65	36
Cultivar	Scirocco	Mavera & Florate	Mavera & Florate	Mavera
Topping date	Jun 15	Dec 5	-	-

Data collection

In this study, aerial environment data were used for the crop simulations. Temperature and relative humidity were measured using a complex sensor (AQ3020, Aosong Electronics, Guangzhou, China); radiation was measured using a pyranometer (SQ-110, Apogee Instrument Inc., Logan, UT, USA). The collected data were saved on a cloud platform (ioFarm, ioCrops Inc., Seoul, Korea). The missing environmental data were interpolated using linear interpolation and U-Net (Moon et al. 2021).

The growth data were collected with the destructive investigation. The investigation was conducted five times for each cultivation except the cultivation in the latter half of 2021. At that time, the crops were investigated only at the end of the cultivation to exclude biases from crop population decrease. For organ DWs, destructive organs were dried for 72 hours at 80 °C in a forced-air drying oven (HB-503LF, Hanbaek Co. Ltd., Bucheon-si, Gyeonggi-do, Korea). Since by the destructive investigation varied the number of plants, the harvest data were normalized to fruits per plant using the total number of crops.

Leaf area was measured from the image using Easy Leaf Area (Easlon and Bloom, 2014). Plant height was calculated from the higher value between summations of the node lengths of each stem. The other length factors were measured using a digital vernier caliper.

For the processed input factors, growing degree days (GDD) were

calculated by daily average temperature and the base temperature (T_{base}).

$$\text{GDD} = \frac{\sum_{t=0}^{23} T_t}{24} - T_{base} \quad (3\text{-}2)$$

where T_t hourly temperature of the day. T_{base} was set to 10. Vapor-pressure deficit (VPD) was calculated from saturation vapor pressure (SAP) using temperature and relative humidity (Eqs. 3-3, 3-4).

$$\text{SVP} = 0.6113 \times \exp\left(5423\left(\frac{1}{273.15} - \frac{1}{273.15+T}\right)\right) \quad (3\text{-}3)$$

$$\text{VPD} = \text{SVP}\left(1 - \frac{RH}{100}\right) \quad (3\text{-}4)$$

where T is greenhouse temperature (°C) and RH is relative humidity (%).

Computation

AdamOptimizer was used to train deep learning models (Kingma and Ba 2017). Batch and layer normalizations were used for regularization (Ioffe and Szegedy 2015; Ba et al. 2016). A deep learning library in Python, TensorFlow (v. 2.6.0), was used to build the model (Abadi et al. 2016). All deep learning computations were conducted using a Linux server with one CPU (ThreadRipper 2990WX, AMD, Santa Clara, CA) and one GPU having 35.58 TFlops (RTX 3090, NVIDIA, Santa Clara, CA). The existing crop models were simulated only with CPUs.

RESULTS

Simulated crop growth from DeepCrop

Trained DeepCrop was evaluated with the data from the first and the second halves of 2021, represented as 2021-1 and 2021-2, and it showed reasonable simulations for the test data (Figs. 3-7, 3-8). The output tendencies were varied, although the model shared the same encoder. Some simulation results showed a declining section in the middle of the cultivation. DeepCrop somewhat overestimated the vegetative growth factors after 100 DAT; the final predicted FW and DW of total vegetative organs were > 19% and > 30%, respectively. The tendency was evident for the FWs of 2021-1, although the final total FW in 2021-2 was overestimated with > 30%. For the tendency of harvested fruits, the simulated factors of 2021-1 were similar to the observed values, and those of 2021-2 were not. The value in 2021-2 was already saturated at > 0.2 kg per plant in DAT 130. However, the final FW and DW of harvested fruits could be accurately predicted in 2021-2. Overall, the simulation reasonably followed the tendency of the observed growth for the diverse target factors without considering the interactions of each factor and the relevant formula.

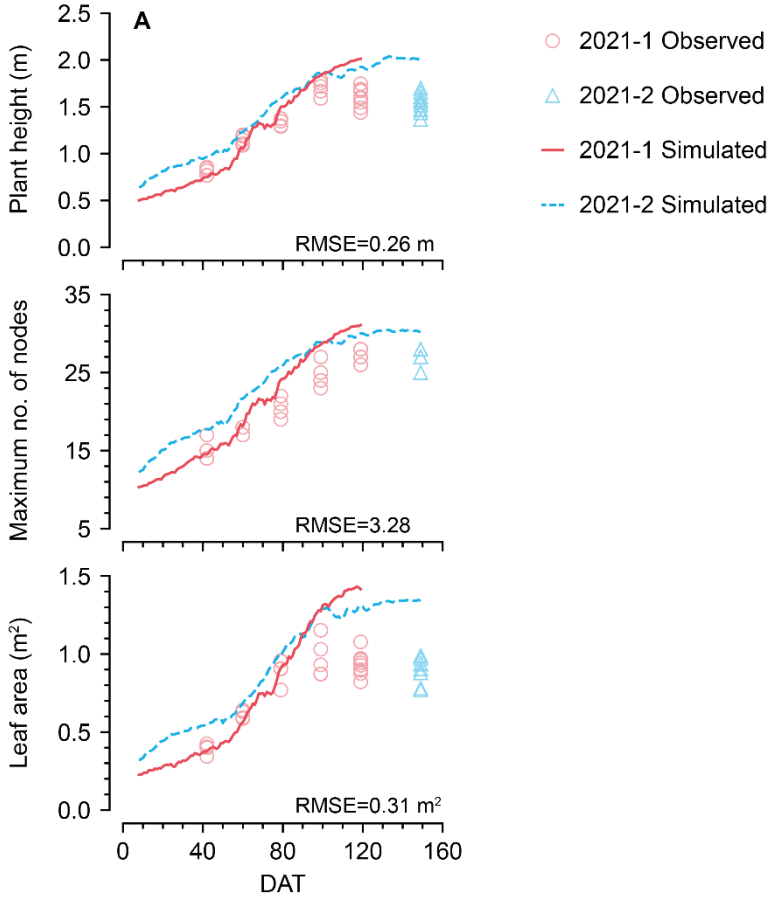

Fig. 3-7. Simulated physiology from DeepCrop. (A) Property output and leaf area. Leaf area was predicted by the Leaf decoder. (B) Simulated number of organs. (C) Total summation of node lengths, node diameters, harvested fruit length, and harvested fruit height. All data represent the value per plant.

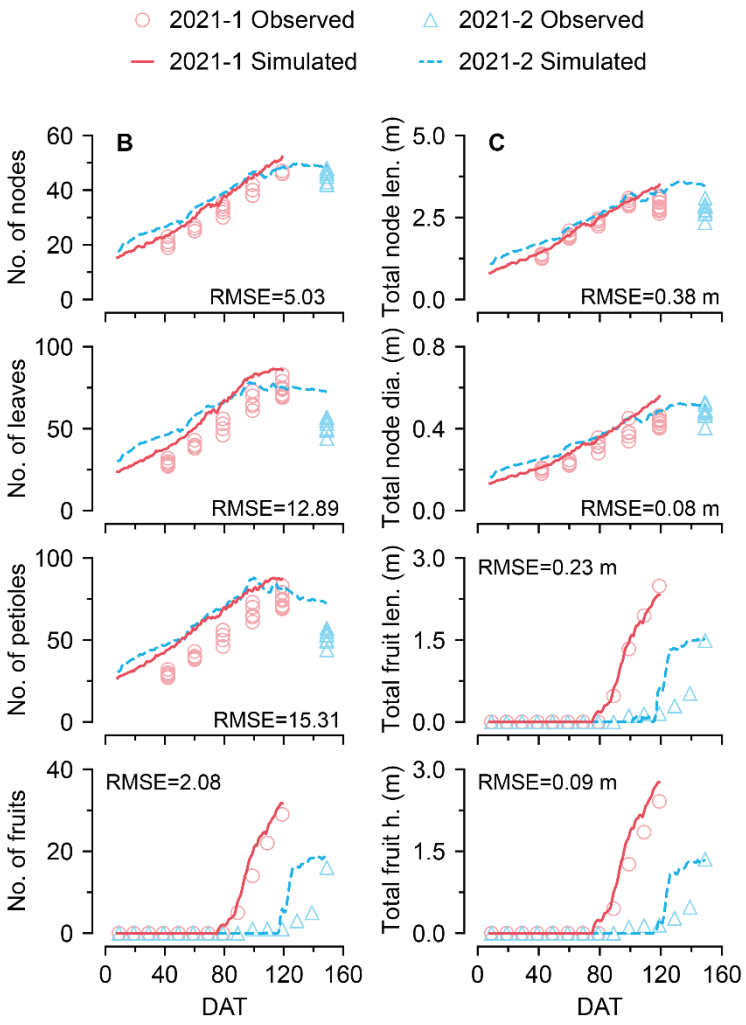

Fig. 3-7. (Continued from the previous page).

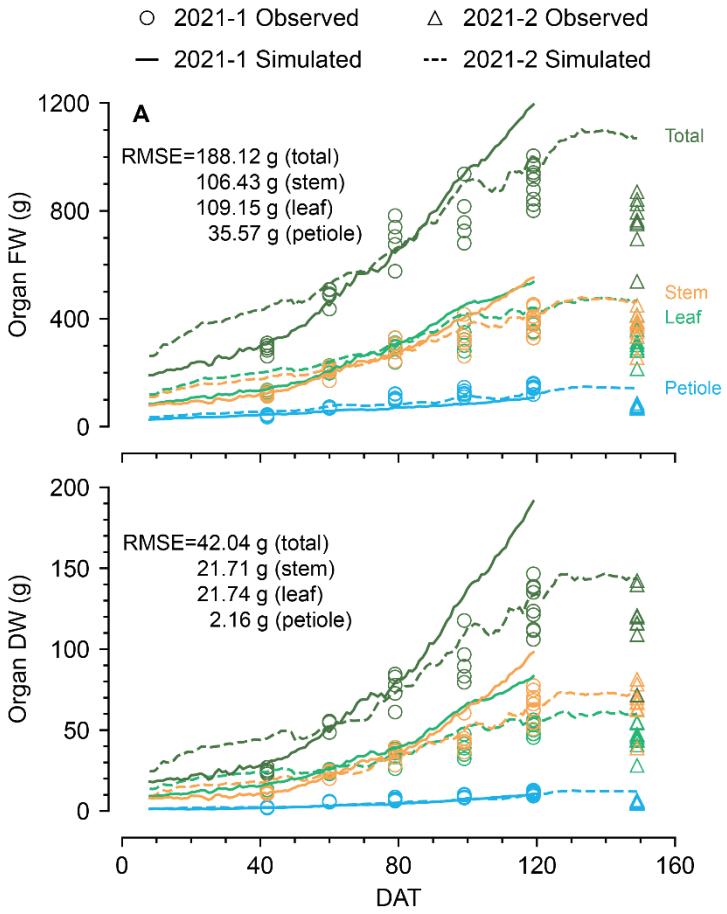

Fig. 3-8. Simulated assimilation results from DeepCrop. (A) Fresh weights (FWs) and dry weights (DWs) of the vegetative organs. (B) cumulative FWs and DWs of the harvested fruits. All data represent the value per plant.

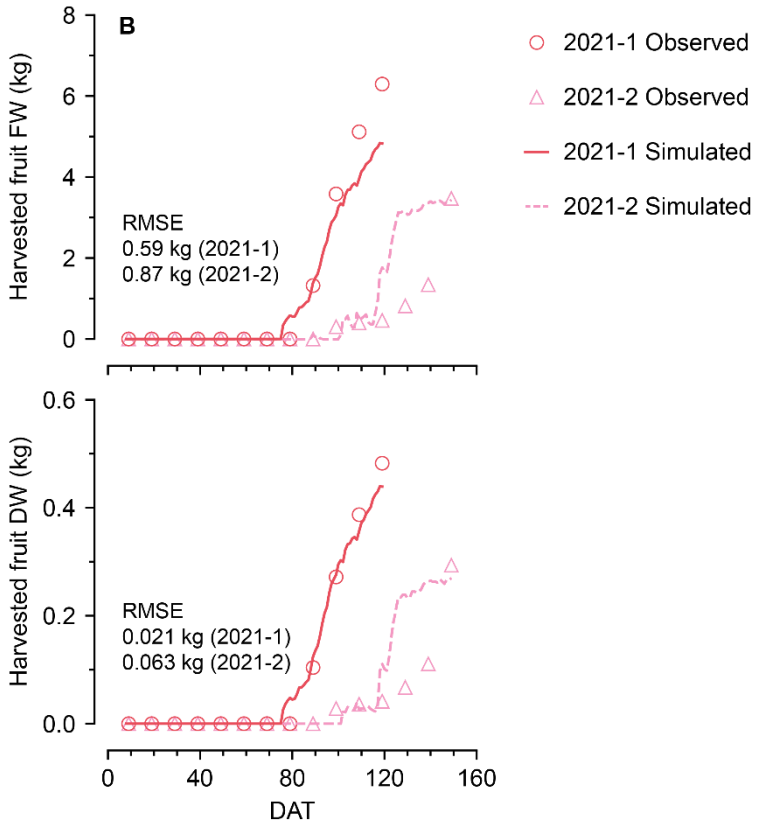

Fig. 3-8. (Continued from the previous page).

Model evaluation and comparison

DeepCrop was compared with existing accessible process-based crop models and simple predictors based on deep learning algorithms. Modeling efficiency (EF) and normalized root mean squared error (NRMSE) showed different tendencies; however, DeepCrop recorded the highest EF (= 0.76) and the lowest NRMSE (= 0.18) compared to the other accessible models, although advanced horticultural models such as HORTISIM could not be listed (Fig. 3-9). According to EFs, food and feed crop models were not effectively calibrated for sweet pepper showing lower EFs than the average of 2020, although the targets were limited to organ DWs; however, two calibrated models recorded the lowest NRMSE among the compared models. The crop models that initially targeted sweet pepper were also unable to simulate the given data except for the calibrated DSSAT models. SW-DSS showed the lowest EF of < 0.2 among the calibrated models, and the DSSAT models with original parameter sets seemed to be biased showing negative EFs. The calibrated DSSAT models showed competitive EF (= 0.67) and NRMSE (= 0.26); however, these models adjusted the planting density to two times higher value for the unit conversion from value per ha to value per plant. That is, the compared FWs, DWs, and leaf area were 200% of the original simulation from the DSSAT models.

For the deep learning models, long short-term memory (LSTM) showed the highest performance with the EF of 0.58 and NRMSE of 0.25, but it was not simply comparable because the deep learning models were not process-

based. Specific results of the compared models are given in Supplementary Material.

According to the ablation test showing the negative EFs, adequate selection of the input features was the most deterministic factor of DeepCrop performance (Fig. 3-10A). Not every input feature was adequate for the simulation; adding more information did not ensure higher performance. Providing cumulative input and manipulated input improved the model performance. For the loss objectives, dividing the loss for each decoder made the model converge because unified loss also showed the negative EF (Fig. 3-10B). Domain knowledge, such as the loss of total FWs and DWs, was also enhanced the model robustness with increasing EF by 0.2. Similar to the input features, more loss objectives based on trivial plant physiology did not ensure model convergence. All structural ablations decreased the EF from 1.2 to 0.1, and the existence of the decoders was the decision factor increasing the EF the most (Fig. 3-10C). Excluding the original attention mechanism and modified algorithms also decreased model stability also showing negative EFs. Increasing the memory length that determined the output length for the decoders did not guarantee an improvement in model performance showing lower EFs and higher NRMSEs (Fig. 3-10D).

The t-SNE results showed two distinctive clusters (Fig. 3-11A). Environment and growth factors did not perfectly reflect the division; however, the factors were primarily divided into high and low values. Four cultivations

did not have a completely different distribution, but the harvest decoder showed distinct distributions of harvested fruit DW for the first and second half of the year. The input sequences were utilized in balance according to the attention weights (Fig. 3-11B). The attention tendencies of the Leaf and Harvest decoders were different. In the latter part of the cultivation, both attentions were relatively narrowed according to the increased dark regions.

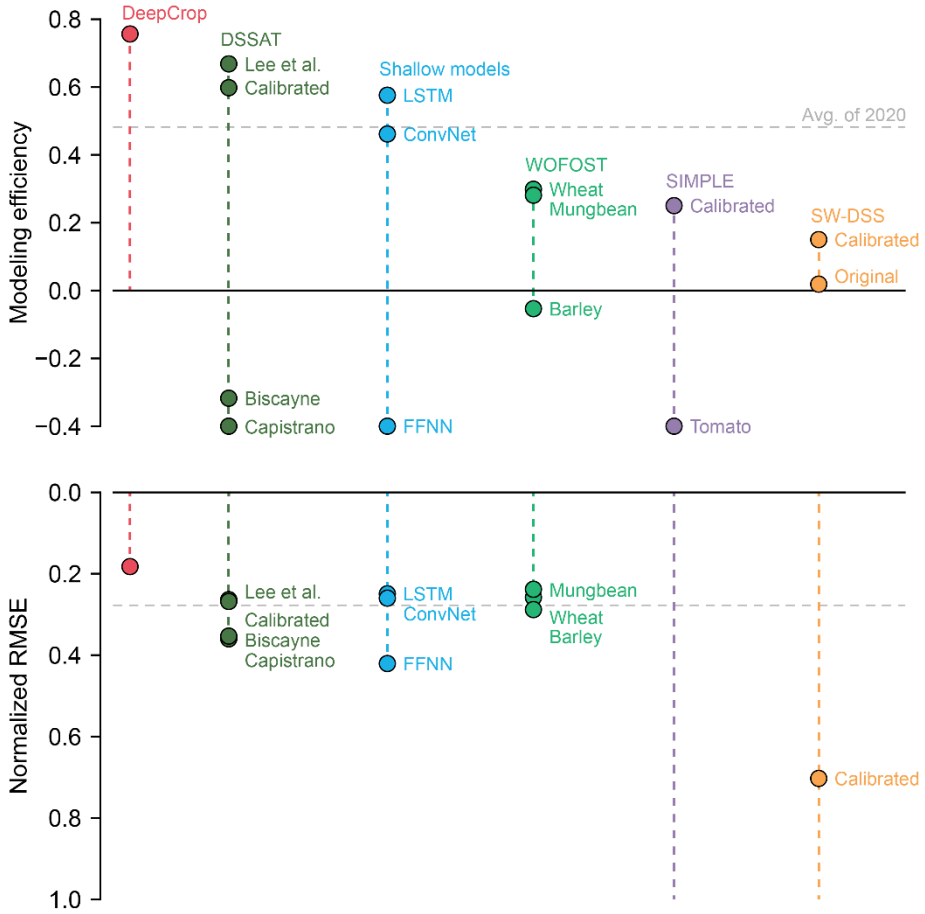

Fig. 3-9. Model performance of existing models. The modeling efficiency and normalized root mean squared error (normalized RMSE) were calculated using the 2021-2. FFNN, LSTM, and 1D ConvNet represent feedforward neural network, long short-term memory, and one-dimensional convolutional neural network, respectively; WOFOST, DSSAT, SIMPLE, and SW-DSS represent World Food Studies, Decision Support System for Agrotechnology Transfer, a simple crop model, and a sweet pepper model for a decision support system, respectively. For WOFOST, the top three calibrated models were depicted. The normalized RMSEs out of the axis boundary were omitted.

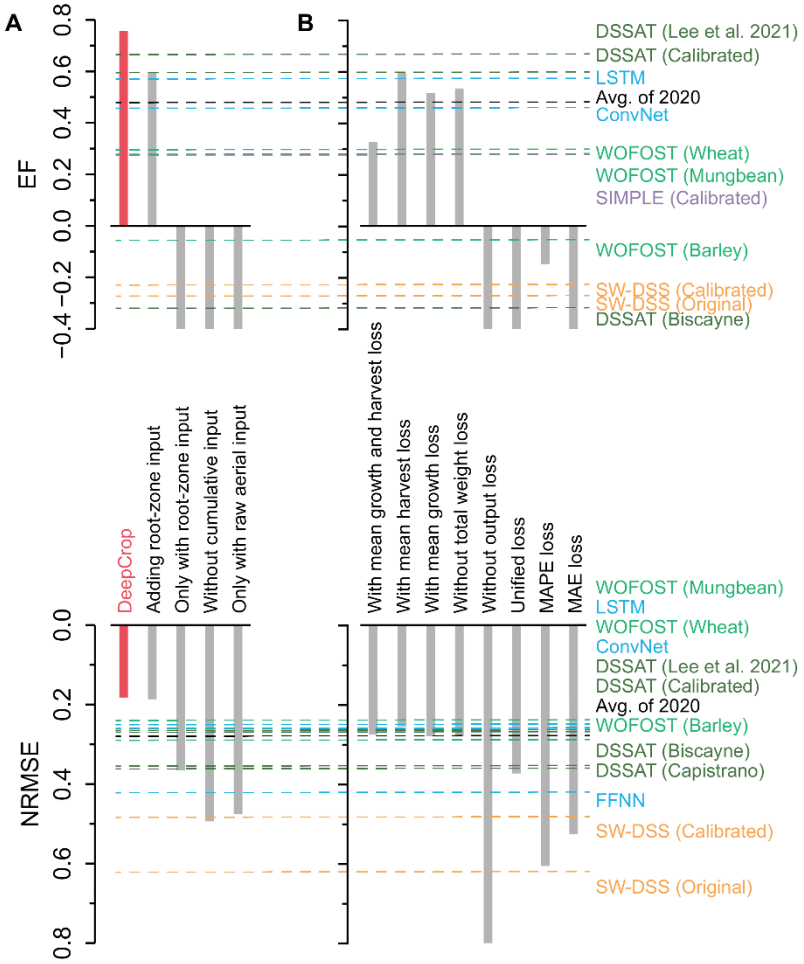

Fig. 3-10. DeepCrop with ablation. The dashed lines are the accuracy of the corresponding models. The ablation test was conducted for variations in (A) input, (B) training procedure, (C) model structure, and (D) memory length. The results outlying the depicted axis are not shown.

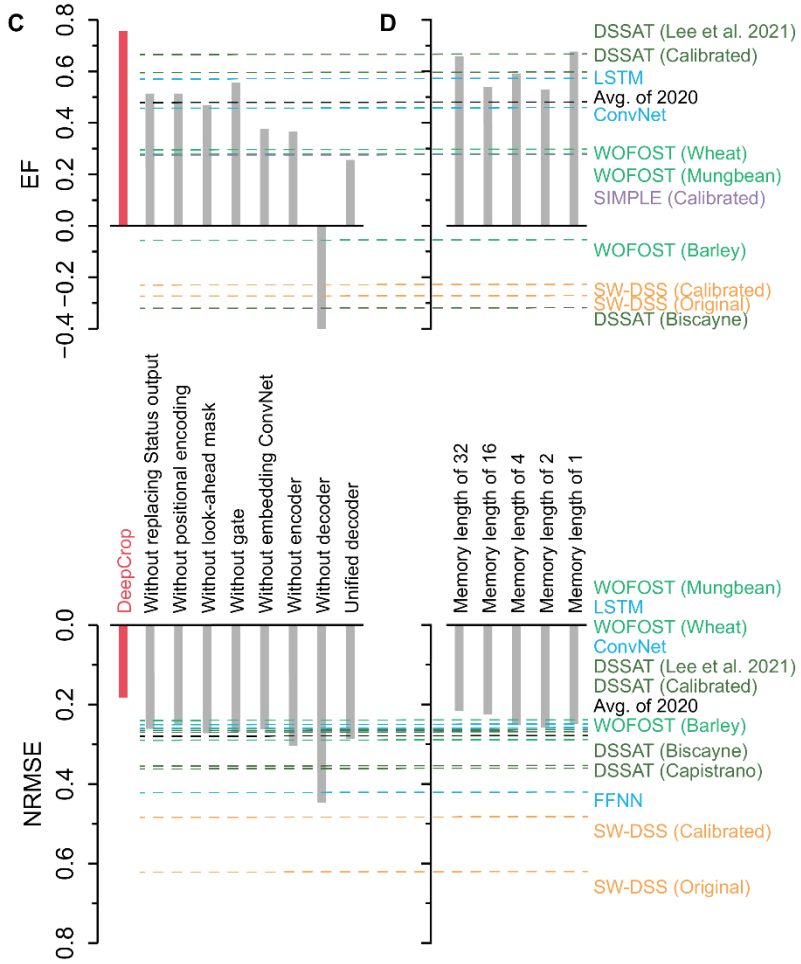

Fig. 3-10. (Continued from the previous page).

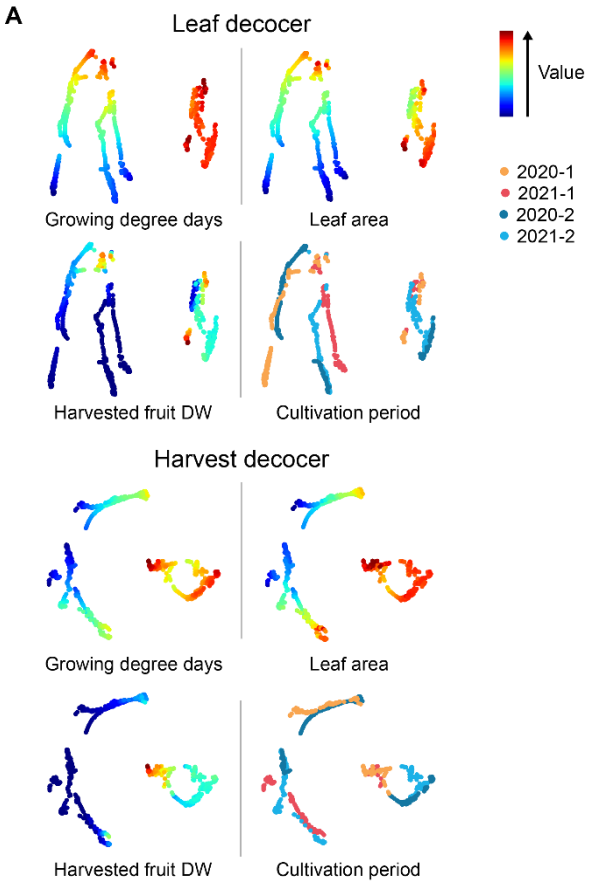

Fig. 3-11. Two-dimensional t-distributed stochastic neighbor embedding (t-SNE) for the output of the last hidden layer (A) and attention weights (B) yielded by the Leaf and Harvest decoders. Fully-trained DeepCrop was used to yield the output. Two decoders were selected as representatives of the vegetative and reproductive representations. Attention weights were extracted from the DAT 20 and 80 to represent the early and later part of the cultivation, respectively. The columns of the attention weight yielded from each head in the attention mechanism. Only 2021-1 data were used for the attention weights.

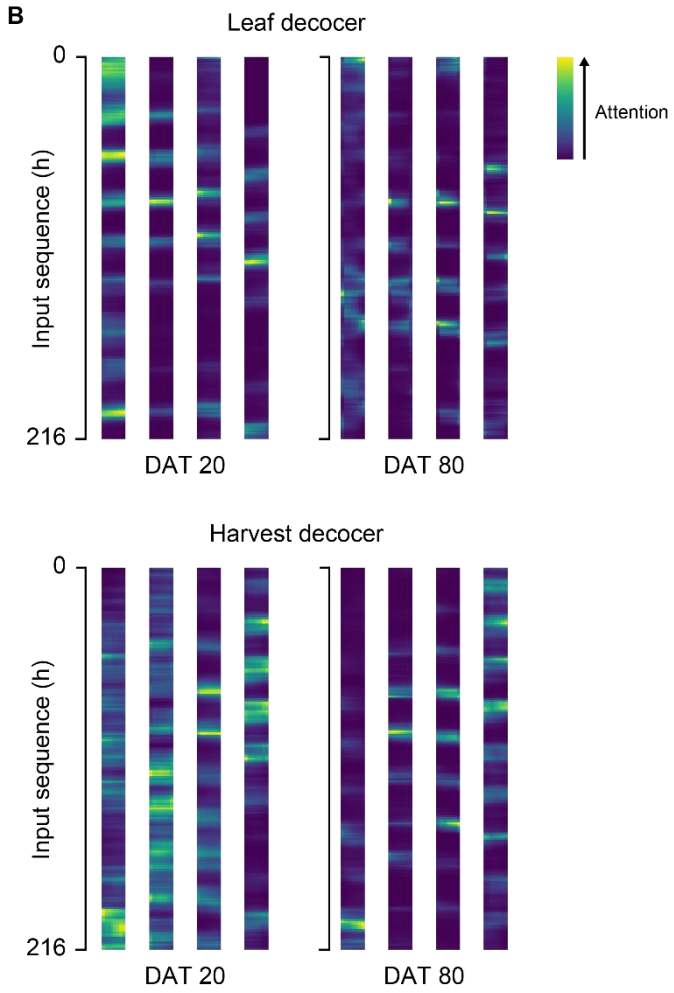

Fig. 3-11. (Continued from the previous page).

DISCUSSION

Attention mechanism with multitask decoders was able to interpret the interactions of crop and environment with high performance. It has been reported that sharing root layers and dividing the tasks that have similarities but differ in the final output can improve the performance (Caruana 1997; Ruder 2017a). Therefore, multitask decoders could be the core structure. In this study, the neural network models with shallow structures also showed acceptable scores. Theoretically, it has been verified that one layer of neural networks can interpret all forms of functions (Hornik 1991). Crop growth is a relatively simple target for deep learning algorithms, so shallow models can achieve high performance if the models are technically well fitted. However, the compared deep learning models did not receive crop growth as input; the models were a predictor, not a process-based crop model. Therefore, shallow models cannot interpret large datasets with several differences in crops, scales, etc. In addition, Transformer is faster in calculation, and the model can have a deeper structure (Vaswani et al. 2017), and the performance gap between LSTM and DeepCrop could increase with the amount of data.

Understandably, sweet peppers in greenhouses could have a significant disjunction with food and feed crop models for open fields. Crop models in WOFOST share the same physiology module (Van Diepen et al. 1989; de Wit et al. 2019), but it seems that the module significantly differs from sweet

peppers. However, the original sweet pepper models also failed to simulate the test data. The existing models without adjusted planting density were not compatible because they yielded the low accuracies despite the calibration. Therefore, it can be said that the functions in crop models are overfitted to their dataset and research scales. Crop model ensembles or simplified estimation factors could improve simulation performance (Wang et al. 2017; Müller et al. 2021; Kimm et al. 2021); however, the methodologies cannot be a fundamental solution for overfitting, resulting in fragmentation of the crop models.

For DeepCrop, the model selection and training did not require a meticulous understanding of the plant physiology and crop modeling; consideration of suitable functions and parameters was not essential. Existing crop models must modify the innate functions if the model robustness cannot be secured with calibration for new data (Xu et al. 2010; Hsiao et al. 2019; Kimm et al. 2021). On the other hand, the same deep learning models can be retrained for the new task in any case (Zhuang et al. 2020; Qiu et al. 2020); even if a model with better performance appears, that model also has the same properties under deep learning. For example, the developed DeepCrop did not include CO_2 concentration as input, but the value can be added, similar to the ablation test (Fig. 3-10D). Therefore, DeepCrop can be retrained using the same methodology, including a new dataset such as CO_2 fertilization, and it can improve the accessibility to crop models.

DeepCrop simulation adequately followed the growing tendency from

scratch according to the high EF, but the model should be inspected because it could be potentially improved. Specifically, DeepCrop overestimated the test data despite the high score. This seems to be due to the difference in cultivation management, such as planting density and pruning. Crop growth was somewhat insufficient because of some inhibitory factors such as high planting density and unfavorable weather; therefore, fruiting was deliberately delayed, which resulted in an inverse tendency of cumulative harvested fruits. That is, the data were insufficient to interpret hidden physiological patterns perfectly, so DeepCrop depended too much on the last cultivation. However, the model was adequately trained according to the simulation result. This yielded different results for 2021-1 and 2021-2. The model recognized seasonal differences that were difficult to grasp with only a given input. Similar to the other models, it was impossible to fully comprehend the phenology of sweet pepper with four cultivation datasets. Nevertheless, the model was adequately trained with limited conditions; therefore, the simulation result concretely showed the potential of DeepCrop for the larger datasets. More types of data will enable the identification of clear growth patterns and an understanding of crops without human knowledge (Silver et al. 2017). In addition, DeepCrop is still a black box model, but the studies to reveal the reasoning process are ongoing (Wang and Yeung 2016; Angelov and Soares 2020); DeepCrop can learn the intermediate output such as assimilation from a sufficient number of data and features, and it can also make the model explainable (Newman and Furbank

2021).

The t-SNE distribution also supports that the recognition of the growth pattern of DeepCrop can be analyzed out of the black box. DeepCrop could interpret the relationship between the environment and growth without being biased by a certain factor. Four cultivations did not show completely different distributions, and the developed model was not biased to a certain cultivation period. In particular, two clusters can be regarded as vegetative and reproductive stage divisions. The attention weights showed different tendencies by the crop development stage and the output decoder. Differences by input factors also showed, although it was relatively weak. The weights could include the detailed information about the environmental influences on crops. Therefore, more datasets would enable the analysis of DeepCrop reasoning.

Currently, since the data are scarce because of the characteristics of the crop production, all processes, including input feature selection, model construction, model training, best model selection, and model test must be carefully conducted. For the input used in this study, growing degree days, vapor-pressure deficit, and the difference between the day and night temperature are often used for crop modeling (Xu et al. 2010; de Wit et al. 2019; Hammer et al. 2019). Therefore, utilizing domain knowledge with insufficient data could improve model convergence. However, careless repetition of redundant information can cause overfitting. According to the ablation test, excessive input features in the small dataset caused overfitting, although deep

learning can autonomously extract features from raw data. Applying an end-to-end deep learning framework seems premature (Lischeid et al. 2022), so the balance should be kept in input feature selection.

The training process was also able to influence the robustness of crop modeling. Dividing the loss function by the multitask learning was adequate for the model performance, but too many loss objectives resulted in counter effects. Gradient descent is linear-algebraically sophisticated (Panageas and Piliouras 2016; Ruder 2017b). Better loss objectives should be found for obvious objectives such as the number of leaves equal to the number of petioles. Specializing tasks and trainable losses with more features can yield a stable and accurate model. For the output setting in the training process, guiding the output with known values also slightly improved the model performance. However, guiding only with Status output was not that effective, so more variations of guiding output should be identified.

The discordance in metrics showed the necessity of diversified evaluation for deep learning models that are hard to analyze the reasoning process. The main problem could be a scarcity of labels. Finding adequate metrics for scarce data or continuous measuring devices to increase the number of labels should be introduced.

CONCLUSION

In this study, a process-based crop model that was fully constructed with deep learning algorithms was developed and evaluated. DeepCrop consists of an attention mechanism and multitask decoders. Trained DeepCrop showed the highest accuracy in selected metrics, EF and NRMSE. With the precedents in the other research fields, the model can be trained only with raw data without domain knowledge. DeepCrop does not require consideration of the internal formula corresponding to the changes in input features, so the same structure can be applied to various studies unless the target task is identical. In this study, advanced horticultural models were not compared; since the model structure and the relevant workflow are explained, further studies that compare DeepCrop to those models can be conducted. Therefore, developed DeepCrop can improve the accessibility of crop models and mitigate fragmentation problems in crop model studies.

LITERATURE CITED

Abadi M, Barham P, Chen J, Chen Z, Davis A, Dean J, Devin M, Ghemawat S, Irving G, Isard M, et al. (2016) TensorFlow: A System for Large-Scale Machine Learning. In: 12th USENIX Symposium on Operating Systems Design and Implementation (OSDI 16). USENIX Association, Savannah, GA, pp 265–283.

Altes-Buch Q, Quoilin S, Lemort V (2019) Greenhouses: A Modelica Library for the Simulation of Greenhouse Climate and Energy Systems. pp 533–542.

Angelov P, Soares E (2020) Towards explainable deep neural networks (xDNN). Neural Net 130:185–194.

Antle J, Basso B, Conant RT, Godfray HCJ, Jones JW, Herrero M, Howitt RE, Keating BA, Munoz-Carpena R, Rosenzweig C, et al. (2017) Towards a new generation of agricultural system data, models and knowledge products: Design and improvement. Agric Syst 155:255–268.

Ba JL, Kiros JR, Hinton GE (2016) Layer Normalization. arXiv preprint arXiv:1607.06450.

Benos L, Tagarakis AC, Dolias G, Berruto R, Kateris D, Bochtis D (2021) Machine Learning in Agriculture: A Comprehensive Updated Review. Sensors 21:3758.

Bergstra J, Komer B, Eliasmith C, Yamins D, Cox DD (2015) HyperOpt: a

Python library for model selection and hyperparameter optimization. Comput Sci Discov 8:014008.

Caruana R (1997) Multitask Learning. Machine Learning 28:41–75.

Chapagain R, Remenyi TA, Harris RMB, Mohammed CL, Huth N, Wallach D, Rezaei EE, Ojeda JJ (2022) Decomposing crop model uncertainty: A systematic review. Field Crops Res 279:108448.

Chenu K, Porter JR, Martre P, Basso B, Chapman SC, Ewert F, Bindi M, Asseng S (2017) Contribution of Crop Models to Adaptation in Wheat. Trends Plant Sci 22:472–490.

Chorowski JK, Bahdanau D, Serdyuk D, Cho K, Bengio Y (2015) Attention-Based Models for Speech Recognition. In: Cortes C, Lawrence N, Lee D, Sugiyama M, Garnett R (eds) Advances in Neural Information Processing Systems. Curran Associates, Inc., Montreal, Canada.

de Wit A, Boogaard H, Fumagalli D, Janssen S, Knapen R, van Kraalingen D, Supit I, van der Wijngaart R, van Diepen K (2019) 25 years of the WOFOST cropping systems model. Agric Syst 168:154–167.

Easlon HM, Bloom AJ (2014) Easy Leaf Area: automated digital image analysis for rapid and accurate measurement of leaf area. Appl Plant Sci 2:1400033.

Gijzen H, Heuvelink E, Challa H, Marcelis LFM, Dayan E, Cohen S, Fuchs M (1998) HORTISIM: a model for greenhouse crops and greenhouse climate. Acta Hortic 441–450.

Hammer G, Messina C, Wu A, Cooper M (2019) Biological reality and parsimony in crop models—why we need both in crop improvement! in silico Plants 1:diz010.

Han K, Wang Y, Chen H, Chen X, Guo J, Liu Z, Tang Y, Xiao A, Xu C, Xu Y, Yang Z, Zhang Y, Tao D (2022) A Survey on Vision Transformer. IEEE Trans Pattern Anal Mach Intell 1–1.

He J, Jones JW, Graham WD, Dukes MD (2010) Influence of likelihood function choice for estimating crop model parameters using the generalized likelihood uncertainty estimation method. Agric Syst 103:256–264.

He K, Zhang X, Ren S, Sun J (2016) Deep Residual Learning for Image Recognition. Las Vegas, USA, pp 770–778.

Holzworth D, Huth NI, Fainges J, Brown H, Zurcher E, Cichota R, Verrall S, Herrmann NI, Zheng B, Snow V (2018) APSIM Next Generation: Overcoming challenges in modernising a farming systems model. Environ Model Softw 103:43–51.

Hoogenboom G, Porter CH, Boote KJ, Shelia V, Wilkens PW, Singh U, White JW, Asseng S, Lizaso JI, Moreno LP, et al. The DSSAT crop modeling ecosystem. In: Boote KJ (ed) Advances in Crop Modeling for a Sustainable Agriculture. Burleigh Dodds Science Publishing, Cambridge, United Kingdom, pp 173–216.

Hornik K (1991) Approximation capabilities of multilayer feedforward networks. Neural Net 4:251–257.

Hsiao J, Yun K, Moon KH, Kim S-H (2019) A process-based model for leaf development and growth in hardneck garlic (Allium sativum). Ann Bot 124:1143–1160.

Ioffe S, Szegedy C (2015) Batch Normalization: Accelerating Deep Network Training by Reducing Internal Covariate Shift. In: Proceedings of the 32nd International Conference on Machine Learning. PMLR, pp 448–456.

Jones JW, Antle JM, Basso B, Boote KJ, Conant RT, Foster I, Godfray HCJ, Herrero M, Howitt RE, Janssen S, et al. (2017) Brief history of agricultural systems modeling. Agric Syst 155:240–254.

Kamilaris A, Prenafeta-Boldú FX (2018) A review of the use of convolutional neural networks in agriculture. J Agric Sci Technol 156:312–322.

Katzin D, van Henten EJ, van Mourik S (2022) Process-based greenhouse climate models: Genealogy, current status, and future directions. Agric Syst 198:103388.

Kimm H, Guan K, Jiang C, Miao G, Wu G, Suyker AE, Ainsworth EA, Bernacchi CJ, Montes CM, Berry JA, Yang X, Frankenberg C, Chen M, Köhler P (2021) A physiological signal derived from sun-induced chlorophyll fluorescence quantifies crop physiological response to environmental stresses in the U.S. Corn Belt. Environ Res Lett 16:124051.

Kingma DP, Ba J (2017) Adam: A Method for Stochastic Optimization. arXiv preprint arXiv:1412.6980.

Koirala A, Walsh KB, Wang Z, McCarthy C (2019) Deep learning – Method

overview and review of use for fruit detection and yield estimation. Comput Electron Agric 162:219–234.

LeCun Y, Bengio Y, Hinton G (2015) Deep learning. Nature 521:436–444.

Lee JW, Moon T, Son JE (2021) Development of Growth Estimation Algorithms for Hydroponic Bell Peppers Using Recurrent Neural Networks. Horticulturae 7:284.

Lischeid G, Webber H, Sommer M, Nendel C, Ewert F (2022) Machine learning in crop yield modelling: A powerful tool, but no surrogate for science. Agric For Meteorol 312:108698.

Mikolov T, Chen K, Corrado G, Dean J (2013) Efficient Estimation of Word Representations in Vector Space. arXiv Preprint arXiv:1301.3781.

Moon T, Lee JW, Son JE (2021) Accurate Imputation of Greenhouse Environment Data for Data Integrity Utilizing Two-Dimensional Convolutional Neural Networks. Sensors 21:2187.

Müller C, Franke J, Jägermeyr J, Ruane AC, Elliott J, Moyer E, Heinke J, Falloon PD, Folberth C, Francois L, et al. (2021) Exploring uncertainties in global crop yield projections in a large ensemble of crop models and CMIP5 and CMIP6 climate scenarios. Environ Res Lett 16:034040.

Mnih V, Kavukcuoglu K, Silver D, Rusu AA, Veness J, Bellemare MG, Graves A, Riedmiller M, Fidjeland AK, Ostrovski G, et al. (2015) Human-level control through deep reinforcement learning. Nature 518:529–533.

Nash JE, Sutcliffe JV (1970) River flow forecasting through conceptual models

part I — A discussion of principles. J Hydrol 10:282–290.

Newbery F, Qi A, Fitt BD (2016) Modelling impacts of climate change on arable crop diseases: progress, challenges and applications. Curr Opin Plant Biol 32:101–109.

Newman SJ, Furbank RT (2021) Explainable machine learning models of major crop traits from satellite-monitored continent-wide field trial data. Nat Plants 7:1354–1363.

Niu Z, Zhong G, Yu H (2021) A review on the attention mechanism of deep learning. Neurocomputing 452:48–62.

Osinga SA, Paudel D, Mouzakitis SA, Athanasiadis IN (2022) Big data in agriculture: Between opportunity and solution. Agricultural Systems 195:103298.

Panageas I, Piliouras G (2016) Gradient Descent Only Converges to Minimizers: Non-Isolated Critical Points and Invariant Regions. arXiv Preprint 1605.00405.

Peng B, Guan K, Tang J, Ainsworth EA, Asseng S, Bernacchi CJ, Cooper M, Delucia EH, Elliott JW, Ewert F, et al. (2020) Towards a multiscale crop modelling framework for climate change adaptation assessment. Nat Plants 6:338–348.

Qiu X, Sun T, Xu Y, Shao Y, Dai N, Huang X (2020) Pre-trained models for natural language processing: A survey. Sci China Technol Sci 63:1872–1897.

Ruder S (2017a) An Overview of Multi-Task Learning in Deep Neural Networks. arXiv Preprint arXiv:1706.05098.

Ruder S (2017b) An overview of gradient descent optimization algorithms. arXiv Preprint arXiv:1609.04747.

Sánchez-Molina JA, Pérez N, Rodríguez F, Guzmán JL, López JC (2015) Support system for decision making in the management of the greenhouse environmental based on growth model for sweet pepper. Agric Syst 139:144–152.

Scaife MA, Jones D (1976) The relationship between crop yield (or mean plant weight) of lettuce and plant density, length of growing period, and initial plant weight. J Agric Sci 86:83–91.

Silver D, Schrittwieser J, Simonyan K, Antonoglou I, Huang A, Guez A, Hubert T, Baker L, Lai M, Bolton A, Chen Y, Lillicrap T, Hui F, Sifre L, van den Driessche G, Graepel T, Hassabis D (2017) Mastering the game of Go without human knowledge. Nature 550:354–359.

Tan X, Qin T, Soong F, Liu T-Y (2021) A Survey on Neural Speech Synthesis. arXiv Preprint arXiv:2106.15561.

Van Diepen C van, Wolf J, Van Keulen H, Rappoldt C (1989) WOFOST: a simulation model of crop production. Soil Use Manag 5:16–24.

Vaswani A, Shazeer N, Parmar N, Uszkoreit J, Jones L, Gomez AN, Kaiser Ł, Polosukhin I (2017) Attention is All you Need. In: Advances in Neural Information Processing Systems. Curran Associates, Inc.

Wang E, Martre P, Zhao Z, Ewert F, Maiorano A, Rötter RP, Kimball BA, Ottman MJ, Wall GW, White JW et al. (2017) The uncertainty of crop yield projections is reduced by improved temperature response functions. Nat Plants 3:1–13.

Wang H, Yeung D-Y (2016) Towards Bayesian Deep Learning: A Framework and Some Existing Methods. IEEE Trans Knowl Data Eng 28:3395–3408.

Xu R, Dai J, Luo W, Yin X, Li Y, Tai X, Han L, Chen Y, Lin L, Li G, Zou C, Du W, Diao M (2010) A photothermal model of leaf area index for greenhouse crops. Agric For Meteorol 150:541–552.

Yang B, Xu Y (2021) Applications of deep-learning approaches in horticultural research: a review. Hortic Res 8:1–31.

Zhang H, Goodfellow I, Metaxas D, Odena A (2019) Self-Attention Generative Adversarial Networks. arXiv Preprint arXiv:1805.08318.

Zhao C, Liu B, Xiao L, Hoogenboom G, Boote KJ, Kassie BT, Pavan W, Shelia V, Kim KS, Hernandez-Ochoa IM, Wallach D, Porter CH, Stockle CO, Zhu Y, Asseng S (2019) A SIMPLE crop model. Eur J Agron 104:97–106.

Zhuang F, Qi Z, Duan K, Xi D, Zhu Y, Zhu H, Xiong H, He Q (2020) A Comprehensive Survey on Transfer Learning. arXiv Preprint arXiv:1911.02685.

GENERAL DISCUSSION

Summary of the chapters

Chapter 1-1 explained the procedure to construct infrastructure before applying the deep learning approach to agriculture, which has insufficient data conditions. Verifying the performance of transfer learning with greenhouse environment and representative deep learning models showed the applicability of the deep learning models to the agricultural data. Based on transfer learning, the developed DeepCrop would be applied to the limited data condition, which is inevitable in agricultural systems.

In Chapter 1-2, it was verified that the U-Net algorithm that processes medical images could be adapted to the tabular data having a greenhouse environment. With unfavorable conditions for the sensors in agriculture, data imputation helps the collected agricultural data to be utilized for the data science tasks. In addition, the application example of the U-Net structure also showed high applicability of the deep learning algorithms, which supports the ability of DeepCrop to be applied to various data types.

The topic of Chapter 2 was crop model calibration for model comparison. HyperOpt was introduced as a tool to calibrate a crop model to the given data condition. The HyerOpt algorithm is derived from the Bayesian optimization method, so it does not require domain knowledge for the methodology. HyperOpt can calibrate many models with the same methodology, so the

calibrated models can be the baseline at least, which could be a factor in judging the model performance. In addition, the calculation of the Bayesian optimization can be parallelized, so the algorithm can use GPU acceleration. GPU-based HyperOpt would calibrate model parameters much faster.

Chapter 3 verified the performance of DeepCrop and contained procedures to build a process-based crop model using deep learning in practice and to compare the performance with other models. The core invention of this study was Chapter 3; however, in addition to the specific model called DeepCrop, the whole protocol of constructing and evaluating DeepCrop in the limited conditions of agriculture will be a reference, contributing to another 'realization of deep learning in the agriculture.'

Desirable future for DeepCrop

For the dissemination of DeepCrop, a possible direction is to assemble an open-source-based community. The open-source strategy can become a robust infrastructure for technological progress in the current information age with global networks. The trained DeepCrop with partial crop data could not play a sufficient role of alleviating fragmentation of crop modeling. Relating environment and crop response with limited data is too easy for deep learning. DeepCrop would show remarkable performances for any scale, crop, and factors, similar to chapter 3. The data with various conditions are required for DeepCrop robustness. DeepCrop should be a means of uniting the crop

modeling research community. In the end, information sharing would be the most necessary for a comprehensive interpretation of crop physiology. If each research team conducts separate research, fragmentation will not be resolved, similar to existing end-to-end deep learning models. DeepCrop should be utilized for diverse inputs and outputs first; then, the consensus of DeepCrop will result in an open-source-based community of crop modeling research groups of various sizes.

Empirical difficulties of crop modeling and deep learning application

Crop modeling and deep learning have dissimilar research basis. In this section, empirical and subjective challenges within mixing two immiscible studies are shared. This practical example could help reduce trials and errors for applying deep learning; then, this paper would be completed as a reference protocol. Please note that all contents discussed in this section are based on personal experience and may be very misleading depending on the reader's research base.

Unfortunately, using model was a main difficulty for the crop modeling. For example, open-source crop modeling programs like DSSAT have numerous add-ons, but the data processing is still in the 90s. The programs became inconvenient to handle the current big data. Individual research groups commonly customize the program partially, which could result in similar problems with the private models.

Using individual crop models required a ‘guesswork.’ Similar research groups periodically publish follow-up papers on those private models, but essential information to reproduce the model in practice is missing in many reports. Unclarified formula and parameters differed by the research scale, so a third person have to guess the proper formula.

In this regard, the problem for using crop models was a lack of practical information. The accessibility of the crop models was set to a core problem as mentioned in Literature Review, and it was a fundamental reason for considering a full deep neural network crop model outside the existing models.

Meanwhile, deep learning is in direct opposite: proper and correct information should be identified among too much information. Public materials are prevalent, including private blogs, lectures, and YouTubes in addition to scientific reports. It has made developing a new algorithm easier, that results in more deep learning models. Most of the models can be reproduced with the published information; if not, curious developers make and share a replica in no time. Therefore, finding adequate information for the own target task was a hurdle of deep learning. That is the reason that this thesis was aimed to write as a developmental protocol containing sufficient information as possible.

Most of all, the biggest challenging hurdle for applying deep learning was different data types and amounts. General tasks for the crop production are regressions. Deep learning models have to be customized for the different data type, and it inevitably requires in-depth understanding for deep learning. When

exploring crop physiology and deep learning, balancing the two was a challenge. For the difficulty in data collection, growing crops and collecting necessary data were labor intensive, and the painstakingly collected data were insufficient to apply deep learning with ‘standard protocols’. The lack of data confuses whether training failures are caused by the model or the data. In this condition, wrong training process can also yield plausible results; the model robustness should be verified in multiple perspectives. In spite of the above challenges, this study tried to establish appropriate standards. We expect this thesis to be transformed, compared, and criticized as a baseline by new studies for deep learning applications.

GENERAL CONCLUSION

In this thesis, a protocol to apply deep learning to process-based crop models was established. Fundamental studies for distinctive data condition were conducted before deep learning application. Finally, a process-based crop model with full deep learning algorithms, DeepCrop, was developed. DeepCrop recorded the highest model efficiency compared to the existing crop models. Since the same structure of deep neural networks can be retrained with heterogeneous inputs and outputs, DeepCrop can be widely applied regardless of the research scales and objectives. As a protocol, this thesis tried to set adequate criteria: deep learning models were trained using adequate datasets without data leakage; the developed and introduced models were compared with existing methods based on multiple perspectives; the reasonability of the training process was also inferred outside the accuracies. This thesis would be the first step to unifying fragmented crop models and reducing redundancy in crop model research using deep learning. DeepCrop does not require considering internal formula corresponding to the changes in input features, and its structure and the relevant workflow were explained; therefore, the model can easily be studied and improved with any purpose and dataset with the established protocol.

ABSTRACT IN KOREAN

농업 시스템에서 발생하는 문제들은 작물과 환경의 상호작용 하에 복잡하게 얽혀 있다. 작물 모델링은 대상을 단순화하는 방법으로써, 농업에서 일어나는 현상을 추상화하고 해석하는 과정이다. 모델링을 통해 대상을 이해하는 것은 농업 분야의 학술적 및 사회적 결정을 지원할 수 있다. 지난 수년 간 절차 기반 작물 모델은 농업의 문제들을 해결하여 작물 생산성 및 품질을 증진시켰으며, 현재 작물 모델링에 남아있는 과제들은 다차원 정보를 다방향에서 분석할 수 있는 작물 모델을 필요로 하게 되었다. 이를 만족시킬 수 있는 지침으로써, 복잡한 농업적 과제들을 목표로 딥러닝 알고리즘이 도입되었다. 그러나, 이 알고리즘들은 낮은 데이터 완결성 및 높은 연구 다양성 때문에 기존의 작물 모델들을 대체하지는 못했다. 본 연구에서는 딥러닝 방법론을 이용하여 절차 기반 작물 모델을 구축하는 개발 프로토콜을 확립하였다. Literature Review에서는 딥러닝과 작물 모델에 대해 소개하고, 농업으로의 딥러닝 적용 연구가 많음에도 이 프로토콜이 필요한 이유를 설명하였다. 제1장과 2장에서는 국내 여러 지역의 데이터를 이용하여 전이 학습 및 U-Net 구조를 활용하여 딥러닝 모델 적용을 위한 기반을 마련하고, 베이지안 최적화 방법인 HyperOpt를 사용하여 기존 모델과 딥러닝 기반 모델을 비교하기 위해 시험적으로 WOFOST 작물 모델을 보정하는 등 모델 개발을 위한 기반 연구를 수행하였다. 마지막으로, 제3장에서는 주의 메커니즘 및 다중 작업 디코더를 가진 완전 심층 신경망 절차 기반 작물 모델인 DeepCrop을 수경재배 파프리카(*Capsicum annuum* var. *annuum*) 대상으로 개발하였다. 데이터 완결성을 위한 기술들은 적합한 정확도를 보여주었으며, 전체 챕터 데이터에 적용하였다. HyperOpt는 식량 및 사료 작물 모델들을 파프리카 대상으로 보정할 수 있었다. 따라서, 제3장의 비교 대상 모델들에 대해 HyperOpt를 사용하였다. DeepCrop은 환경

데이터를 이용하고 여러 생육 지표를 예측하도록 학습되었다. 학습에 사용하지 않은 데이터를 이용하여 학습된 DeepCrop를 평가하였으며, 이 때 비교 모델들 중 가장 높은 모형 효율(EF=0.76)과 가장 낮은 표준화 평균 제곱근 오차(NRMSE=0.18)를 보여주었다. DeepCrop은 높은 적용성을 기반으로 다양한 범위와 목적을 가진 연구에 사용될 수 있을 것이다. 모든 방법들이 주어진 작업을 적절히 풀어냈고 DeepCrop 개발의 근거가 되었으므로, 본 논문에서 확립한 프로토콜은 작물 모델의 접근성을 향상시킬 수 있는 획기적인 방향을 제시하였고, 작물 모델 연구의 통합에 기여할 수 있을 것으로 기대한다.

추가 주요어: 기계학습, 인공지능, 작물 시뮬레이션 모델, 다중작업 학습, 트랜스포머

학번: 2019-35122

APPENDIX

Table A1. References, crops, and numbers of meta-analyzed data of Fig. 1.

Reference	Crop	Number of analyzed data	
		Open field	Greenhouse
Maureira et al. (2022)	Tomato	1	3
Yuan and Zhang (2021)	Tomato	1	1
	Cucumber	1	1
Angmo1 et al. (2021)	Tomato	1	2
Shen et al . (2021)	Cherry	1	1
Zhang et al. (2021)	Various crops	2	2
Ntinas et al. (2020)	Tomato	0	2
Yildizhan (2018)	Strawberry	1	1
Ntinas et al. (2017)	Tomato	2	5
Stanghellini (2014)	Tomato	1	4
Khoshnevisan et al. (2014)	Strawberry	1	1
Khoshnevisan et al. (2013)	Strawberry	1	1
Kuswardhani et al. (2013)	Tomato	1	1
	Chili	2	2
	Lettuce	1	1
Yousefi et al. (2012)	Cucumber	1	1
Page et al., (2012)	Tomato	1	3
Martínez-Blanco et al. (2011)	Tomato	2	2
Muñoz et al. (2008)	Tomato	1	1
Khah et al. (2006)	Tomato	4	4
Ozkan et al. (2005)	Grape	1	1

Table A3-1. Calibrated coefficients of WOFOST. The coefficient values with colons represent the values for the corresponding variables such as development stage or temperature.

Item	Description	Value		
		Wheat	Mung bean	Barley
TEFFMX	Maximum effective temperature for emergence	100	100	100
TBASEM	Base temperature for emergence	0	0	0
TSUMEM	Temperature sum from sowing to emergence	0	0	0
SPAN	Life span of leaves growing at 35°C	400	400	400
DVSI	Initial development stage at the start of simulation	0.48	0.63	0.89
TBASE	Lower threshold temperature for ageing of leaves	21.37	11.39	14.54
RGRLAI	Maximum relative increase in LAI	1.61	3.59	3.35
TSUM1	Temperature sum from emergence to anthesis	676	733	713
TSUM2	Temperature sum from anthesis to maturity	1402	1200	1274
CVO	Conversion efficiency of assimilates into storage organ	0.45	0.91	0.94
CVL	Conversion efficiency of assimilates into leaf	0.85	0.51	0.36
SLATB	Specific leaf area as a function of development stage	0: 0.026 1: 0.014 2: 0.019	0: 0.030 1: 0.043 2: 0.014	0: 0.035 1: 0.021 2: 0.023

SSATB	Specific stem area as a function of development stage	0: 0.054 1: 0.051 2: 0.011	0: 0.012 1: 0.036 2: 0.001	0: 0.042 1: 0.031 2: 0.001
KDIFTB	Extinction coefficient for diffuse visible light as function of development stage	0: 0.813 1: 0.129 2: 0.817	0: 0.237 1: 0.384 2: 0.636	0: 0.179 1: 0.651 2: 0.756
AMAXTB	Maximum leaf CO_2 assimilation rate as a function of development stage	0: 35.66 1: 19.10 2: 34.54	0: 29.55 1: 33.08 2: 30.26	0: 39.95 1: 22.18 2: 24.45
RFSETB	Reduction factor for senescence as function of development stage	0: 0.085 1: 0.903 2: 0.044	0: 0.532 1: 1.000 2: 0.840	0: 0.448 1: 0.713 2: 0.906
FRTB	Fraction of total dry matter increase partitioned to roots as a function of development stage	0: 0.28 1: 0.40 2: 0.07	0: 0.20 1: 0.18 2: 0.43	0: 0.39 1: 0.03 2: 0.01
FLTB	Fraction of above ground dry matter increase partitioned to leaves as a function of development stage	0.0: 0.90 0.5: 0.40 1.0: 0.93 1.5: 0.70 2.0: 0.16	0.0: 0.57 0.5: 1.00 1.0: 0.29 1.5: 0.05 2.0: 0.29	0.0: 0.99 0.5: 0.63 1.0: 0.83 1.5: 0.84 2.0: 0.26
FSTB	Fraction of above ground dry matter increase partitioned to stems as a function of development stage	0.0: 0.09 0.5: 0.50 1.0: 0.01 1.5: 0.01 2.0: 0.49	0.0: 0.16 0.5: 0.00 1.0: 0.30 1.5: 0.27 2.0: 0.32	0.0: 0.01 0.5: 0.27 1.0: 0.06 1.5: 0.14 2.0: 0.41

FOTB	Fraction of above ground dry matter increase partitioned to storage organs as a function of development stage	0.0: 0.01 0.5: 0.10 1.0: 0.07 1.5: 0.29 2.0: 0.35	0.0: 0.27 0.5: 0.00 1.0: 0.41 1.5: 0.68 2.0: 0.39	0.0: 0.00 0.5: 0.10 1.0: 0.11 1.5: 0.02 2.0: 0.33
EFFTB	Initial light-use efficiency of CO_2 assimilation of single leaves as function of mean daily temperature	0: 0.75 10: 1.57 20: 0.27 30: 1.23 40:1.99	0: 0.22 10: 1.32 20: 0.92 30: 1.78 40:1.74	0: 1.47 10: 1.06 20: 0.23 30: 1.02 40:0.76
DTSMTB	Daily increase in temperature sum as function of average temperature	0: 25.9 15: 99.9 30: 71.3 45: 87.1	0: 63.2 15: 43.6 30: 99.9 45: 64.0	0: 52.9 15: 84.7 30: 52.7 45: 43.4

Table A3-2. Original and calibrated coefficients of DSSAT.

Item	Description	Value			
		Biscayne	Capistrano	Lee et al. (2021)	Calibrated
EM-FL	Time between plant emergence and flower appearance	22.0	37.0	40.0	21.99
FL-SH	Time between first flower and first pod	11.0	10.0	10.0	10.33
FL-SD	Time between first flower and first seed	15.0	15.0	15.0	15.64
SD-PM	Time between first seed and physiological maturity	100.0	100.0	330.0	95.80
LFMAX	Maximum leaf photosynthesis rate at 30°C, 350 vpm CO_2, and high light	1.10	0.98	0.98	1.071
SLAVR	Specific leaf area of cultivar under standard growth conditions	250.0	275.0	275.0	299.3
SIZLF	Maximum size of full leaf	300.0	250.0	350.0	250.0
XFRT	Maximum fraction of daily growth that is partitioned to seed + shell	0.75	0.85	0.60	0.627
SFDUR	Seed filling duration for pod cohort at standard growth conditions	25.0	25.0	40.0	25.0
SDLIP	Fraction oil in seeds	0.050	0.050	0.050	0.051
PM06	Proportion of time between first seed and physiological maturity	0.75	0.75	0.0	0.0
FL-VS	Time from first flower to last leaf on main stem	53.0	53.0	330.0	330.0

Table A3-3. Original and calibrated coefficients of a sweet pepper model from Sánchez-Molina et al. (2015).

Item	Description	Value	
		Original	Calibrated
V_{cmax}	Maximum carboxylation velocity	200	81.29
f_c	Assimilation conversion factor	0.29	0.30
Γ^*	CO_2 compensation point	Temp. dependent func.	36.03
T_{ref}	Reference temperature	25.0	15.1
r_l	Leaf ratio for maintenance respiration rate	0.030	0.004
r_s	Stem ratio for maintenance respiration rate	0.015	0.004
r_r	Root ratio for maintenance respiration rate	0.015	0.001
r_f	Fruit ratio for maintenance respiration rate	0.010	0.002
T_{base}	Base temperature for thermal time	10	13.86
VS	Days of vegetative stage	30	52

Table A3-4. Original and calibrated coefficients of SIMPLE.

Item	Description	Value	
		Tomato (SunnySD)	Calibrated
T_{sum}	Cumulative temperature requirement from sowing to maturity	2800	2931
HI	Potential harvest index	0.68	0.89
I_{50A}	Cumulative temperature requirement for leaf area development to intercept 50% of radiation	520	712
I_{50B}	Cumulative temperature till maturity to reach 50% radiation interception due to leaf senescence.	400	2717
T_{base}	Base temperature for phenology development and growth	6	17.7
T_{opt}	Optimal temperature for biomass growth	26	29.6
RUE	Radiation use efficiency (above ground only and without respiration)	1.00	0.56
T_{heat}	Threshold temperature to start accelerating senescence from heat stress	32	39.6
T_{ext}	The extreme temperature threshold when RUE becomes 0 due to heat stress	45	41
S_{CO2}	Relative increase in RUE per ppm elevated CO2 above 350 ppm	0.07	0.02
$fSolar_{max}$	The maximum fraction of radiation interception that a crop can reach	0.95	0.67

Table A3-5. Structure of FFNN, LSTM, and ConvNet. Dense and Conv are a fully connected layer and a convolution layer, respectively; Maxpool and Flatten represent the maximum pooling and flattening, respectively. Parameters for Conv are denoted as "{type of layer}{kernel size}-{number of filters}," and parameters for the other layers are denoted as "{type of layer}-{number of nodes in the layer}." ResBlock represents a residual block. Refer to Fig. A3-1 for the detailed structure.

Model	FFNN	LSTM	1D ConvNet
Input size		216×7	
Layers	Dense-256	BiLSTM-256	Conv7-32
	BatchNorm	LayerNorm	BatchNorm
	Dense-256	BiLSTM-256	MaxPool
	BatchNorm	LayerNorm	ResBlock-16
	Flatten	Dense-32	ResBlock-32
	Dense-19	Dense-19	ResBlock-32
			ResBlock-64
			ResBlock-128
			Flatten
			Dense-16
			BatchNorm
			Dense-16
			BatchNorm
			Dense-19
Output size		1×19	

Table A3-6. Parameters used for each model construction and training. Hyphens represent unused values for the corresponding model.

Hyperparameter	FFNN	LSTM	1D ConvNet
Nonlinearity function	Tanh; Sigmoid	Tanh; Sigmoid	ReLU
Normalization	Batch	Layer	Batch
Batch size	128	128	128
Kernel initializer	-	-	Glorot normal
Padding	-	-	Same
Learning rate	0.001	0.002	0.0015
Epsilon	1e-08	1e-08	1e-08
β_1	0.9	0.9	0.9
β_2	0.999	0.999	0.999
Learning rate decay	0.1	0.1	0.1

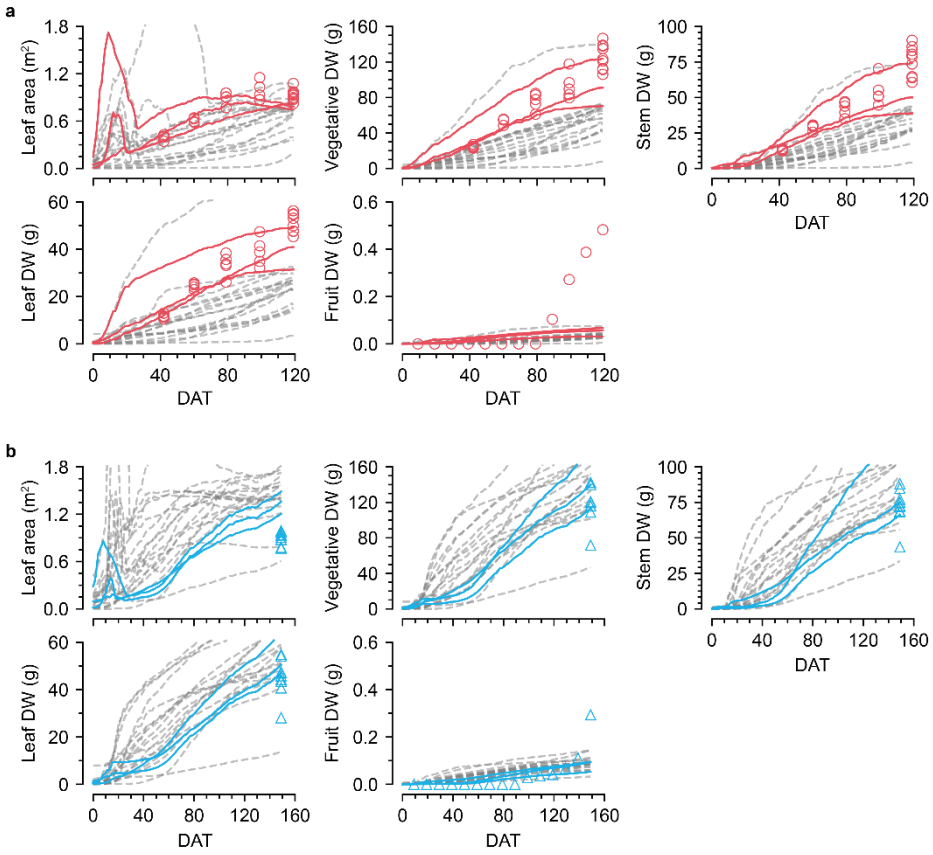

Fig. A3-1. Simulated growth factors of calibrated WOFOST crop models for (A) 2020-1 and (B) 2020-2. Colored solid and gray dashed lines represent the calibrated models that showed top three performance and the others, respectively. Symbols represent observed growth factors.

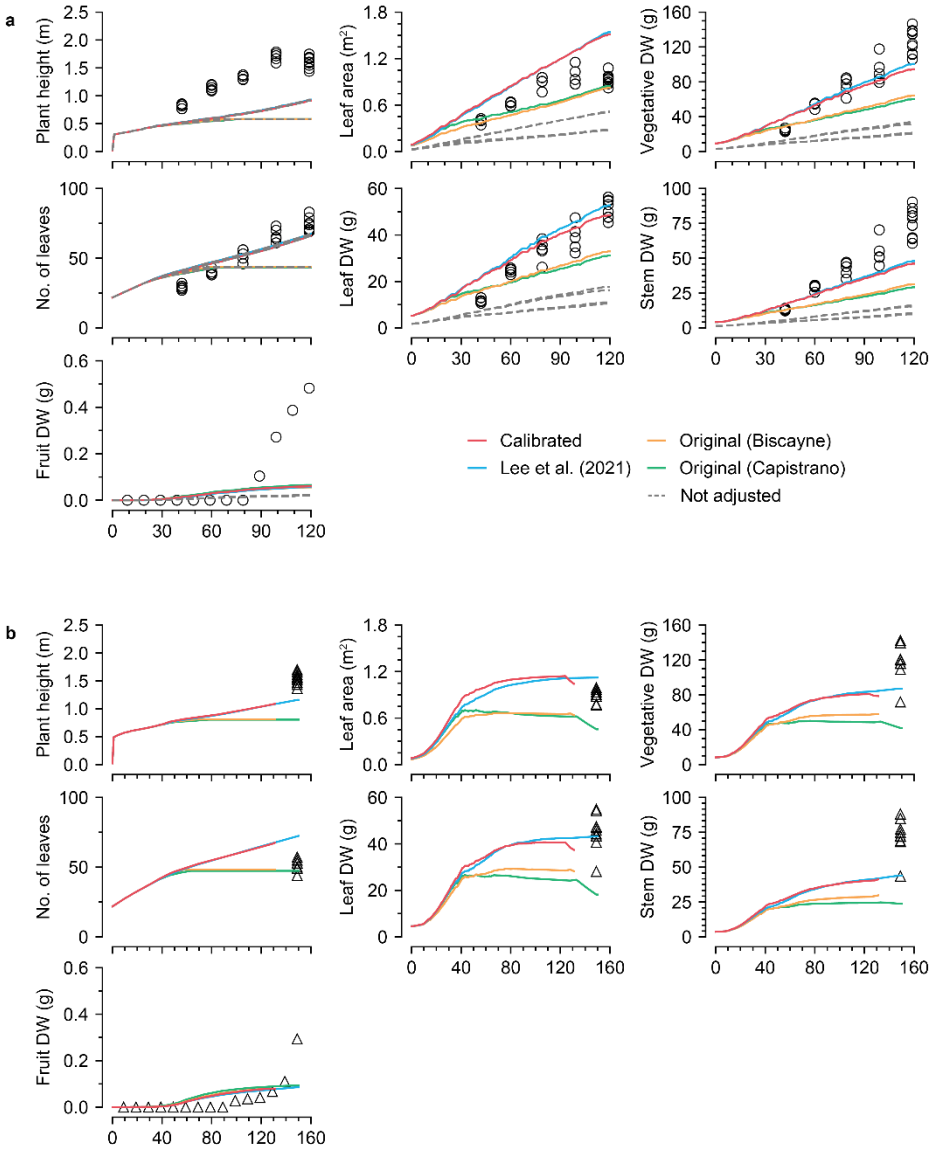

Fig. A3-2. Simulated growth factors of sweet pepper model in DSSAT for (A) 2021-1 and (B) 2021-2. Symbols represent observed growth factors. Gray dashed line represents the simulated 2021-1 without adjusted planting density.

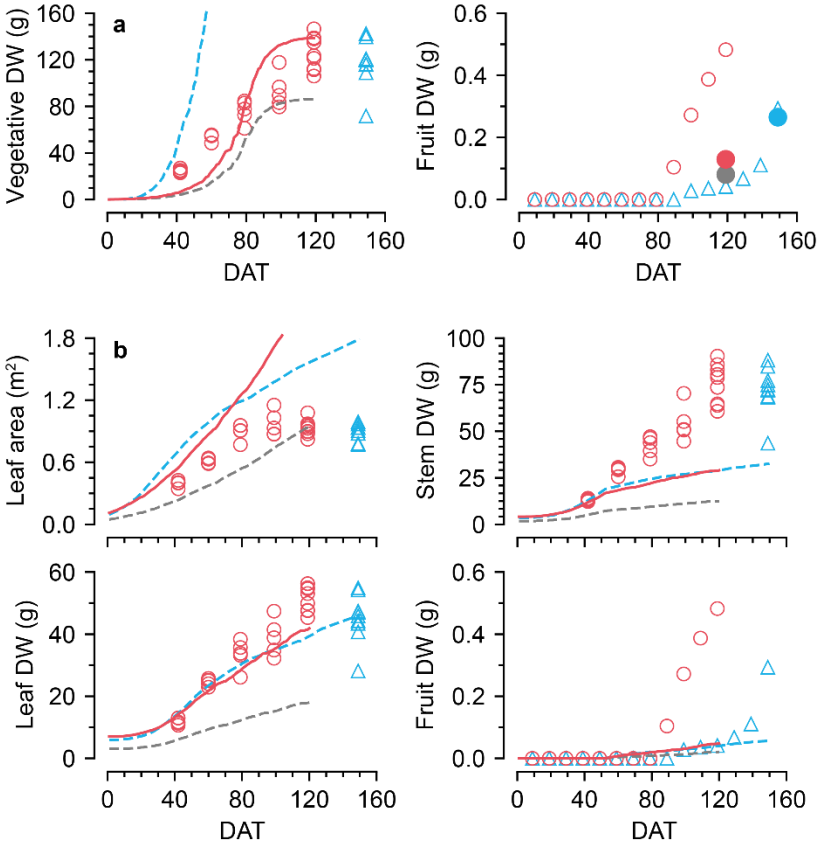

Fig. A3-3. Simulated growth factors of (A) SIMPLE crop model and (B) a sweet pepper model for decision support Sánchez-Molina et al. (2015).

References for Fig. 1 and Table A1

Angmo P, Phuntsog N, Namgail D, Chaurasia OP, Stobdan T (2021) Effect of shading and high temperature amplitude in greenhouse on growth, photosynthesis, yield and phenolic contents of tomato (*Lycopersicum esculentum* Mill.). Physiol Mol Biol Plants 27:1539–1546.

Khah EM, Kakava E, Mavromatis A, Chachalis D, Goulas C (2006) Effect of grafting on growth and yield of tomato (*Lycopersicon esculentum* Mill.) in greenhouse and open-field. J Appl Hortic 5.

Khoshnevisan B, Rafiee S, Mousazadeh H (2013) Environmental impact assessment of open field and greenhouse strawberry production. Eur J Agron 50:29–37.

Khoshnevisan B, Shariati HM, Rafiee S, Mousazadeh H (2014) Comparison of energy consumption and GHG emissions of open field and greenhouse strawberry production. Renew Sust Energ Rev 29:316–324.

Kuswardhani N, Soni P, Shivakoti GP (2013) Comparative energy input–output and financial analyses of greenhouse and open field vegetables production in West Java, Indonesia. Energy 53:83–92.

Martínez-Blanco J, Muñoz P, Antón A, Rieradevall J (2011) Assessment of tomato Mediterranean production in open-field and standard multi-tunnel greenhouse, with compost or mineral fertilizers, from an agricultural and environmental standpoint. J Clean Prod 19:985–997.

Maureira F, Rajagopalan K, Stöckle CO (2022) Evaluating tomato production

in open-field and high-tech greenhouse systems. J Clean Prod 337:130459.

Muñoz P, Antón A, Nuñez M, Paranjpe A, Ariño J, Castells X, Montero JI, Rieradevall J (2008) Comparing the environmental impacts of greenhouse versus open-field tomato production in the mediterranean region. Acta Hortic 1591–1596.

Ntinas GK, Dannehl D, Schuch I, Rocksch T, Schmidt U (2020) Sustainable greenhouse production with minimised carbon footprint by energy export. Biosyst Eng 189:164–178.

Ntinas GK, Neumair M, Tsadilas CD, Meyer J (2017) Carbon footprint and cumulative energy demand of greenhouse and open-field tomato cultivation systems under Southern and Central European climatic conditions. J Clean Prod 142:3617–3626.

Ozkan B, Fert C, Karadeniz CF (2007) Energy and cost analysis for greenhouse and open-field grape production. Energy 32:1500–1504.

Page G, Ridoutt B, Bellotti B (2012) Carbon and water footprint tradeoffs in fresh tomato production. J Clean Prod 32:219–226.

Shen J, Zhang P, Chang Y, Zhang L, Hao Y, Tang S, Xiong X (2021) The environmental performance of greenhouse versus open-field cherry production systems in China. Sustain Prod Consum 28:736–748.

Stanghellini C (2014) Horticultural production in greenhouses: efficient use of water. Acta Hortic 25–32.

Yildizhan H (2018) Energy, exergy utilization and CO_2 emission of strawberry

production in greenhouse and open field. Energy 143:417–423.

Yousefi M, Darijani F, Jahangiri AA (2012) Comparing energy flow of greenhouse and open-field cucumber production systems in Iran. Afr J Agric Res 7:624–628.

Yuan Y, Zhang X (2021) Comparison of agrochemicals allocation efficiency between greenhouse and open-field vegetables in China. Sci Rep 11:12807.

Zhang F, Liu F, Ma X, Guo G, Liu B, Cheng T, Liang T, Tao W, Chen X, Wang X (2021) Greenhouse gas emissions from vegetables production in China. J Clean Prod 317:128449.

References for Fig. 4

Chorowski JK, Bahdanau D, Serdyuk D, Cho K, Bengio Y (2015) Attention-based models for speech recognition. In: Cortes C, Lawrence N, Lee D, Sugiyama M, Garnett R (eds) Advances in Neural Information Processing Systems. Curran Associates, Inc., Montreal, Canada.

Chung J, Gulcehre C, Cho K, Bengio Y (2014) Empirical evaluation of gated recurrent neural networks on sequence modeling. arXiv Preprint arXiv:1412.3555.

Devlin J, Chang M-W, Lee K, Toutanova K (2019) BERT: pre-training of deep bidirectional Transformers for language understanding. arXiv Preprint arXiv:1810.04805.

Dosovitskiy A, Beyer L, Kolesnikov A, Weissenborn D, Zhai X, Unterthiner T,

Dehghani M, Minderer M, Heigold G, Gelly S, Uszkoreit J, Houlsby N (2021) An image is worth 16x16 words: Transformers for image recognition at scale. arXiv Preprint arXiv:2010.11929.

Gehring J, Auli M, Grangier D, Yarats D, Dauphin YN (2017) Convolutional sequence to sequence learning. In: Proceedings of the 34th International Conference on Machine Learning. PMLR, pp 1243–1252.

He K, Zhang X, Ren S, Sun J (2016) Deep residual learning for image recognition. Las Vegas, USA, pp 770–778.

Kalchbrenner N, Espeholt L, Simonyan K, Oord A van den, Graves A, Kavukcuoglu K (2017) Neural machine translation in linear time. arXiv Preprint arXiv:1610.10099.

Krizhevsky A, Sutskever I, Hinton GE (2012) ImageNet classification with deep convolutional neural networks. In: Pereira F, Burges CJ, Bottou L, Weinberger KQ (eds) Advances in Neural Information Processing Systems. Curran Associates, Inc., Lake Tahoe, USA.

Kumar K, Kumar R, de Boissiere T, Gestin L, Teoh WZ, Sotelo J, de Brébisson A, Bengio Y, Courville AC (2019) MelGAN: generative adversarial networks for conditional waveform synthesis. In: Wallach H, Larochelle H, Beygelzimer A, d'Alché-Buc F, Fox E, Garnett R (eds) Advances in Neural Information Processing Systems. Curran Associates, Inc.

Lan Z, Chen M, Goodman S, Gimpel K, Sharma P, Soricut R (2020) ALBERT: a lite BERT for self-supervised learning of language representations. arXiv

Preprint arXiv:1909.11942.

Li N, Liu S, Liu Y, Zhao S, Liu M (2019) Neural speech synthesis with Transformer network. Proc AAAI Conf Artif Intell 33:6706–6713.

Li Y, Choi D, Chung J, Kushman N, Schrittwieser J, Leblond R, Eccles T, Keeling J, Gimeno F, Lago AD, et al. (2022) Competition-level code generation with AlphaCode. arXiv Preprint arXiv:2203.07814.

Oord AV, Kalchbrenner N, Kavukcuoglu K (2016a) Pixel Recurrent Neural Networks. In: Proceedings of The 33rd International Conference on Machine Learning. PMLR, pp 1747–1756.

Oord A van den, Dieleman S, Zen H, Simonyan K, Vinyals O, Graves A, Kalchbrenner N, Senior A, Kavukcuoglu K (2016b) WaveNet: a generative model for raw audio. arXiv Preprint arXiv:1609.03499.

Radford A, Metz L, Chintala S (2016) Unsupervised representation learning with deep convolutional generative adversarial networks. arXiv Preprint arXiv:1511.06434.

Sutskever I, Vinyals O, Le QV (2014) Sequence to Sequence Learning with Neural Networks. In: Ghahramani Z, Welling M, Cortes C, Lawrence N, Weinberger KQ (eds) Advances in Neural Information Processing Systems. Curran Associates, Inc., Montreal, Canada.

Suwajanakorn S, Seitz SM, Kemelmacher-Shlizerman I (2017) Synthesizing Obama: learning lip sync from audio. ACM Trans Graph 36:1–13.

Szegedy C, Liu W, Jia Y, Sermanet P, Reed S, Anguelov D, Erhan D, Vanhoucke

V, Rabinovich A (2015) Going deeper with convolutions. Boston, USA, pp 1–9

van den Oord A, Kalchbrenner N, Espeholt L, kavukcuoglu koray, Vinyals O, Graves A (2016) Conditional image generation with PixelCNN decoders. In: Lee D, Sugiyama M, Luxburg U, Guyon I, Garnett R (eds) Advances in Neural Information Processing Systems. Curran Associates, Inc., Barcelona, Spain.

Vaswani A, Shazeer N, Parmar N, Uszkoreit J, Jones L, Gomez AN, Kaiser Ł, Polosukhin I (2017) Attention is all you need. In: Guyon I, von Luxburg U, Bengio S, Wallach H, Fergus R, Vishwanathan S, Garnett R (eds) Advances in Neural Information Processing Systems. Curran Associates, Inc., Long Beach, USA.

Wang Y, Skerry-Ryan RJ, Stanton D, Wu Y, Weiss RJ, Jaitly N, Yang Z, Xiao Y, Chen Z, Bengio S, Le Q, Agiomyrgiannakis Y, Clark R, Saurous RA (2017) Tacotron: towards end-to-end speech synthesis. arXiv Preprint arXiv:1703.10135.

Zhang H, Goodfellow I, Metaxas D, Odena A (2019) Self-attention generative adversarial networks. arXiv Preprint arXiv:1805.08318.